10-1-2018

Elucidating the Mechanisms of Apoptosis Induced by a Novel Geranylgeranyl Diphosphate Synthase Inhibitor in T-cell Acute Lymphoblastic Leukemia

Sherry Agabiti
sherry.su@uconn.edu

Elucidating the Mechanisms of Apoptosis Induced by a Novel Geranylgeranyl Diphosphate Synthase Inhibitor in T-cell Acute Lymphoblastic Leukemia

Sherry Su Agabiti, Ph.D.

University of Connecticut, 2018

T-cell acute lymphoblastic leukemia (T-ALL) is a rare but aggressive T-cell malignancy that is a subset of acute lymphoblastic leukemia. T-ALL comprises approximately 15% of childhood and 25% of adult cases. It is most common in children but these patients can relapse. While the 5-year survival rate in children (80%) has improved significantly due to advances in chemotherapy, primary resistant and relapsed cases are still dismal which argue for more treatment options. Many current therapies target T-ALL through DNA damage or synthesis often causing toxicity in healthy cells. Our lab has identified and developed novel agents that induce apoptosis in T-ALL cells, which are selective inhibitors of the enzyme geranylgeranyl diphosphate synthase (GGDPS). GGDPS is an enzyme in the isoprenoid biosynthesis pathway that produces geranylgeranyl diphosphate (GGPP) whose lipid moiety is post-translationally attached to small GTPases allowing GTPases to be membrane-associated and exert their function at the membrane. Here, I investigate the mechanism of apoptosis induced by GGDPS inhibitors and compare GGDPS inhibitors with current therapies. GGDPS inhibition is more potent than zoledronate, an isoprenoid biosynthesis pathway inhibitor used clinically against bone malignancies. Interestingly, GGDPS inhibitors are minimally toxic towards healthy PBMCs compared to zoledronate. GGDPS inhibitors and zoledronate also alter membrane localization of different small GTPases. I establish the role of ERK activation and caspase cleavage in GGDPS

inhibitor-induced apoptosis, and importantly, I also determine that GGDPS inhibition-induced apoptosis is also mediated by Notch1, ATM and c-abl. C-abl is at the crux of the DNA damage response pathway as it is both involved in DNA damage repair and DNA damage-induced apoptosis. Interestingly, T-ALL cells show high levels of DNA damage yet do not undergo apoptosis. I predict that GGDPS inhibition circumvents this evasion of apoptosis through depleting levels of active Notch1, and allowing for the activation of ATM, and cleaving of c-abl. Therefore, I hypothesize that GGDPS inhibition targets cells with high levels of DNA damage. Overall, I explore how T-ALL cells use Notch1, ATM, and c-abl to avoid DNA damage-induced apoptosis and how inhibition of GGDPS overcomes this regulation.

Elucidating the Mechanisms of Apoptosis Induced by a Novel Geranylgeranyl Diphosphate Synthase Inhibitor in T-cell Acute Lymphoblastic Leukemia

Sherry Su Agabiti

B.S. University of Connecticut, 2012

A Dissertation

Submitted in Partial Fulfillment of the

Requirements for the Degree of

Doctor of Philosophy

at the

University of Connecticut

2018

APPROVAL PAGE

Doctor of Philosophy Dissertation

Elucidating the Mechanisms of Apoptosis Induced by a Novel Geranylgeranyl Diphosphate Synthase Inhibitor in T-cell Acute Lymphoblastic Leukemia

Presented by

Sherry Su Agabiti, B.S.

Major Advisor

Andrew J. Wiemer, Ph.D.

Associate Advisor

Debra Kendall, Ph.D.

Associate Advisor

Brian Aneskievich, Ph.D.

Associate Advisor

Nathan Alder, Ph.D.

Associate Advisor

Olga Vinogradova, Ph.D.

University of Connecticut
2018

Acknowledgments

Thanks to my advisor, Dr. Andrew Wiemer, for letting me work on this project, for being patient, listening to my half-baked ideas, and giving great advice. Thank you for taking a chance on me. Your commitment to mentorship has not gone unnoticed and will not be forgotten.

Thanks to my committee members: Dr. Alder, Dr. Aneskievich, Dr. Kendall and Dr. Vinogradova for your support, availability, commitment, questions and suggestions. I truly appreciate the time and effort put into making me a more independent researcher. To my lab mates: Jin, Ashley, Megan, and Mike thanks for all the great conversations and the support. To Dr. Christine Hsiao, for always being willing to read a draft of a manuscript and for the help with cloning and trouble shooting all things molecular biology. Assistance with flow cytometry from Dr. Carol Norris and Dr. Wu He is gratefully acknowledged. To Leslie Lebel, our graduate student advocate, for always being helpful (we are ever grateful). To Willie Dong and Jin Li, thanks for all the help with doing extra cell viability studies. To Andrew Hederman and Dipali Mistri, thank you for running viability assays. To Dr. RC Dash thanks for patiently teaching me docking. And to Dr. Mike Poe thanks for patiently teaching me synthesis. To Chelle, Sarah, Bekah and Tabitha, your friendship and support in this endeavor has been invaluable to me. To Dad, thank you for instilling a love of learning, analysis, and cats. I'm grateful that you've always provided and been there for me. Mom, thank you for all the sacrifices you made for me (including your own Ph.D.) and thanks for always being willing to send over a protocol. I hope this makes you proud. Dear Dan- you're cool. Thanks for talking me through the tough days, holding down the fort, always making me laugh and always being there for me. You're the best. To God, your grace is sufficient. And to you, dear reader, for taking the time to read through this and for tolerating my penchant for hyphens.

Table of Contents

CHAPTER 1. MOLECULAR MECHANISMS LINKING GERANYLGERANYL DIPHOSHATE SYNTHASE TO CELL SURVIVAL AND PROLIFERATION.

Abstract

Geranylgeranyl diphosphate is a twenty-carbon isoprenoid phospholipid whose lipid moiety can be post-translationally incorporated into proteins to promote membrane association. The process of geranylgeranylation has been implicated in anti-proliferative effects of clinical agents that inhibit enzymes of the mevalonate pathway (i.e. statins and nitrogenous bisphosphonates) as well as experimental agents that deplete geranylgeranyl diphosphate. Inhibitors of geranylgeranyl diphosphate synthase are an attractive way to block geranylgeranylation because they utilize beneficial chemical features of the bisphosphonate substructure and take advantage of a unique position of the enzyme within the biosynthetic pathway. Here, we describe recent advances in geranylgeranyl diphosphate synthase expression and inhibitor development with a particular focus on the molecular mechanisms that link geranylgeranyl diphosphate to cell proliferation via geranylgeranylated small GTPases. This chapter was adapted from a previous publication (Agabiti et al., 2016).

Introduction

Post-translational attachment of a lipid group to a protein is commonly used by cells to promote association of the protein with a biological membrane (Palsuledesai and Distefano, 2015). The enzymes of protein prenylation specifically utilize intermediates of cellular isoprenoid biosynthesis as substrates to modify one or two cysteine residues near the C-terminus of the protein. Prenylation may refer to incorporation of the fifteen-carbon molecule farnesyl

diphosphate (farnesylation) or the twenty-carbon geranylgeranyl diphosphate (geranylgeranylation) onto a protein. The specific modification depends upon the amino acid sequence found at the C-terminus of that particular protein. Both types of prenylation are directed by the CaaX motif- composed of a cysteine followed by three additional amino acid residues (Reid et al., 2004), though in some Rab proteins geranylgeranylation can occur at two cysteine residues with other consensus sequences.

Because many small GTPases of the Ras superfamily are prenylated, inhibition of protein prenylation has been viewed as a potential therapeutic target for diseases in which GTPases contribute to the pathogenesis (Berndt et al., 2011, Hottman and Li, 2014, Cox et al., 2015). The majority of these studies have examined disrupting farnesylation of Ras family members H-, N- and K-Ras, which are known oncogenes. Other small GTPases, such as RhoA, also have been reported to play roles in survival and proliferation of malignant cells (Qiu et al., 1995, Ghosh et al., 1999, Allal et al., 2000, Yoshida et al., 2009) and altering the membrane localization of RhoA can reduce proliferation (Adnane et al., 1998, Li et al., 2002, Denoyelle et al., 2003, Fromigue et al., 2006, Tang et al., 2006, Zhu et al., 2013). While these and other studies have clearly shown that disruption of prenylation can reduce proliferation of malignant cells, the clinical potential of prenylation inhibitors for treatment of disease is often limited because: 1) prenylated proteins can be critical to the function of healthy normal cells, 2) direct inhibition of prenylation enzymes in cells can be overcome by activation of alternative prenylation pathways, and 3) prenylation and the membrane association that it promotes is not always required for protein activity. Although much effort has been devoted to pre-clinical development of prenyl transferase inhibitors, these compounds have not yet gained clinical relevance.

In contrast, bisphosphonate-based inhibitors of cellular isoprenoid biosynthesis and protein prenylation have achieved clinical success (Ebetino et al., 2011, Clezardin et al., 2011). Although they can be associated with mechanism-based side effects such as osteonecrosis in a small percentage of patients, these drugs greatly reduce the risk of fractures resulting from osteoporosis (Russell et al., 2008). Additionally, they are now frequently used for treatment of cancer-related skeletal complications (Ibrahim et al., 2003) that arise from both solid tumor metastases (Gnant, 2012) and hematological diseases such as myeloma (Terpos et al., 2014) where they prevent growth of the malignant cells in the bone environment. The nitrogen-containing bisphosphonates appear to function primarily by blocking isoprenoid biosynthesis (Amin et al., 1992, Shipman et al., 1998) leading to protein prenylation (van Beek et al., 1999b, Bergstrom et al., 2000). In osteoclasts, this results in loss of bone resorption but in malignant cells this reduces proliferation. Nitrogenous bisphosphonates overcome some of the limitations of prenyltransferase inhibitors in this regard because they exhibit reduced effects on healthy cells through enriched distribution to the bone compartment and they prevent alternative prenylation through inhibiting an upstream enzyme, farnesyl diphosphate synthase (FDPS).

While FDPS is the molecular target of the clinical bisphosphonates, the molecular mechanism of action is often linked to downstream depletion of geranylgeranyl diphosphate. Therefore, bisphosphonate-based compounds that target other enzymes of isoprenoid biosynthesis (Wiemer et al., 2009) leading to geranylgeranyl diphosphate production may be viable therapies for GTPase-dependent disorders affecting the bone environment (Wiemer et al., 2011), and could be useful tools for understanding the biological consequences of geranylgeranyl diphosphate depletion in cells. This mini-review examines recent developments in our understanding of the relationship between geranylgeranyl diphosphate synthase (GGDPS) and

cell survival and proliferation, which are affected by geranylgeranylated proteins in the membrane domain.

Expression and regulation of GGDPS

GGDPS is a ubiquitously-expressed 35 kDa enzyme found within the isoprenoid biosynthetic pathway (also known as the mevalonate pathway) (Wiemer et al., 2011) (Figure 1). In human cells, GGDPS has been reported to form a large multimeric complex, which was initially characterized as an octomer (tetramer of dimers) (Kuzuguchi et al., 1999) but subsequently reported as a hexamer (trimer of dimers) (Kavanagh et al., 2006a). Further biochemical studies appear to support the octomer model (Miyagi et al., 2007). Like FDPS, GGDPS is a prenyl synthase enzyme. Together, these enzymes produce the farnesyl diphosphate and geranylgeranyl diphosphate, respectively. GGDPS catalyzes the condensation of farnesyl diphosphate and isopentenyl diphosphate to geranylgeranyl diphosphate via an ionization-condensation-elimination mechanism (Poulter et al., 1978). Thus, depletion of either substrate may decrease GGDPS activity. GGDPS also has an additional binding site where geranylgeranyl diphosphate may bind and inhibit the enzymatic activity (Kavanagh et al., 2006a, Guo et al., 2007). Farnesyl diphosphate and geranylgeranyl diphosphate, can subsequently be utilized as substrates by the prenyl transferase enzymes (farnesyl transferase and geranylgeranyl transferases I and II) as described above. Post-translational incorporation of the prenyl moiety increases membrane association of modified proteins, which is generally but not always required for normal activation and signaling.

Many isoprenoid biosynthetic pathway enzymes are regulated at the transcriptional level to control isoprenoid production (Figure 2). The classical model of this effect is observed when statin drugs are used to inhibit HMG-CoA reductase leading to the depletion of intracellular

cholesterol (Brown and Goldstein, 1980). Cholesterol depletion triggers a restorative feedback response mediated by sterol regulatory element binding transcription factors, which upon translocation into the nucleus induce transcription of HMG-CoA reductase (Hua et al., 1993, Brown and Goldstein, 1997, Brown and Goldstein, 2009) (Figure 2A). It is unclear whether GGDPS expression is strongly dependent on sterol regulatory elements, though evidence suggests that its regulation by these factors is not as dramatic as the upstream enzymes such as HMG-CoA reductase. Nonetheless, inhibition of GGDPS leads to diversion of farnesyl diphosphate into sterol synthesis, which has an effect that is opposite to that of statins and nitrogenous bisphosphonates-decreased transcription of HMG-CoA reductase (Wiemer et al., 2011). Thus, in contrast to HMG-CoA reductase inhibition, cells appear to have a reduced ability to overcome the effects of GGDPS inhibition at the transcriptional level.

Sterol regulatory elements are not the only potential transcriptional regulators of GGDPS and other isoprenoid pathway enzymes. Activation of the extracellular signal-regulated kinase (ERK) pathway can activate the zinc-dependent transcription factor early growth response gene 1 (EGR1) to regulate expression of HMG-CoA reductase and other sterol pathway enzymes (Gokey et al., 2011) (Figure 2B). In contrast to transcription controlled by sterol regulatory elements, constitutively active EGR1 may also regulate GGDPS expression by upregulating transcription of the GGDPS gene, which forms a positive feedback loop (Shen et al., 2011). This pathway can be activated by insulin (Yu et al., 2011) and toxins such as cigarette smoke extract (Shen et al., 2011), which stimulate the ERK pathway and promote accumulation of EGR1 (Tao et al., 2013). But the relationship between EGR1 and GGDPS needs further investigation as inhibition of EGR1 transcription had no effect on GGDPS mRNA and protein levels in MCF-7 breast cancer cells (Tao et al., 2013).

Upregulation and/or dysregulation of the isoprenoid biosynthetic pathway enzymes including GGDPS has been indicated in oncogenic progression (Pandyra et al., 2015), demonstrating an important link between isoprenoids and cell survival and proliferation. For example, dysregulation of the mevalonate pathway by ectopic expression of HMG-CoA reductase promotes transformation of liver cells (Clendening et al., 2010). Additionally, mutant p53 can contribute to malignant cell morphology in mammary tissue in a way that is dependent upon the mevalonate pathway (Freed-Pastor et al., 2012). In cells depleted of mutant p53, the addition of mevalonate pathway metabolites could compensate for the loss of mutant p53 by restoring the invasive morphology. GGDPS itself is associated with development of liver cancer. In tissue from hepatocellular carcinoma patients, GGDPS mRNA expression was elevated in 85.29% of tumor tissue compared to surrounding cells (Yu et al., 2014). Correspondingly, they found that GGDPS protein expression was increased in tumor tissue compared to adjacent tissue in 11 of 15 patients.

While GGDPS expression is ubiquitous and its enzymatic product is often required for proliferation (Benford et al., 1999, van de Donk et al., 2003, Inoue et al., 2005, Brinkkoetter et al., 2006, Baulch-Brown et al., 2007, Sonnemann et al., 2007, Wiemer et al., 2007, Yanae et al., 2011, Tsubaki et al., 2013, Zafar et al., 2014), there is only limited evidence, as described in the preceding paragraph, to suggest a higher degree of GGDPS mutation in malignant cells relative to normal cells. Therefore, GGDPS inhibitors could be best classified as anti-metabolites targeting membrane domain proteins (Bennis et al., 1993, Mo and Elson, 2004). Even without malignant versus normal selectivity, therapeutic specificity could still be obtained by tissue-

specific distribution such as that which directs bisphosphonates to localize to the bone environment due to the affinity of the substructure for calcium.

Geranylgeranyl diphosphate synthase inhibitors

Bisphosphonate-based drugs, such as alendronate (Figure 3, compound **1**), have been used therapeutically in humans for over half a century (Ebetino et al., 2011). In fact, the nitrogenous bisphosphonates that inhibit FDPS gained therapeutic use prior to determination of their molecular mechanism of action. These agents were selected in part because of the usefulness of the bisphosphonate substructure for binding calcium ions. It was later revealed that the nitrogenous bisphosphonates act as potent inhibitors of FDPS. However, the cellular effects of bisphosphonates on osteoclast-mediated bone resorption are not due to depletion of the immediate enzymatic product, farnesyl diphosphate, but rather to depletion of the subsequent molecule in the pathway, geranylgeranyl diphosphate (van beek et al., 1999a). Around the same time, it was demonstrated that the bisphosphonate substructure is useful for targeting inhibitors such as compound **2** to squalene synthase (Ciosek et al., 1993). As bisphosphonates can be viewed as analogs of diphosphates, one could readily hypothesize that other enzymes that metabolize diphosphate, such as GGDPS, may also be targeted by bisphosphonate-based drugs.

Initial studies on GGDPS demonstrated that lipophilic bisphosphonates such as compound **3** inhibit the enzyme, while the nitrogenous bisphosphonate drugs do not (Bergstrom et al., 2000, Szabo et al., 2002). Given this knowledge, it was hypothesized that bisphosphonates bearing isoprenoid substituents may also function as GGDPS inhibitors. We synthesized and characterized an initial library of bis-prenyl bisphosphonates (Shull et al., 2006) including digeranyl bisphosphonate (**4**), demonstrating potent inhibition of cellular geranylgeranylation

with no effect on cellular farnesylation. Subsequent studies revealed nanomolar inhibition of GGDPS with no inhibition of FDPS (Wiemer et al., 2007, Wiemer et al., 2008a).

Lipophilic bisphosphonates bind up to three sites in the GGDPS enzyme (Guo et al., 2007), including both the substrate binding pockets of isopentenyl diphosphate and farnesyl diphosphate, as well as a geranylgeranyl diphosphate product/inhibitory binding site. Further studies comparing bis-prenyl and mono-prenyl bisphosphonates showed potent GGDPS inhibition of both types of compounds (Wiemer et al., 2008a). Structural analysis demonstrated that branched bisphosphonates such as digeranyl bisphosphonate (DGBP) bind to the enzyme with the bisphosphonate in complex with two magnesium ions and the dual alkyl chains extending into the farnesyl diphosphate substrate and the geranylgeranyl diphosphate product binding sites (Chen et al., 2008).

Shorter-chain mono-alkyl nitrogenous bisphosphonates (e.g. compound **5**) allow for dual inhibition of FDPS and GGDPS (Zhang et al., 2009). Compound **5** demonstrated good anti-tumor activity in a mouse model of breast cancer. Additionally, the authors argued that these GGDPS inhibitors may be effective anti-malarial compounds, due to their two-fold effect (Zhang et al., 2013): 1) inhibition of the parasite GGDPS enzyme causes direct inhibition of parasite growth, and 2) inhibition of human FDPS causes activation of a human immune response through indirect activation of gamma delta T cells. Both mono-aromatic non-nitrogenous bisphosphonates (Barney et al., 2010) and triazole-based compounds such as compound **6** appear to retain specificity for inhibition of GGDPS over FDPS, in contrast to mono-alkyl nitrogenous bisphosphonates which appear to inhibit both FDPS and GGDPS (Zhou et al., 2014). In fact, a recently identified triazole-based compound (**7**) is the most potent GGDPS inhibitor described to date (Wills et al., 2015).

While most reports have examined modifications to the bisphosphonate substructure, non-bisphosphonate inhibitors of GGDPS have also been recently described (e.g. compound **8**) (Chen et al., 2013). Although these compounds are significantly less potent inhibitors of GGDPS, they retain specificity over FDPS. Lack of the bisphosphonate would be expected to increase peripheral distribution, which could increase the relevance for treatment of non-bone disorders that are dependent upon geranylgeranylation. However, this strategy may also result in increased toxicity towards healthy peripheral tissues. Taken together, a diverse group of bisphosphonate and non-bisphosphonate based GGDPS inhibitors has been developed, yielding a variety of options with respect to target specificity and cellular availability that could determine the consequences of geranylgeranyl diphosphate depletion.

GGDPS inhibitors as anti-proliferative agents targeting small GTPases

Several groups have examined the anti-proliferative activity of compounds that inhibit the enzymes of the isoprenoid pathway. The major premise is that protein prenylation is vital to cell growth and survival and that blocking prenylation through isoprenoid depletion would negatively impact cell health. While it is straightforward to broadly determine whether prenylation is required for proliferation in a given system, it is more difficult to determine which specific prenylated proteins mediate the effect. This problem is especially difficult with respect to geranylgeranylation, because approximately two thirds of the over 150 prenylated proteins are predicted to be geranylgeranylated rather than farnesylated (Reid et al., 2004, Maurer-Stroh et al., 2007). Many of these proteins are small GTPases of the Ras superfamily, which is typically divided into five families based on sequence and functional homology (Ras, Rho, Rab, Ran and Arf) (Wennerberg et al., 2005). While the Ras family GTPases are known to regulate proliferation, these proteins are predominately farnesylated and usually geranylgeranylated only

when their farnesylation is blocked. In contrast, the Rho and Rab GTPases, while predominately geranylgeranylated, are traditionally thought to function mainly in cytoskeletal reorganization and vesicle trafficking, respectively. Their roles in proliferation are less clear. Here, we examine the connection between geranylgeranylated small GTPases and the anti-proliferation phenotype caused by geranylgeranyl diphosphate depletion in order to determine whether GGDPS inhibitors would reduce proliferation by affecting a particular GTPase or GTPase family.

In some cases, the anti-proliferative effect caused by isoprenoid depletion using HMG-CoA reductase inhibitors (statin drugs) or FDPS inhibitors (bisphosphonate drugs) is dependent upon reduced prenylation of oncogenic small GTPases. The primary rationale for developing direct prenylation inhibitors (e.g. farnesyl transferase inhibitors) as anti-cancer agents stemmed from the finding that H- N- and K-Ras, which are among the most commonly mutated oncogenes, are primarily farnesylated (Cox et al., 2015). Isoprenoid biosynthesis inhibitors or farnesyl transferase inhibitors can block Ras prenylation, in turn reducing Ras signaling and preventing cellular growth. For example, in some human leukemia cells the HMG-CoA reductase inhibitor lovastatin potentiates the cell toxicity of a checkpoint inhibitor, which is abrogated by ectopic expression of constitutively active Ras leading to elevated downstream ERK signaling (Dai et al., 2007).

At times some Ras isoforms can be geranylgeranylated when their farnesylation is blocked (Whyte et al., 1997), suggesting that farnesyl transferase is not an ideal target for disrupting Ras prenylation. Some groups have proposed combining farnesyl transferase inhibitors with geranylgeranyl transferase inhibitors to achieve complete Ras blockade (Lobell et al., 2001). However, another potential route to overcome this limitation is to utilize a prenyl synthase inhibitor which acts upstream to deplete both farnesyl and geranylgeranyl diphosphate,

and block both routes of prenylation. For example, exposure to a lipophilic bisphosphonate decreases the plasma membrane levels of K-Ras and H-Ras and leads to caspase dependent apoptosis (Xia et al., 2014). Targeting only farnesyl transferase lacked clinical efficacy, therefore targeting multiple isoprenoid enzymes may be more advantageous (Cox et al., 2015), provided that unwanted toxicity to healthy cells can be avoided through other means such as tumor-specific delivery.

Although Ras is mutated in a number of cancers like pancreatic and lung adenocarcinomas (McCormick, 2015, Padavano et al., 2015), the majority of prenylated proteins are not mutated in cancer (Alan and Lundquist, 2013). Notable exceptions are that dominant negative RhoA can be found in angioimmunoblastic T-cell lymphoma and mutated RhoH can be found in non-Hodgkin lymphoma and multiple myeloma (Preudhomme et al., 2000, Nagata et al., 2016). However, even these non-mutated prenylated proteins can still be targets for cancer therapy because of their role in cell proliferation. Targeting prenylation requires that both the protein and its prenylated state are important in proliferation. For instance, Rac, which is a substrate of geranylgeranyl transferase I, has been shown to be involved in proliferation and decreasing prenylation decreases proliferation (Baba et al., 2008). Despite these advantages, it is challenging to identify the specific protein involved in the pathway because many GTPases share effector and regulatory proteins and the exogenous expression of one GTPase may influence the activity of other GTPases.

Taking those caveats into account, most studies have implicated geranylgeranylation of Rho family proteins, specifically RhoA, as a mediator of the anti-proliferative effects of geranylgeranyl diphosphate depletion. For example, depletion of geranylgeranyl diphosphate interrupts the transition from G1 to S phase in thyroid cells by preventing a decrease in p27

expression (Hirai et al., 1997). The phenotype is rescued by co-incubation with exogenous geranylgeranyl diphosphate. However, in the presence of botulinum C3 exoenzyme (which specifically inhibits Rho proteins), geranylgeranyl diphosphate is unable to rescue the phenotype. Thus, the authors concluded that geranylgeranylation of Rho is required for proliferation of these cells.

In vascular smooth muscle cells, statins induce an apoptotic effect, which is rescued by co-incubation with either farnesyl or geranylgeranyl diphosphate, indicating a role for geranylgeranylation in the apoptotic mechanism. Overexpression of constitutively active RhoA (L63) reduces the effect of the statin on apoptotic DNA laddering (Blanco-Colio et al., 2002). In endothelial cells, statins potentiate apoptosis induced by tumor necrosis factor-α. This effect is due to reduced RhoA geranylgeranylation, because the phenotype can be mimicked by expression of a dominant negative RhoA construct (N19). More importantly, the effect of the statin can be rescued by expression of constitutively active RhoA (L63) (Tang et al., 2006). In osteosarcoma cells, statin treatment induces caspase-dependent apoptosis. Here, the authors demonstrated that atorvastatin increases caspase activity, which is rescued by constitutively active RhoA (V14) but not wild-type RhoA (Fromigue et al., 2006). In a well-designed study, Allal et al. generated plasmids coding for farnesylated-RhoA and farnesylated-RhoB in which the CAAX domain is mutated to a farnesylation sequence (CVLS) as opposed to the normal geranylgeranylation sequence (CVLV). They found that farnesylated-RhoB and not farnesylated RhoA evades G_0/G_1 cell cycle arrest induced by geranylgeranyl transferase inhibition (Allal et al., 2002). Together, these studies provide mechanistic evidence for a requirement of not only Rho but also of Rho geranylgeranylation for cell proliferation and survival.

While disruption of RhoA geranylgeranylation resulting in mislocalization has negative consequences on proliferation and survival, it is unclear in some cases whether disruption of geranylgeranylation inhibits or activates RhoA signaling. For example, in HepG2 cells, a decrease in RhoA activity is implicated in mediating apoptosis via lipophilic statins (Maeda et al., 2010). These effects are rescued by addition of geranylgeranyl diphosphate. Similarly, in colorectal cancer cells, treatment with a statin induces apoptosis, which is rescued by exogenous geranylgeranyl diphosphate but not farnesyl diphosphate (Zhu et al., 2013). In contrast to the HepG2 cells, partial rescue of the statin-induced phenotype is observed not only with RhoA silencing, but also with Rac1 silencing, Rac1 inhibitors, and expression of dominant negative Rac1 (N17). This led the authors to suggest not only that both RhoA and Rac1 mediate the effects of statins in this system, but also that statins elevate (rather than reduce) Rho and Rac signaling activity, which leads to apoptosis.

These results agree with a prior study that observed GTPase activation in macrophages that had been treated with nitrogenous bisphosphonates. In the macrophage system, increases are observed in RhoA, Rac1, and Cdc42 GTP binding in response to isoprenoid depletion. The authors propose that mislocalization of the improperly prenylated proteins may restrict their ability to interact with their regulatory partners. Furthermore, in this system Rac1 silencing was able to block the increase in p38 phosphorylation that was also observed (Dunford et al., 2006).

The Ras family members RalA and RalB have also been implicated in the phenotypes caused by inhibition of geranylgeranylation (Falsetti et al., 2007). Here, the authors examined the mechanism of growth inhibition that was induced by geranylgeranyl transferase type I inhibitors in pancreatic cancer cells. Treatment with the geranylgeranyl transferase inhibitors causes anchorage-independent growth and induces apoptosis. These studies used RalA and RalB

constructs in which the CAAX prenylation signal had been altered to allow these naturally geranylgeranylated proteins to be modified instead by farnesylation. Interestingly, the farnesylated RalB construct rescued the apoptotic phenotype while expression of the farnesylated RalA construct rescued the anchorage-independent growth phenotype.

Rap1 is another geranylgeranylated GTPase that may play a role in tumor malignancy. While mechanistic studies demonstrating functional significance of Rap1 prenylation to the anti-proliferative phenotypes of isoprenoid biosynthesis inhibitors are lacking, the development of antibodies to the non-prenylated form of Rap1 have facilitated the *in vitro* study of geranylgeranylation by eliminating the need for preparing cytoplasmic and membrane fractions for Western blot analysis. Rap1 is routinely used as a biomarker for cellular geranylgeranylation, and is especially useful for in tissue studies in which tissue for analysis is limited, precluding analysis by subcellular fractionation. For example, Rap1 geranylgeranylation was detected to be impaired by GGDPS inhibitors at metastatic sites in the adrenal gland and mesenteric metastatic sites, while it was not altered in non-tumorous adrenal glands. Corresponding with the inhibition of Rap1 prenylation, mice treated with the GGDPS inhibitor also show reduced tumor burden (Reilly et al., 2015a).

An important advantage of GGDPS inhibition is the ability to impair geranylgeranylation of proteins that are modified by both geranylgeranyl transferase type I, which I modifies Rho family proteins like Rho, Rac, cdc42 and type II, which modifies members of the Rab family (Stigter et al., 2012). These proteins have been traditionally associated with regulation of membrane trafficking, however there is recent evidence implicating Rab prenylation in the anti-proliferative effect of isoprenoid depletion. For example, it has been reported that overexpression

of Rab27B can promote tumor growth (Hendrix et al., 2010). Mutants of Rab27B that are deficient in their prenylation lack this effect.

The impact of Rab GTPases is also seen in inhibitor studies. Both zoledronate and a geranylgeranyl transferase inhibitor decrease the membrane to cytoplasmic ratios of RhoA, Cdc42 and Rab6. Most notably, the effects of zoledronate are similar to that of a geranylgeranyl transferase II inhibitor suggesting that the effects of zoledronate likely depend on the geranylgeranylation of Rab proteins including Rab6. Zoledronate ultimately induces apoptosis in some cells and S-phase cell cycle arrest in others. An inhibitor of geranylgeranyl transferase II also demonstrated a similar effect, and the authors suggested that zoledronate-mediated apoptosis was driven by loss of Rab geranylgeranylation (Okamoto et al., 2014).

In addition to roles in cell proliferation regulation, Rab geranylgeranylation has been implicated in regulation of autophagy. Geranylgeranyl diphosphate depletion in response to GGDPS inhibition increases expression of LC3-II (Wasko et al., 2011, Dykstra et al., 2015), indicative of autophagy (Tanida et al., 2008). Co-incubation with exogenous geranylgeranyl diphosphate prevented accumulation of LC3-II and impairment of Rab geranylgeranylation caused by isoprenoid depletion. Dykstra found that geranylgeranyl transferase I inhibitor (GGTI-2133) is not able to induce LC3-II accumulation despite effective inhibition of geranylgeranylation (Dykstra et al., 2015). Moreover, knockdown of GGDPS induces autophagy and delays tumor growth *in vivo* (Jiang et al., 2014).

Conclusion

While many papers have shown that depletion of isoprenoids or small GTPases has a negative impact on proliferation and viability, fewer have investigated whether the anti-proliferative effects of isoprenoid depletion can be rescued by molecular manipulation of a

prenylated small GTPase. The more successful approaches have been to rescue proliferation with either an alternatively prenylated construct or a constitutively active construct, or fail to rescue with exogenous isoprenoid plus a dominant negative construct or inhibitor. In some cases, GTPase mislocalization causes activation rather than inactivation, and the phenotype can be directly rescued with a GTPase inhibitor. The studies described herein show that although there are dozens of predicted geranylgeranylated proteins, the anti-proliferative mechanism of geranylgeranyl diphosphate depletion can at times rest on mislocalization of a single geranylgeranylated small GTPase. RhoA geranylgeranylation has been the most frequently described critical lynchpin, but the phenomenon varies by model system, with Rac, Ral, and even Rab geranylgeranylation mediating the anti-proliferative effects in some models. By extension, inhibitors of GGDPS or the geranylgeranyl transferases may be most relevant to indications that depend upon the function of RhoA or its related proteins. Future studies on the consequences of disrupting geranylgeranylation would be aided by molecular approaches that identify the specific GTPase(s) involved.

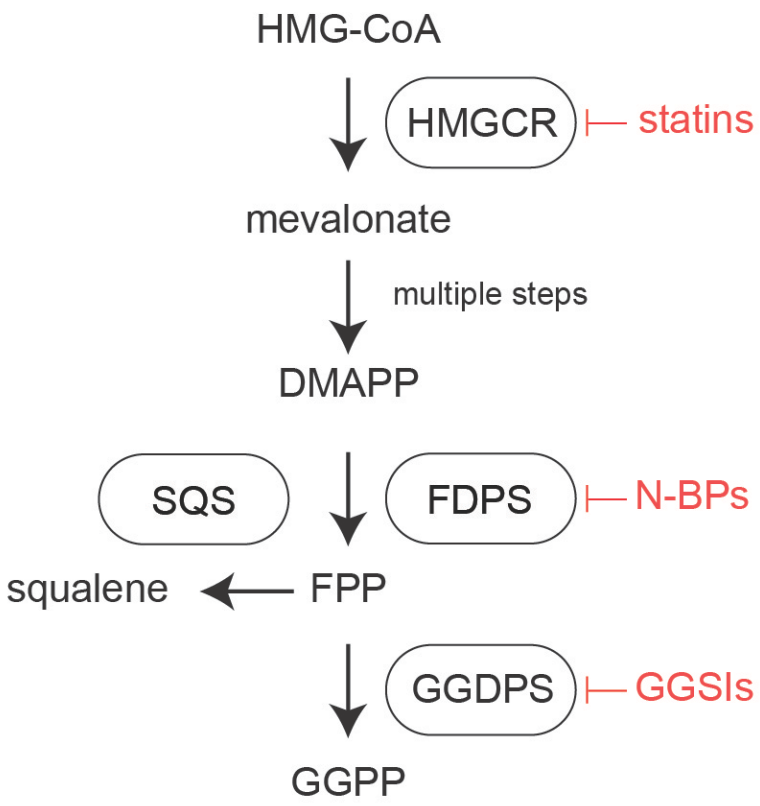

Figure 1. Location of geranylgeranyl diphosphate synthase (GGDPS) within the human isoprenoid biosynthetic pathway.

The first and rate-limiting step of human isoprenoid synthesis is the conversion of HMG-CoA to mevalonate by HMG-CoA reductase (HMGCR). This enzyme is the molecular target of the statin drugs. Several steps downstream, farnesyl diphosphate synthase (FDPS) catalyzes the production of farnesyl diphosphate (FPP) from dimethylallyl diphosphate DMAPP and two equivalents of isopentenyl diphosphate (IPP). This enzyme is the molecular target of the nitrogenous bisphosphonates. Farnesyl diphosphate is a key branch point of isoprenoid metabolism, giving rise to squalene in a reaction catalyzed by squalene synthase (SQS) and geranylgeranyl diphosphate (GGPP) in the GGDPS reaction.

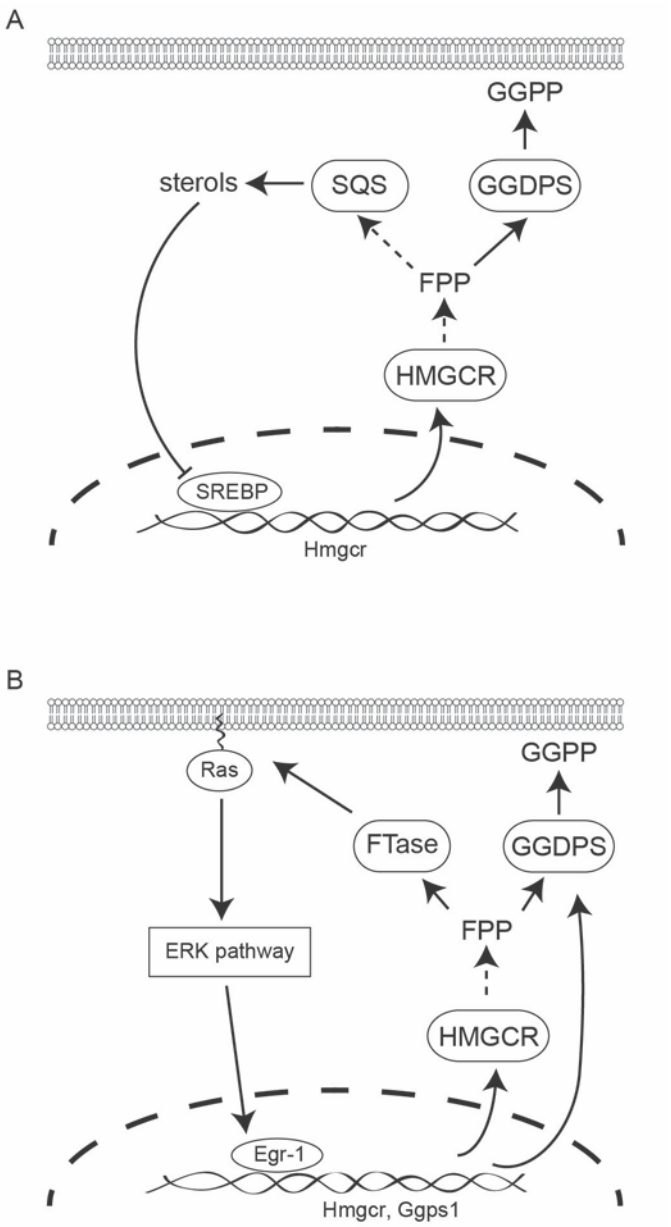

Figure 2. Key feedback mechanisms that control isoprenoid biosynthetic gene expression at the transcriptional level.

A) Sterol regulatory element-binding proteins (SREBPs) regulate transcription of HMG-CoA reductase and other enzymes of isoprenoid biosynthesis in response to cellular sterol levels, which indirectly affects synthesis of geranylgeranyl diphosphate. B) Egr-1 regulates transcription

of isoprenoid biosynthesis in response to activation of the ERK pathway, which directly regulates GGPDS expression at the transcriptional level.

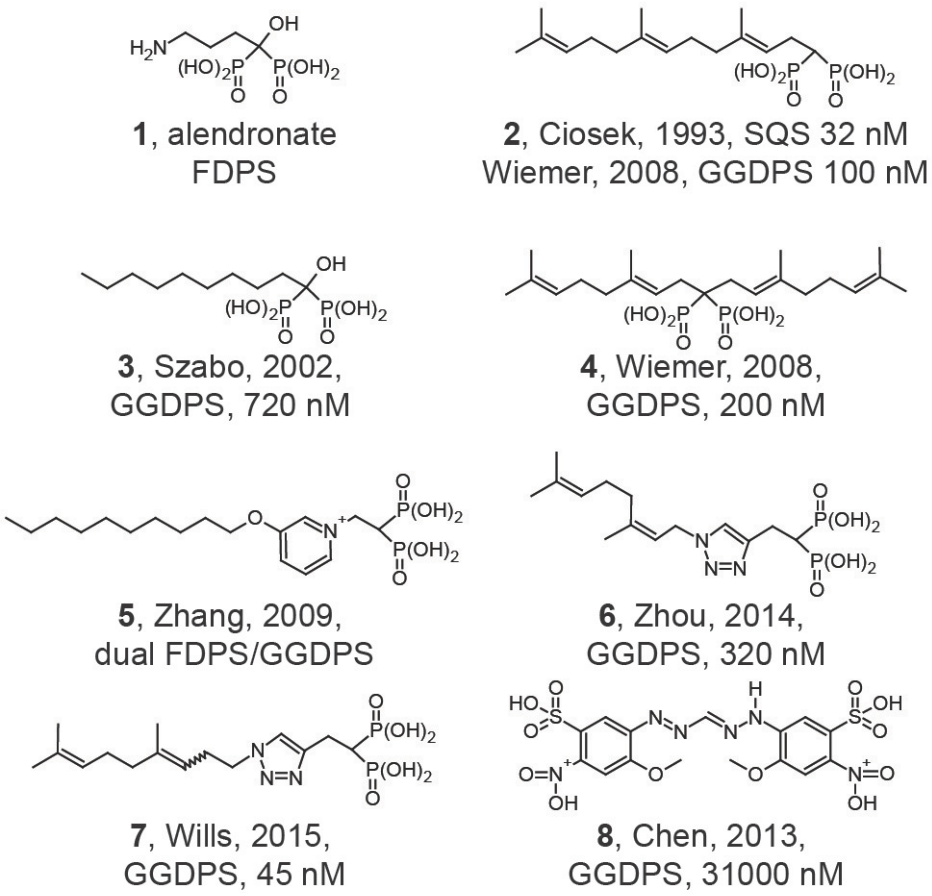

Figure 3. Structural evolution of GGDPS inhibitors.

Small nitrogen-containing bisphosphonates are inhibitors of farnesyl diphosphate synthase (FDPS). Lipophilic bisphosphonates can inhibit the enzymes of farnesyl diphosphate metabolism, including GGDPS and squalene synthase. Branched bisalkyl bisphosphonates retain specificity for GGDPS. Non bisphosphonate inhibitors of GGDPS have also been identified.

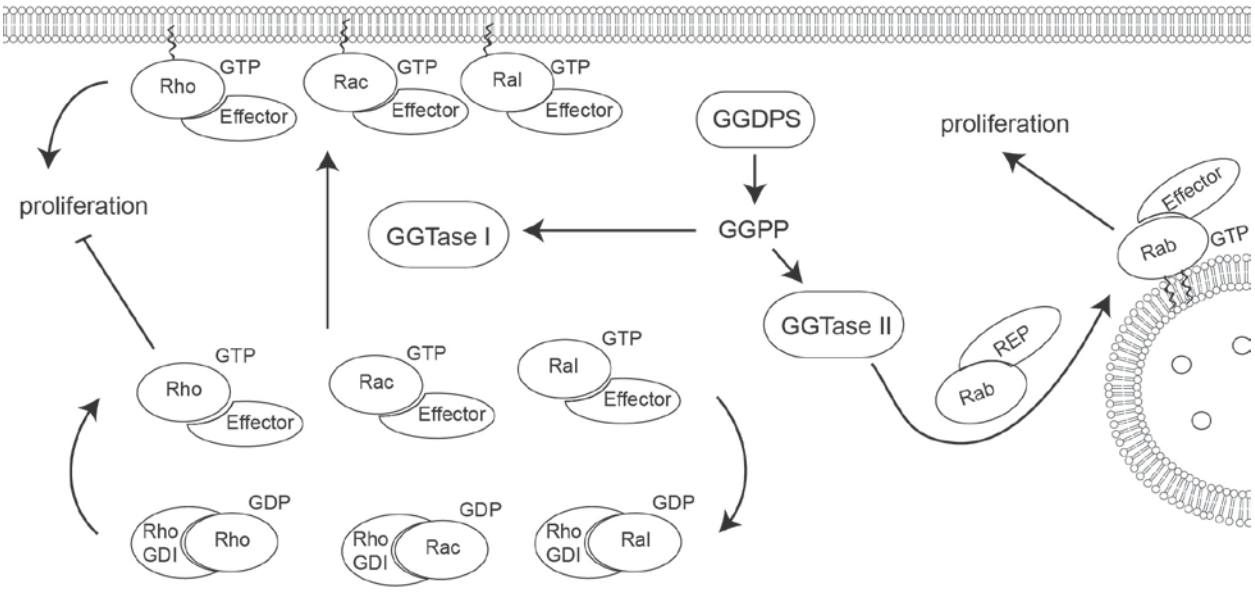

Figure 4. Geranylgeranylation of small GTPases including Rac, Rho, Rab, and Cdc42 promotes localization to the membrane domain, affecting proliferation.

Geranylgeranyl transferase I catalyzes the addition of geranylgeranyl diphosphate to the C-terminus of Rho, Rac, or Cdc42 while geranylgeranyl transferase II catalyzes the addition of one or two geranylgeranyl moieties to Rab GTPases. Rab GTPases are primarily involved in vesicle trafficking, though disruption of Rab geranylgeranylation can affect cell viability and proliferation. Rho, Rac, and Cdc42 are involved in proliferation in addition to adhesion and migration regulation.

CHAPTER 2: GERANYLGERANYL DIPHOSPHATE SYNTHASE INHIBITION INDUCES APOPTOSIS THAT IS DEPENDENT UPON GGPP DEPLETION, ERK PHOSPHORYLATION AND CASPASE ACTIVATION

Abstract

Bisphosphonates are diphosphate analogs that inhibit the intermediate enzymes of the mevalonate pathway. Here, we compared the effects of a farnesyl diphosphate synthase (FDPS) inhibitor, zoledronate, and a geranylgeranyl diphosphate synthase (GGDPS) inhibitor, digeranyl bisphosphonate (DGBP), on lymphocytic leukemia cell proliferation and apoptosis. Both zoledronate and DGBP inhibited proliferation with DGBP doing so more potently. DGBP was markedly less toxic than zoledronate towards the viability of healthy human peripheral blood mononuclear cells. Addition of GGPP, but not farnesyl diphosphate (FPP), prevented the anti-proliferative effects of DGBP. Both GGPP and FPP partially rescued the effects of zoledronate. Co-treatment with DGBP and zoledronate was antagonistic. To further assess the effects of the bisphosphonates, we analyzed annexin V and PI staining via flow cytometry and found that DGBP induced apoptosis more potently than zoledronate. Western blots show that DGBP treatment altered expression and membrane affinity of some but not all geranylgeranylated small GTPases, activated caspases, and increased ERK phosphorylation. Importantly, the anti-proliferative effects of DGBP were blocked by treatment with a caspase inhibitor and by treatment with a MEK inhibitor. Together, our findings indicate that DGBP is a more potent and selective compound than zoledronate in inducing apoptosis mediated through pathways that include caspases and MEK/ERK. These findings support the further development of GGDPS inhibitors as anticancer therapeutics. This chapter was adapted from a previous publication (Agabiti et al., 2017).

Introduction

Bisphosphonates are used widely for treatment of osteoporosis and other indications related to bone and calcium metabolism (Russell and Rogers, 1999, Licata, 2005, Russell et al., 2008). These compounds are structural analogs of diphosphates that are resistant to metabolism because they contain a carbon atom in place of the connecting oxygen atom normally found in the diphosphate (Martin et al., 1999, Licata, 2005). The bisphosphonate structure is critical for binding to the active sites of pharmacological targets including the enzyme farnesyl diphosphate synthase (FDPS) (Cheng and Oldfield, 2004, Guo et al., 2007). At the same time, the bisphosphonate structure impacts the pharmacokinetics of these drugs as it has a strong affinity for binding to calcium, thus promoting bone distribution (Ebetino et al., 2011). These compounds primarily function by inhibiting cellular functions in the bone microenvironment. This is especially important for osteoporosis therapy, because bisphosphonates can reduce osteoclast-mediated bone resorption and ultimately strengthen bone density (Roelofs et al., 2006, Russell et al., 2008).

Because of its activity in the bone microenvironment, the 3rd generation bisphosphonate zoledronate also has become useful for treatment of metastatic bone disease associated with solid tumors (Body, 2006, Stresing et al., 2007, Clezardin et al., 2011, Gnant, 2012) as well as multiple myeloma (Aparicio et al., 1998, Baulch-Brown et al., 2007, Guenther et al., 2010, Terpos et al., 2014, Tsubaki et al., 2015). It is thought that zoledronate functions to reduce the cellular intermediates of isoprenoid biosynthesis including farnesyl diphosphate (FPP) and geranylgeranyl diphosphate (GGPP), which are required for cell proliferation (Figure 5) (Reszka and Rodan, 2004, Okamoto et al., 2014). This disrupts protein geranylgeranylation, a process often required for malignant cell growth (Philips and Cox, 2007, Palsuledesai and Distefano,

2015, Sjogren et al., 2007). However, the mechanisms by which depletion of isoprenoids in transformed cells inhibits proliferation remain unclear. Additionally, the possibility remains that zoledronate or other bisphosphonates may also be used for other malignancies which have bone complications, such as acute T lymphocytic leukemia (Nishida et al., 2003, Kimura et al., 2004, Segawa et al., 2005, Ohtsuka et al., 2005, Chuah et al., 2005, Ishikawa et al., 2007).

Bisphosphonates may ultimately be beneficial for leukemia therapy because leukemia patients frequently experience bone pain due to accumulation of the leukemia cells in the bone and joints (Ishikawa et al., 2007). Additionally, a substantial number of patients experience hypercalcemia, in particular those with leukemias derived from T cells (Kiyokawa et al., 1987). Therefore, bisphosphonates may offer two disease modifying mechanisms to T-cell leukemia-direct inhibition of leukemia cell proliferation that results from their inhibition of isoprenoid biosynthesis (Ishikawa et al., 2007) and relief from hypercalcemia that results from their binding to calcium ions (Ebetino et al., 2011).

While the clinically-used bisphosphonates inhibit the enzyme FDPS (Amin et al., 1992, Rogers et al., 1994, Rogers et al., 1995, Luckman et al., 1998, van Beek et al., 1999b), we have recently explored a new class of bisphosphonates including DGBP (Figure 5), which target the subsequent enzyme in the mevalonate pathway (Wiemer et al., 2009), GGDPS (Shull et al., 2006, Wiemer et al., 2007, Wiemer et al., 2011). The downstream molecular target affords the opportunity to retain the anti-proliferative characteristics of zoledronate which can result from depletion of GGPP while reducing potential side effects that may occur from depletion of FPP. Here, we evaluate the efficacy by which these two classes of bisphosphonates induce cell death in T lymphocytic leukemia and provide insights into the mechanisms through which depletion of isoprenoids leads to leukemia cell death.

Results

DGBP inhibits proliferation of lymphocytic leukemia cell lines more potently than zoledronate

We first compared the effects of two nanomolar inhibitors: zoledronate (a potent clinical inhibitor of FDPS (Kavanagh et al., 2006b)) and DGBP (a specific experimental inhibitor of GGDPS (Wiemer et al., 2007)) on the proliferation of T-cell leukemia lines. Treatment of either Molt-4 or Jurkat cells with varied concentrations of either compound for 72 hours dose-dependently inhibited cell proliferation (Figure 6A/B). In both the Molt-4 and Jurkat cell lines, the anti-proliferative effect of DGBP was stronger than that of zoledronate (half-maximal inhibitory concentration (IC_{50}) of DGBP = 15 μM in Molt-4 cells and 30 μM in Jurkat cells, IC_{50} of zoledronate = 52 μM in Molt-4 cells and 81 μM in Jurkat cells) (Table 1). Both compounds were more potent against proliferation of these lymphocytic cell lines compared to myeloid leukemias, for which concentrations above 100 μM were required (Tsubaki et al., 2013). This surprising effect suggests that lymphocytic leukemias are more sensitive to isoprenoid depletion relative to myeloid leukemias and that inhibition of GGDPS is more anti-proliferative than inhibition of FDPS.

Zoledronate but not DGBP decreases viability of primary PBMCs

To determine whether the compounds have preferential effects on viability of malignant versus normal cells, we tested zoledronate and DGBP for toxicity against primary human peripheral blood mononuclear cells (PBMCs). In contrast to the pattern observed in the leukemia cell lines, zoledronate exhibited a stronger cytotoxic effect against the primary cells than DGBP (Figure 6C). The 72 hour IC_{50} of zoledronate against PBMCs was 63 μM while the IC_{50} for DGBP was 1200 μM. A therapeutic index was determined for each drug by calculating the ratio of the IC_{50} values in the leukemia cell lines versus PBMCs (Table 1), which demonstrates that in

contrast to zoledronate, which offers no selectivity, DGBP is much more selective (80 to 40 fold) against actively proliferating leukemia cells over resting primary blood cells. This finding also suggests that inhibition of FDPS by zoledronate results in cytotoxic effects in addition to the anti-proliferative effects caused by its depletion of GGPP.

GGPP is required for proliferation

To confirm target engagement in these cells, we performed add-back experiments by treatment of the cells with either of the two bisphosphonates for 72 hours in the presence or absence of exogenous GGPP or FPP. As expected, co-treatment with GGPP fully prevented the anti-proliferative effect of the GGDPS inhibitor, DGBP, whereas FPP did not. In these cells, treatment with GGPP resulted in a partial rescue of the zoledronate anti-proliferative effect, as did FPP (Figure 6D). Thus, zoledronate exerts its anti-proliferative effects in part via depletion of GGPP.

The combination of DGBP and zoledronate is antagonistic in Molt-4 cells

To determine if the combination of DGBP and zoledronate more strongly inhibits proliferation of Molt-4 cells, we treated cells for 72 hours with varied doses of the two compounds in a constant ratio determined by their respective potencies. Previously, in the K562 myeloid leukemia line we observed weak synergy between the two compounds (Dudakovic et al., 2008). However, in the Molt-4 T-cell leukemia line we observed strong antagonism with this combination (Figure 6E/F). Here, the combination index values at the experimental concentrations ranged from 2-5 (Table S1). Therefore, the use of dual inhibitors of the FDPS and GGDPS enzymes is not likely to result in enhanced inhibition of proliferation with respect to T-cell leukemias.

DGBP treatment alters protein expression and membrane association of RhoA, Rac and Rap1 but not Cdc42

We examined the effect of DGBP on levels of and membrane localization of a panel of geranylgeranylated proteins including RhoA, total Rac, Cdc42, and Rap1 (Figure 7A/B). Ras, expected to be predominately farnesylated, was used as a control. Treatment with DGBP increased protein expression of RhoA and Rap1 and decreased expression of total Rac (Figure 7C). These changes in protein expression caused by DGBP were prevented by co-incubation with GGPP. DGBP did not alter Cdc42 and Ras protein expression (Figure 7C). Treatment with zoledronate increased the expression of RhoA, which could not be rescued by GGPP co-incubation (Figure 7D). Zoledronate treatment did not appear to alter levels of Rac and Rap1.

As expected, a significant fraction of RhoA, Rac, Rap1 and Ras was membrane associated (Figure 7A/B). Cdc42 was primarily cytosolic. DGBP treatment increased the ratio of cytoplasmic to membrane-associated RhoA, Rac, and Rap1 but not Ras (Figure 7E). In DGBP-treated cells, this change in RhoA and Rap1 resulted from increased total protein which accumulated in the cytosolic fraction. However, the change in Rac localization was driven by decreased total protein levels which also were decreased in the membrane fraction (Figure 7G). The changes in Rac, RhoA, and Rap1 localization induced by DGBP treatment were restored upon co-incubation with GGPP.

Treatment with zoledronate altered Rap1 and Ras cytosolic to membrane ratios (Figure 7F). Although zoledronate reduced GGPP levels as evidenced by its effects on Rap1, zoledronate did not alter the cytosolic to membrane ratios of Rac or RhoA. Interestingly, zoledronate caused Cdc42 to be localized in the membrane while DGBP did not have that effect (Figure 7H). Co-incubation with GGPP restored the effect of zoledronate on Rap1 and Ras. Taken together,

treatment with DGBP broadly affects the expression and localization of geranylgeranylated proteins and does so with a different pattern of activity than zoledronate.

DGBP-induced inhibition of proliferation is not mediated by geranylgeranylated RhoA

This pattern of GTPase regulation in response to DGBP treatment initially led us to hypothesize that the anti-proliferative effects of DGBP were mediated by its effects on RhoA. We asked whether or not overexpression of RhoA could prevent the anti-proliferative effect of DGBP (Figure 8A). We expressed exogenous WT-RhoA and found it was unable to restore the anti-proliferative effect of DGBP. Because the plasmid WT-RhoA would also be geranylgeranylated and blocked by DGBP, we also expressed a mutated RhoA in which the CAAX motif (Hougland et al., 2009) was replaced with one signaling farnesylation (CVLS). Again, farnesylated RhoA was unable to block the anti-proliferative effects of DGBP, as DGBP decreased proliferation of cells transfected with RhoA-CVLS as well as those transfected with the pcDNA3.1+ (empty vector) (Figure 8A).

As it has been reported that active cytosolic RhoA can mediate effects of isoprenoid depletion in some systems (Zhu et al., 2013), we tested whether inhibition of Rho affects DGBP activity. Treatment with a cell permeable C3 transferase, which inhibits Rho activity and has low affinity for Cdc42 and Rac, had no effect on the proliferation in the presence of DGBP or GGPP (Figure 8B). Taken together, this implies that a Rho GTPase, including RhoA, is not the primary GTPase involved in the anti-proliferative effects of DGBP in this model.

DGBP decreases levels of active Rac

Because we observed that DGBP treatment strongly decreased levels of membrane-associated Rac (Figure 7), we assessed how DGBP treatment affects Rac activation as monitored by its GTP binding. We pulled down GTP-bound Rac1 using PAK1-conjugated GST beads and

determined levels of active GTP-bound Rac by Western Blot. GTP-bound Rac1 decreased with DGBP treatment (Figure 8C/D), and was restored to control levels with GGPP co-incubation, suggesting that GGPP depletion decreases the activity of Rac1. We found that NSC 23766, a Rac1 inhibitor, has similar effects on the proliferation as DGBP does (Supplemental Figure 1). Taken together, DGBP treatment reduces Rac1 expression, localization, and GTP binding.

DGBP induces apoptosis more potently than zoledronate

To determine whether the anti-proliferative effects of these bisphosphonates resulted from increased apoptosis, we analyzed annexin V and propidium iodide (PI) staining. Cells were treated with DGBP or zoledronate for 72 hours at varied concentrations. Both compounds increased the percentage of cells in late apoptosis (annexin V+/PI+) but not early apoptosis (annexin V+/PI-) (Figure 9A). Consistent with the proliferation experiments, DGBP was also more potent than zoledronate for induction of apoptosis, with a statistically significant difference observed when cells were treated with 30 μM of either agent (Figure 9A). In these experiments, co-incubation with GGPP rescued the ability of both bisphosphonates to induce late apoptosis (Figure 9B). FPP did not rescue the effect of DGBP, but did partially rescue zoledronate (Figure 9C).

Additionally, induction of apoptosis was examined by Western Blot analysis for the appearance of caspase 3 and caspase 7 cleavage products (Figure 10A/B). DGBP markedly increased both cleaved caspase 3 and caspase 7 at concentrations of 10 μM and 30 μM. In contrast, zoledronate treatment did not cause cleaving of these caspases at equivalent concentrations. However, zoledronate at 100 μM did induce cleaved caspase, but the magnitude of this effect was less than that of DGBP at significantly lower concentrations. Caspase activation by both bisphosphonates was prevented by co-incubation with GGPP (Figure 10C).

Next, we assessed whether the caspase activation was responsible for the anti-proliferative effect of DGBP. To this end, we treated cells with DGBP in the presence or absence of the pan-caspase inhibitor zVAD-FMK (Figure 10D). Again, DGBP dose- dependently inhibited proliferation which was fully blocked by co-incubation with the caspase inhibitor. Taken together, the mechanism by which DGBP and zoledronate reduce proliferation is by induction of caspase-mediated apoptosis, with DGBP exhibiting greater potency.

DGBP-induced apoptosis is mediated by ERK activation

Because a prior study had suggested that depletion of isoprenoids following treatment with an HMG-CoA reductase inhibitor led to alterations in kinase activity (Qi et al., 2013), we investigated the mechanism by which DGBP induces apoptosis by performing Western Blot analysis to detect phosphorylation of the mitogen activated protein kinases ERK, p38 kinase, and JNK. We were unable to detect any changes in phosphorylation of p38 or JNK (not shown), however treatment with DGBP increased phosphorylated ERK, which was prevented by addition of exogenous GGPP (Figure 11A/B). The increase in ERK phosphorylation was apparent at 10 and 30 μM concentrations of DGBP and 100 μM zoledronate, consistent with concentrations that induced caspase cleavage for both compounds. Additionally, co-incubation of GGPP with DGBP decreases levels of phosphorylated ERK (Figure 11A).

We next assessed whether DGBP-induced ERK phosphorylation could be blocked by PD98059, a MEK inhibitor. The induction of ERK phosphorylation by DGBP decreased by co-incubation with PD98059 (Figure 11C), demonstrating that MEK mediates DGBP-induced ERK phosphorylation. At the same time, ERK phosphorylation appears not to be upstream of caspases as the MEK inhibitor did not prevent the effect of DGBP on caspase cleavage (Figure 11C). To further assess the order of activation, we tested whether caspase inhibition would affect ERK

phosphorylation (Figure 11D). Again, cells treated with DGBP displayed high levels of cleaved caspase which was blocked by co-incubation with zVAD-FMK. DGBP-induced ERK phosphorylation was not altered by co-treatement with zVAD-FMK. This finding suggests that MEK activation leading to ERK phosphorylation is not downstream of caspase activation.

We then tested whether ERK phosphorylation was required for inhibition of proliferation and induction of apoptosis by DGBP. We treated cells with DGBP in the presence or absence of PD98059. As a single agent, PD98059 did not affect the cells at concentrations up to 100 μM for 72 h in either the proliferation or apoptosis assays. However, PD98059 was able to partially rescue the anti-proliferative effect (Figure 11E) and the pro-apoptotic effect of DGBP (Figure 11F). Therefore, MEK activity and ERK phosphorylation appears to contribute to DGBP-induced apoptosis.

Rac1 is partially involved in DGBP-mediated effects on viability

To determine whether DGBP-induced apoptosis relied more on RhoA or Rac1, we treated Molt-4 cells with NSC 23766, a Rac1 inhibitor, and Y-27632, a ROCK inhibitor. Treatment of Molt-4 cells with Rac1 inhibitor alone has no significant change with untreated cells. More importantly, NSC treatment in combination with DGBP increases the proliferation of Molt-4 beyond that of DGBP treatment alone (Figure S2). Thus, Rac1 inhibition interrupts the anti-proliferative effect of DGBP. The same ROCK inhibitor and Rac1 inhibitor conditions were used inhibitors were used with DGBP with no significance the DGBP-treated or DGBP and ROCK inhibitor treated conditions. Interestingly, DGBP treatment increased levels of active cdc42 which were ameliorated with GGPP addback (Figure S2). To test whether the PI3K pathway was involved, we investigated levels of phosphorylated Akt with DGBP treatment. DGBP decrease phosphorylated Akt, ableit only slightly (Figure S3). We further tested an MEK1/2 and ERK1/2

dual inhibitor, AZD-6244, and found that it robustly rescued DGBP induced apoptosis in the Molt-4 cells but not in the Jurkat cells (Figure S4). Overall, Rac1 is partially involved in DGBP-mediated decrease in cell viability.

Discussion

Here, we have demonstrated that zoledronate and DGBP inhibit proliferation of T-cell leukemia cells via blocking the intermediate enzymes of the mevalonate pathway. This leads to depletion of cellular GGPP, alterations in protein geranylgeranylation and expression, activation of caspases, and pro-apoptotic signaling through ERK. However, these two bisphosphonates, which have different molecular targets, differ in their potency, selectivity, and their effects on geranylgeranylated proteins.

DGBP inhibits proliferation and induces apoptosis at lower concentrations than zoledronate, which is consistent with results observed in a prostate cancer model, where DGBP also was more potent (Wasko et al., 2011). These results are surprising because zoledronate is approximately 10 fold more potent against purified FDPS than is DGBP against purified GGDPS (Wiemer et al., 2007). We believe the different pattern in cellular activity is a result of a combination of two factors- 1) higher lipophilicity of DGBP relative to zoledronate which enhances access to the cellular enzymes and 2) decreased ability of cells to overcome GGDPS versus FDPS inhibition (Wiemer et al., 2011). While both compounds are active in cells in the micromolar range, bisphosphonates achieve locally high bone concentrations which enable their effects *in vivo* (Fournier et al., 2008, Fournier et al., 2010).

Initially, we hypothesized that increased cellular potency of DGBP relative to zoledronate was due higher permeability compared to zoledronate. However, if cell permeability were the major issue underlying activity, then one might see a similar pattern of activity in the primary

PBMCs. But this pattern is reversed in PBMCs, with zoledronate being more toxic relative to DGBP. This finding argues that the differences in activity between the two compounds results from mechanistic differences caused by inhibition of their respective targets. Indeed, one advantage of targeting GGDPS is that its inhibition cannot be readily overcome by increased isoprenoid flux (Wiemer et al., 2011).

GGDPS inhibitors have two immediate effects- depletion of the product GGPP and elevation of the reactants isopentenyl diphosphate and FPP. In myeloid leukemia cells, we previously observed that co-incubation with GGPP was unable to mitigate all of the effects of DGBP and that elevated levels of FPP can contribute to the anti-proliferative mechanism (Dudakovic et al., 2008). This differs from the current study in which the effects of DGBP were fully rescued by GGPP. Furthermore, the apoptotic effect of DGBP could not be rescued by FPP. Interestingly, the apoptotic effect of zoledronate was only partially rescued by FPP and was nearly fully rescued by GGPP. Taken together, the apoptotic effects of DGBP and zoledronate in these cells are primarily due to GGPP depletion. Because FPP only partially rescued the effects of zoledronate, it is possible that zoledronate may affect GGDPS at high cellular concentrations. In a previous study, zoledronate did not inhibit purified GGDPS up to 10 μM (Wiemer et al., 2007). We predict that cell permeability is a barrier for entry resulting in lower increllular levels than are found in the media, but we cannot exclude the ability of zoledronate at 100 μM to inhibit GGDPS, especially given that GGPP rescues its apoptotic effect.

We observed membrane populations of Rac, RhoA and Rap1 but not Cdc42. GGDPS inhibition increased the cytosolic: membrane ratio of all of the membrane associated geranylgeranylated GTPases examined. Surprisingly, although zoledronate increased the cytosolic: membrane ratio of both Ras and Rap1, it did not significantly alter Rac or RhoA in this

manner, in contrast to a prior report that showed zoledronate caused cytoplasmic Rho accumulation (Chaplet et al., 2004). We found it interesting that Rac and Rho were only altered by DGBP. While it appears that the effect on Rap1 exceeds the effect on Rac and Rho, there is little Rap1 in the cytosol of untreated cells and nearly no change in the in the membrane fraction. In fact, of all the proteins examined, only the membrane fraction of Rac in response to DGBP was decreased, while the other proteins increased their cytosolic fractions. Although membrane association is not always a prerequisite for activity, it is commonly required for activity and its disruption is desirable (Cox et al., 2015, Mohammed et al., 2016, Hahne et al., 2012). Ultimately, the localization of many small GTPases was altered with either compound, indicative of engagement with their respective targets. Interestingly, DGBP treatment altered total expression of Rac, RhoA, and Rap1, albeit in different ways, with Rac expression decreased and RhoA and Rap1 expression increased. Clearly, different pathways must regulate the expression of these proteins.

Given the effects of DGBP on numerous geranylgeranylated proteins, we found it difficult to assess which specific GTPase, if any, is responsible for inhibition of proliferation. We predicted that RhoA was involved as the bulk of the literature suggests it often mediates proliferation (Agabiti et al., 2016), and a well-constructed study showed farnesylated RhoA rescued the effect of GGTase I depletion (Sjogren et al., 2007), but none of the Rho GTPases were involved in the anti-proliferative effects of DGBP. As an alternative, the Rac1 inhibitor caused a decrease in proliferation at a concentration similar to that of DGBP. Although NSC 23766 does not activate ERK (Figure S1), Rac may still be involved in DGBP-mediated apoptosis, as others have seen Rac1 is required for proliferation in response to GGTase I overexpression (Zhou et al., 2013).

How then, does DGBP lead to apoptosis? We hypothesized that MAPK signaling might be affected by changes in protein geranylgeranylation, and found that levels of phosphorylated ERK were altered by DGBP and, to a lesser extent, zoledronate. Therefore, to investigate the ERK pathway as a mechanism of apoptosis, we focused on DGBP, which increased ERK phosphorylation by several fold. This increase in ERK phosphorylation is in contrast to the effect seen in AML as proliferation is blocked by lovastatin and is dependent upon decreased ERK phosphorylation (Wu et al., 2004). There is some precedent for ERK involvement in apoptosis since ERK mediates apoptosis caused by cisplatin (Wang et al., 2000). While we could not establish a causal relationship between p-ERK and caspase, our data that shows DGBP-mediated apoptosis is partially rescued by a MEK inhibitor, suggesting that ERK involvement in apoptosis is late in the stages of apoptosis. Depleting GGPP alters GTPase localization which cleaves caspases leading to apoptosis and phosphorylates ERK also leading to cell death.

In conclusion, in order to use bisphosphonates to best achieve direct anticancer effects in the bone environment, the general strategy of targeting GGDPS likely compares well to targeting FDPS, which is exemplified by increases in cellular potency and selectivity of DGBP versus zoledronate. DGBP works by inhibiting prenylation of some small GTPases which leads to changes in their expression, caspase cleavage, MEK activation, ERK phosphorylation, and apoptosis. Thus, GGDPS inhibitors such as DGBP may produce greater single-agent anti-proliferative effects relative to zoledronate. Additionally, future studies should examine whether GGDPS inhibitors or their prodrugs (Wiemer and Wiemer, 2015) may be a viable strategy to targeting diseases in which Rac plays a role, given the strong reduction in Rac expression, membrane localization, and GTP binding seen with DGBP treatment.

Materials and Methods

Cells and reagents

The T-cell leukemia lines Molt-4 and Jurkat were obtained from ATCC (Manassas, VA). Human peripheral blood mononuclear cells were purified from whole blood obtained from Research Blood Components (Boston, MA) (Hsiao et al., 2014). Annexin-V FITC and propidium iodide were obtained from BD Biosciences (San Jose, CA) and eBioscience (San Diego, CA). GGPP and FPP were obtained from Cayman Chemical (Ann Arbor, MI). AZD-6244 was obtained from APEX Bio (Houston, TX, USA) Zoledronate was obtained from Fisher (Rockford, IL). DGBP was a kind gift from Dr. David Wiemer at the University of Iowa. FBS and other tissue culture supplies were obtained from Thermo Fisher. CellQuantiBlue was obtained from BioAssay Systems (Hayward, CA). zVAD-FMK was obtained from ApexBio (Houston, TX). PD98059 was obtained from LC Labs (Woburn, MA). C3 transferase was obtained from Cyotoskeleton (Denver, CO). Antibodies to ERK (L34F12) pERK (D13.14.4E), cleaved caspase 3 (5A1E), cleaved caspase 7 (D6H1), RhoA (67B9), Rac1/2/3 (polyclonal #2465), p-Akt (Ser473) (D9E) and Cdc42 (11A11) were obtained from Cell Signaling Technology (Danvers, MA). The antibody for beta-actin (Poly6221) was obtained from Biolegend. The anti-tubulin (E7) antibody developed by Michael Klymkowsky was obtained from the Developmental Studies Hybridoma Bank at The University of Iowa. pGEXTK-Pak1 70-117 was obtained from Addgene (Cambridge, MA).

Proliferation/viability assay

Assays were performed as described previously (Wiemer et al., 2013, Oblak et al., 2014, Li et al., 2016). Briefly, 10,000 cells/well of Molt-4 or Jurkat cells in log phase growth or

100,000 cells/well of PBMCs were added to 96-well plates in 100 µL in the presence of test compounds and fresh media. Cells were cultured for 72 hours. During the last 2 hours, cells were labeled with 10 µL of CellQuantiBlue reagent, and were scanned with a Victor plate reader (ex550/em600).

Analysis of apoptosis

Annexin V and PI analysis was performed according to manufacturer protocol (BD Biosciences) as described (Dudakovic et al., 2008). Treated cells were transferred to microcentrifuge tubes, centrifuged at 600 x g for 3 minutes, and then the supernatant was aspirated. Cells were resuspended in 100 µL of binding buffer (10 mM HEPES, 150 mM NaCl, 1 mM $MgCl_2$, 5 mM KCl, and 1.8 mM $CaCl_2$, pH 7.4) then transferred to polystyrene test tubes. Three microliters of FITC annexin V was added, and the cells were incubated for 15 minutes on ice. Two microliters of 50 µg/mL PI solution (Sigma-Aldrich, St. Louis, MO) was added to the cell suspension, and the suspension was mixed and analyzed using a FACSCalibur (BD Biosciences, Franklin Lakes, NJ).

Triton X-114 Separation

Membrane and cytosolic fractions were purified as described previously with some modifications (Bordier, 1981, Wasko et al., 2011). Briefly, cells were resuspended in media at a concentration of 0.75 million cells/mL and cultured for 48 hours with indicated concentrations of compounds or solvent controls. Cells were then spun at 600 x g for 3 minutes, washed with PBS, and resuspended in Triton X-114 lysis buffer (20 mM Tris pH 7.5, 150 mM NaCl, 1% Triton X-114) containing freshly added protease and phosphatase inhibitors including leupeptin (1µg/mL), aprotinin (1µg/mL), pepstatin (1µg/mL), and PMSF (200 µM). Lysate was passed through a 27-gauge needle and centrifuged for 15 minutes at 12,000 x g at 4°C. The resulting supernatant was

transferred to a new tube and incubated at 37°C for 10 minutes in a water bath. Following incubation, the lysate was centrifuged for 12,000 x g for 2 minutes at room temperature. Aqueous phase (upper) was transferred to a new tube and detergent phase (bottom) was diluted with excess buffer.

Western Blot Analysis

Cells were resuspended in fresh media at a concentration of 0.5 million cells/mL. Cells were cultured for 72 hours with indicated concentrations of test compounds or solvent controls. Cells were washed once in PBS and resuspended in lysis buffer (25 mM Tris–HCl pH 7.6, 150 mM NaCl, 1% NP-40, 1% sodium deoxycholate, 0.1% SDS) for 10 minutes on ice followed by centrifugation for 10 minutes at 10,000 x g. Lysis buffer contained a panel of freshly added protease and phosphatase inhibitors including leupeptin (1μg/mL), aprotinin (1μg/mL), PMSF (200 μM), sodium vanadate (200 μM), sodium pyrophosphate (10 μM), sodium fluoride (50 μM), and glycerophosphoric acid (10 μM) (all from Fisher). Proteins were quantified by BCA assay and equivalent masses were loaded onto 10% or 15% SDS-PAGE gels for separation. Proteins were transferred to nitrocellulose membranes and blotted with pERK, ERK, RhoA, Rac1, Cdc42, Rap1, pan-Ras, cleaved caspase 3, or cleaved caspase 7 antibodies. Proteins were visualized using a Licor Odyssey. Alexa-Fluor 680 goat-anti-mouse IgG and IRDye 800CW goat-anti-rabbit IgG were used for detection. Tubulin or beta-actin were used as a loading controls.

Rac1/cdc42 pulldown assay

E. coli (BL21) were transformed with pGEXTK-Pak1 70-117. 50 mL cultures in LB-AMP were grown for 14 hours. The culture was transferred to a flask of 750 mL of LB broth and treated with IPTG (1 mM) for 5 hours. Cells were pelleted by centrifugation and resuspended in

25 mL of lysis buffer (50 mM sodium phosphate, 300 mM NaCl, pH 8.0 with PMSF, aproptinin, leupeptin, pepstatin). The lysate was passed through a French press twice. The lysate was then allowed to bind to glutathione agarose beads overnight at 4º C (Pierce Thermo Scientific). GST beads were washed with equilibration buffer (50 mM Tris, 150 mM NaCl, pH 8.0) and stored at -80º C. Molt-4 cells were lysed according to the Western blotting protocol and the lysate was rotated at 4º C for 45 minutes. Beads were washed with equilibration buffer twice. Western blot procedure was implemented as described above.

Combination Index Analysis

Isobolograms were generated using Calcusyn software (Biosoft, Cambridge, UK). Combination index (CI) values were calculated according to the method of Chou and Talalay as described in the manual (Chou and Talalay, 1984). For each drug, 72-h IC_{50} values were determined by CellQuantiBlue assay. Concentration-response curves were generated for each compound and combination using four 80% dilutions.

RhoA overexpression

Human RhoA was amplified by PCR using the following primers designed to yield a C-terminal faneslyation sequence (-CVLS): 5'-GCT ATC GAA TTC ATG GCT GCC ATC CGG AAG A-3' (forward) and 5'-GCT ATC CTC GAG TCA GCT CAG CAC GCA ACC AGA TTT TTT CTT CCC A-3' (reverse). The amplicon was ligated into the pcDNA3.1(+) plasmid using the EcoRI and XhoI restriction sites. Prior to electroporation, Molt-4 cells were incubated overnight without antibiotics. Cells were then washed and resuspended in serum free media at 2.5 x 10^7 cells/mL. 20 µg of DNA was added to 400µL of cells for 10 minutes at RT. Cells were pulsed using the exponential protocol at 316 V and 500 µF and allowed to incubate at RT for 15 minutes. Cells were allowed to rest for 20 hours before selection with G418 at 400 µg/mL.

Statistical analysis

ANOVA (one-way) was used to calculate significance. Comparisons were done relative to the control or between pairs of conditions as indicated in the graphs. Columns in bar and line graphs represent the mean +/- standard deviation of the indicated number of experimental replicates. An α level of 0.05 was used as the level of significance.

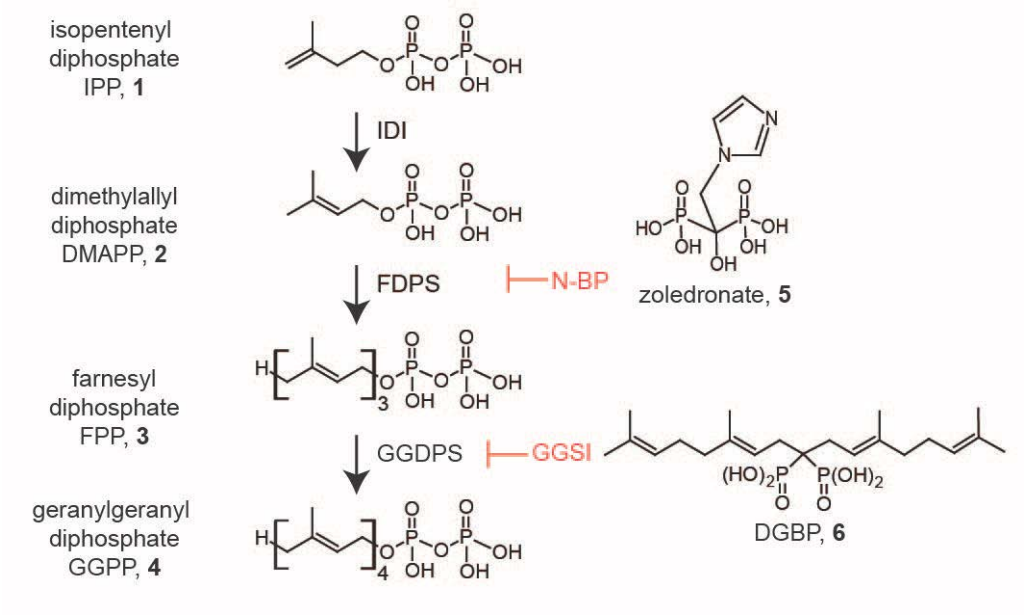

Figure 5. Biosynthesis of GGPP and known isoprenoid biosynthesis pathway inhibitors.

Bisphosphonates such as zoledronate and DGBP inhibit isoprenoid biosynthesis by targeting the enzymes FDPS and GGDPS, respectively. Isopentenyl diphosphate isomerase (IDI) catalyzes the isomerization of isopentenyl diphosphate (1) into DMAPP (2). FDPS then takes one equivalent of DMAPP and two equivalents of isopentenyl diphosphate to form FPP (3). This step can be inhibited by zoledronate (5). Geranylgeranyl diphosphate synthase (GGDPS) then catalyzes the condensation of FPP and isopentenyl diphosphate to form GGPP (4). This step can be inhibited by novel inhibitor DGBP, thus depleting levels of GGPP.

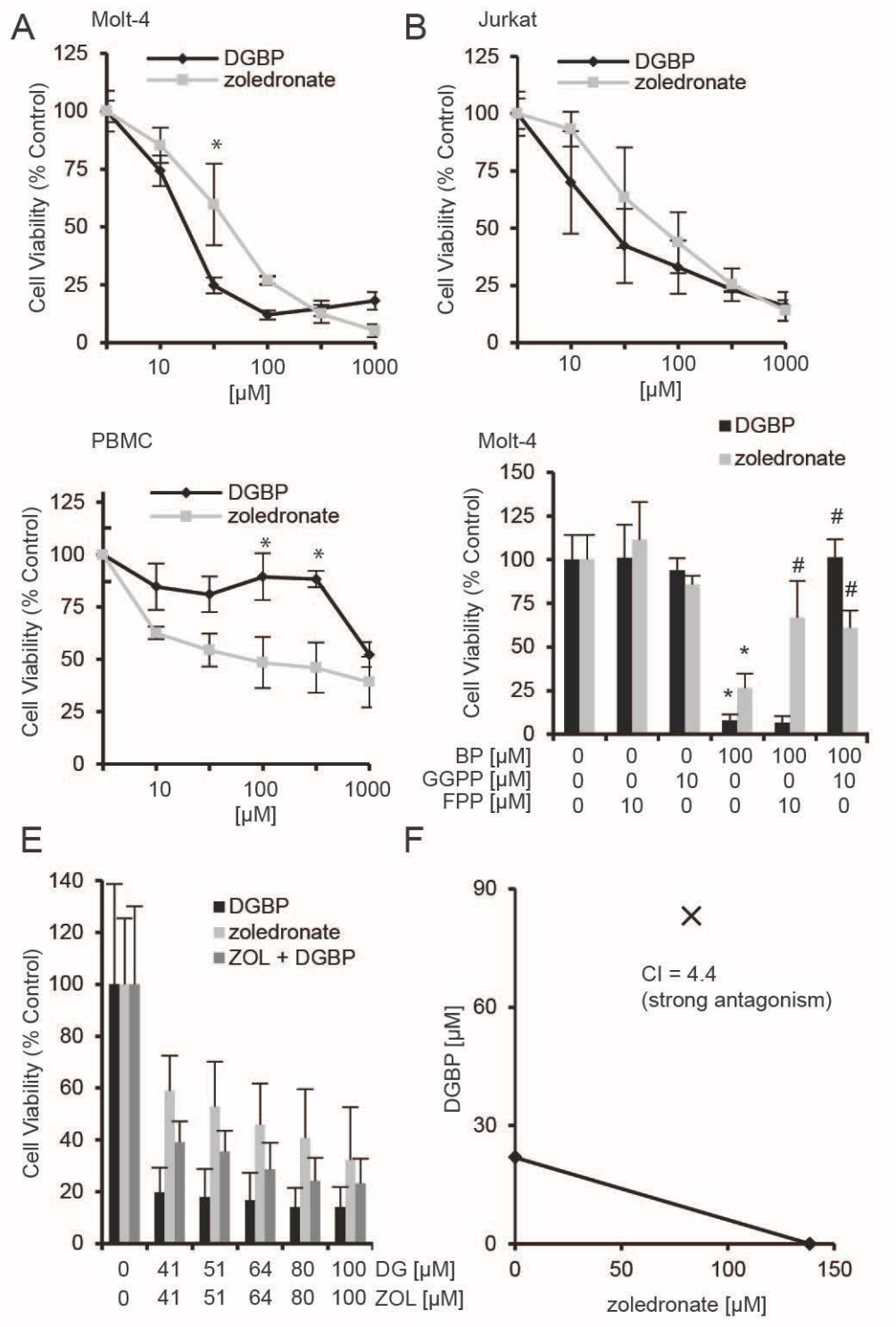

Figure 6. DGBP and zoledronate inhibit proliferation of malignant T lymphocytic cells through depletion of GGPP.

A-C) Dose response curves for Molt-4 and Jurkat cells, and PBMC, treated with either DGBP or zoledronate. Cells were incubated for 72 hours with compound. * indicates significant difference between the two compounds at the indicated drug concentration. D) Growth inhibition caused by DGBP is rescued by co-treatment with GGPP, and not rescued by FPP, while zoledronate is partially rescued by co-treatment with either GGPP or FPP. E) Proliferation of Molt-4 cells with DGBP in combination with zoledronate. F) Isobologram of DGBP with zoledronate. * indicates significant difference with respect to untreated control. # denotes significant difference from treatment with bisphosphonate alone. Statistical significance determined by ANOVA with $p<0.05$ as significant with Tukey's post-hoc analysis. $n = 3$ for all proliferation experiments.

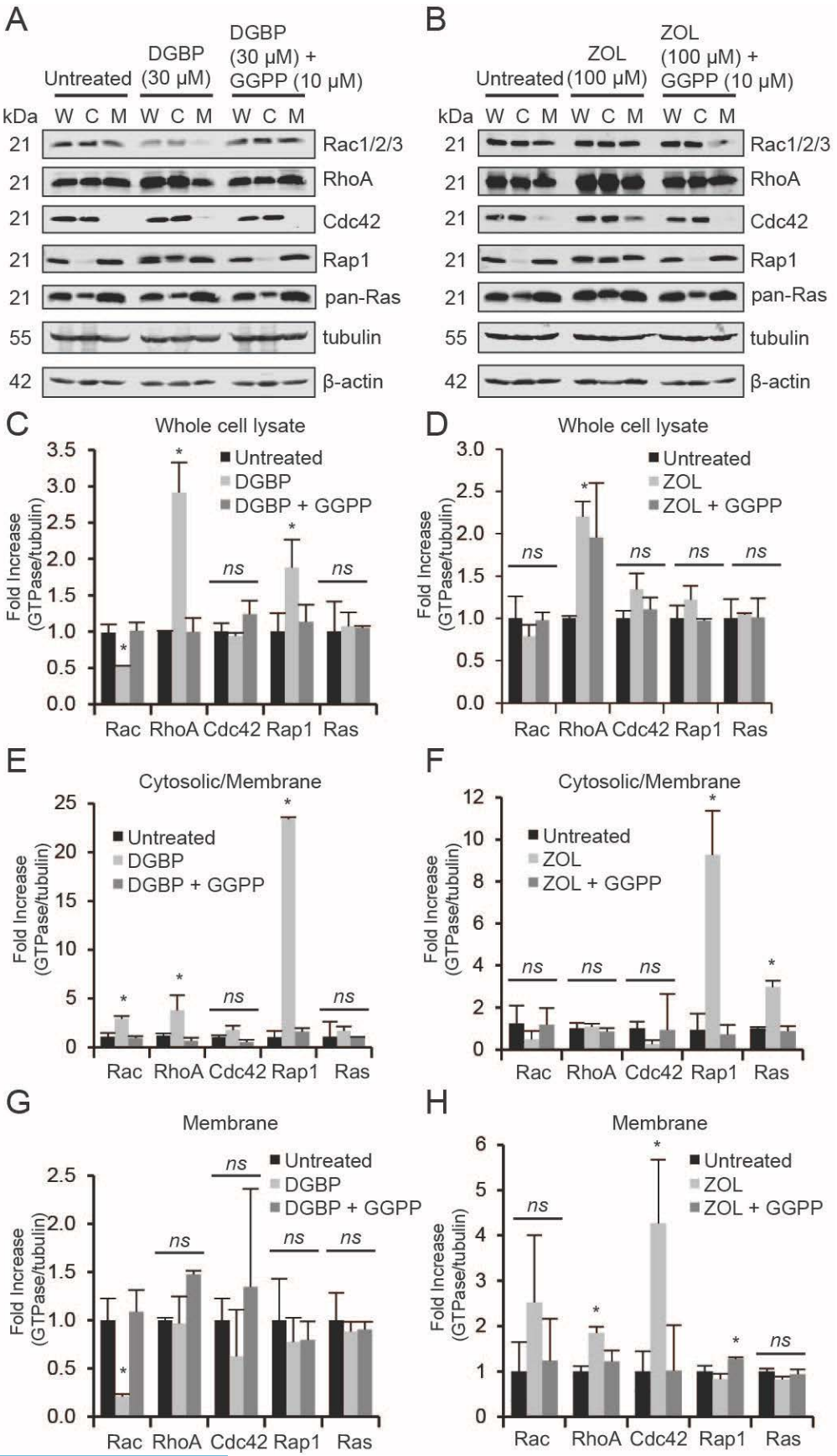

Figure 7. DGBP alters membrane levels of Rac but not RhoA or Cdc42.

A) Western blot of Rac1/2/3, RhoA, Cdc42, Rap1, and pan-Ras in Molt-4 cells treated with DGBP. "W" represents whole cell lysate, "C" represents the cytosolic fraction, and "M" represents the membrane fraction. B) Western blot of RhoA, Rac1/2/3, Cdc42, Rap1 and pan-Ras in Molt-4 cells treated with zoledronate and co-incubated with GGPP. C) Quantification of whole cell lysate fractions of small GTPases with DGBP. C) Whole cell lysate fractions of small GTPases with zoledronate. D) Cytosolic fractions vs. membrane fractions of cells treated with DGBP. D) Ratio of cytosolic fractions: membrane fractions of cells treated with zoledronate. E) Quantification of membrane fractions of Molt-4 cells treated with DGBP and GGPP on left and F) zoledronate and GGPP on right. All data represented as mean ± SD, n=3, *$p<0.05$ by ANOVA with Tukey's post-hoc analysis.

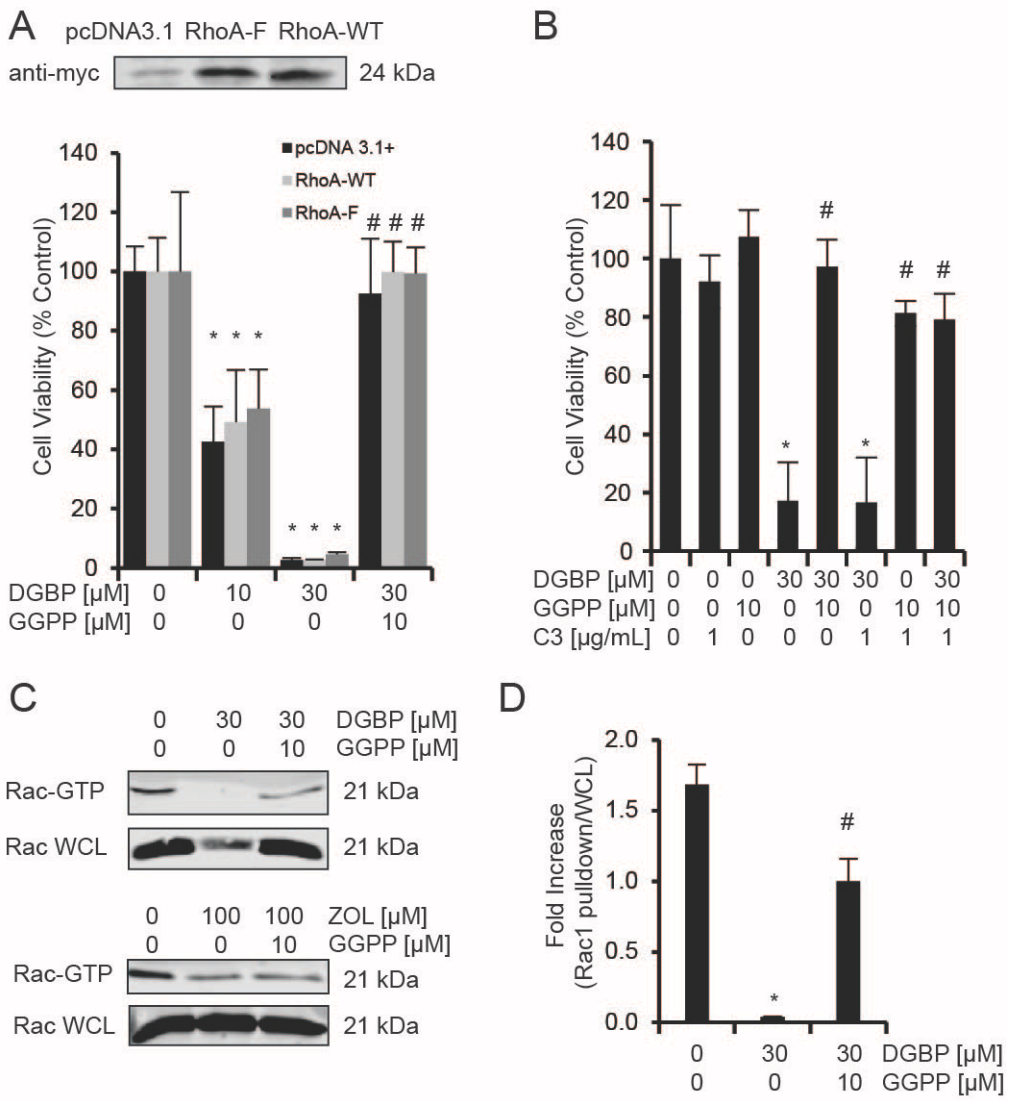

Figure 8. Neither Rho nor Rac is responsible for mediating the anti-proliferative effect of DGBP.

A) Farnesylated RhoA does not bypass the effect of DGBP. 72 hour proliferation of transfected Molt-4 cells. pcDNA3.1 represents the empty vector. Cells were treated with DGBP alone and DGBP with GGPP. B) Cells were treated with C3 transferase alone and in combination with DGBP and GGPP for 72 hours. Proliferation is determined by CellQB assay. *indicates significance with respect to untreated control. # denotes significant difference from treatment

with bisphosphonate alone. C) Western blot analysis of activated Rac1 pull-down. “WCL” represents the whole cell lysate. D) Quantification of Western blot analyses of Rac1 (right). Both quantifications were compared to whole cell levels of GTPase. All data represented as mean ± SD for n=3.

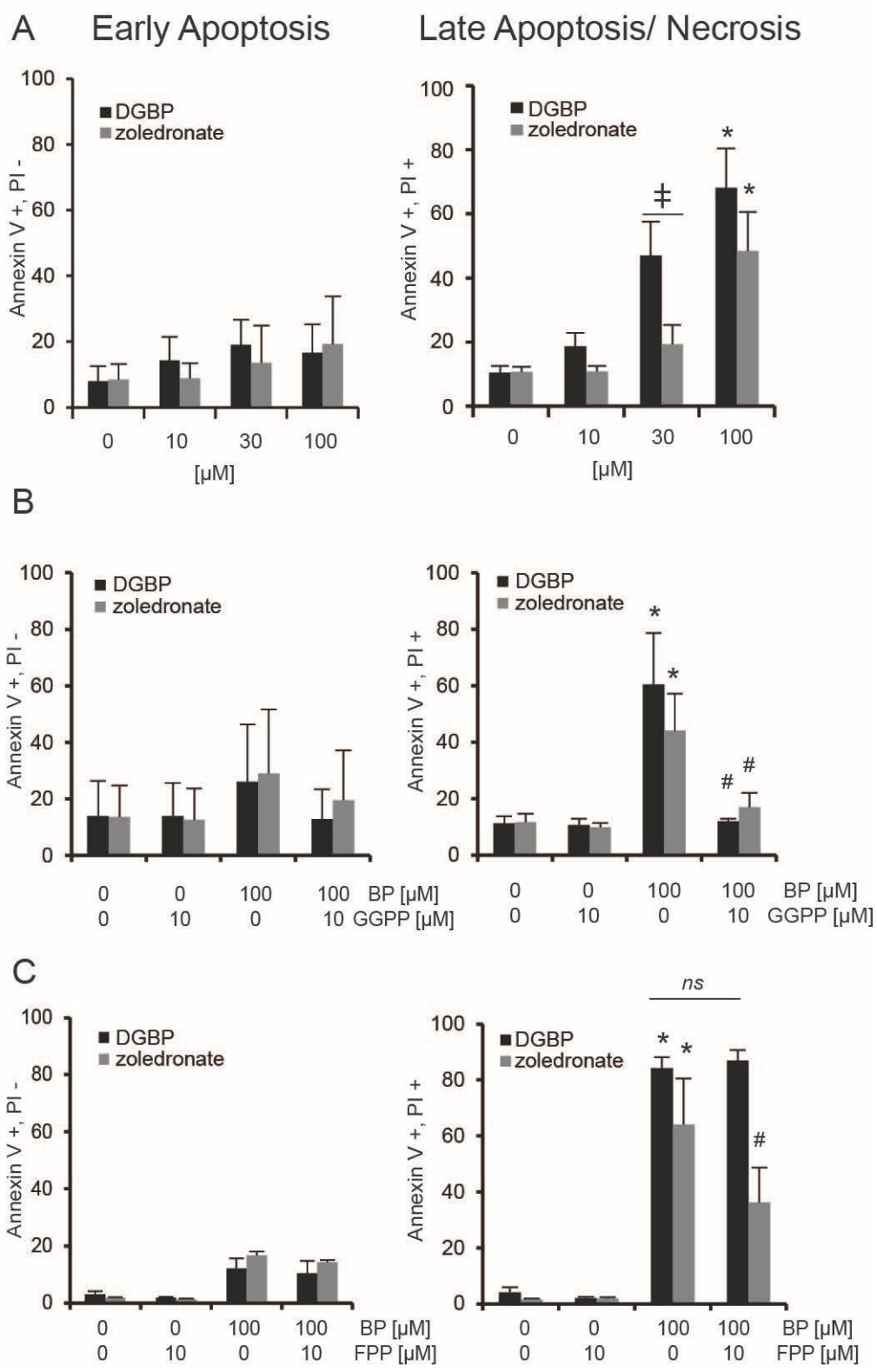

Figure 9. DGBP and zoledronate induce late apoptosis through depletion of GGPP.

A) Annexin V/PI staining of Molt-4 cells as determined by flow cytometry. Dose response of DGBP and zoledronate. Left: early apoptosis, right: late apoptosis. B) Bisphosphonates with co-incubation of GGPP. Cells were incubated for 72 hours with various concentrations of bisphosphonate. Left: early apoptosis, right: late apoptosis. C) Bisphosphonates with co-treatment of FPP. Left: early apoptosis, right: late apoptosis. All data represented as mean ± SD, n=3, * indicates significant difference with respect to untreated control conditions # indicates significant difference with respect to bisphosphonate treated conditions. ‡ denotes significant difference between indicated populations. Statistical significance determined by ANOVA with $p<0.05$ and with Tukey's post-hoc analysis.

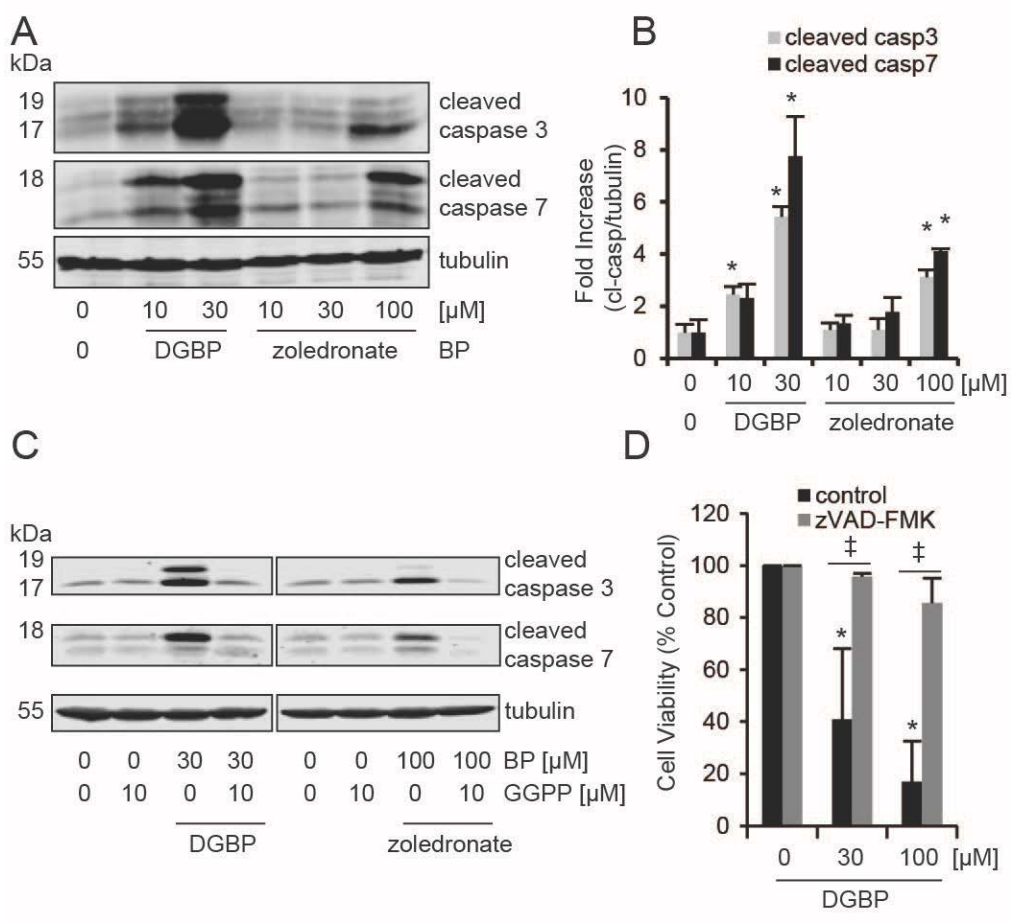

Figure 10. DGBP and zoledronate-mediated apoptosis is through caspase 3 and 7 cleavage.

A) Western blot of cleaved caspase 3/7 in Molt-4 cells with bisphosphate treatment. B) Caspase 3/7 cleavage is greater with DGBP than zoledronate. C) Caspase cleavage is rescued by co-incubation with GGPP. D) Proliferation of Molt-4 cells in presence of different concentrations of DGBP and 100 μM zVAD-FMK (pan-caspase inhibitor). In A, B, C, all data represented as mean ± SD, n=3, * indicates significant difference with respect to untreated control conditions. ‡ denotes significant difference between indicated populations. Statistical significance determined

by ANOVA with $p<0.05$ and with Tukey's post-hoc analysis. Data represented as mean ± SD and n=3.

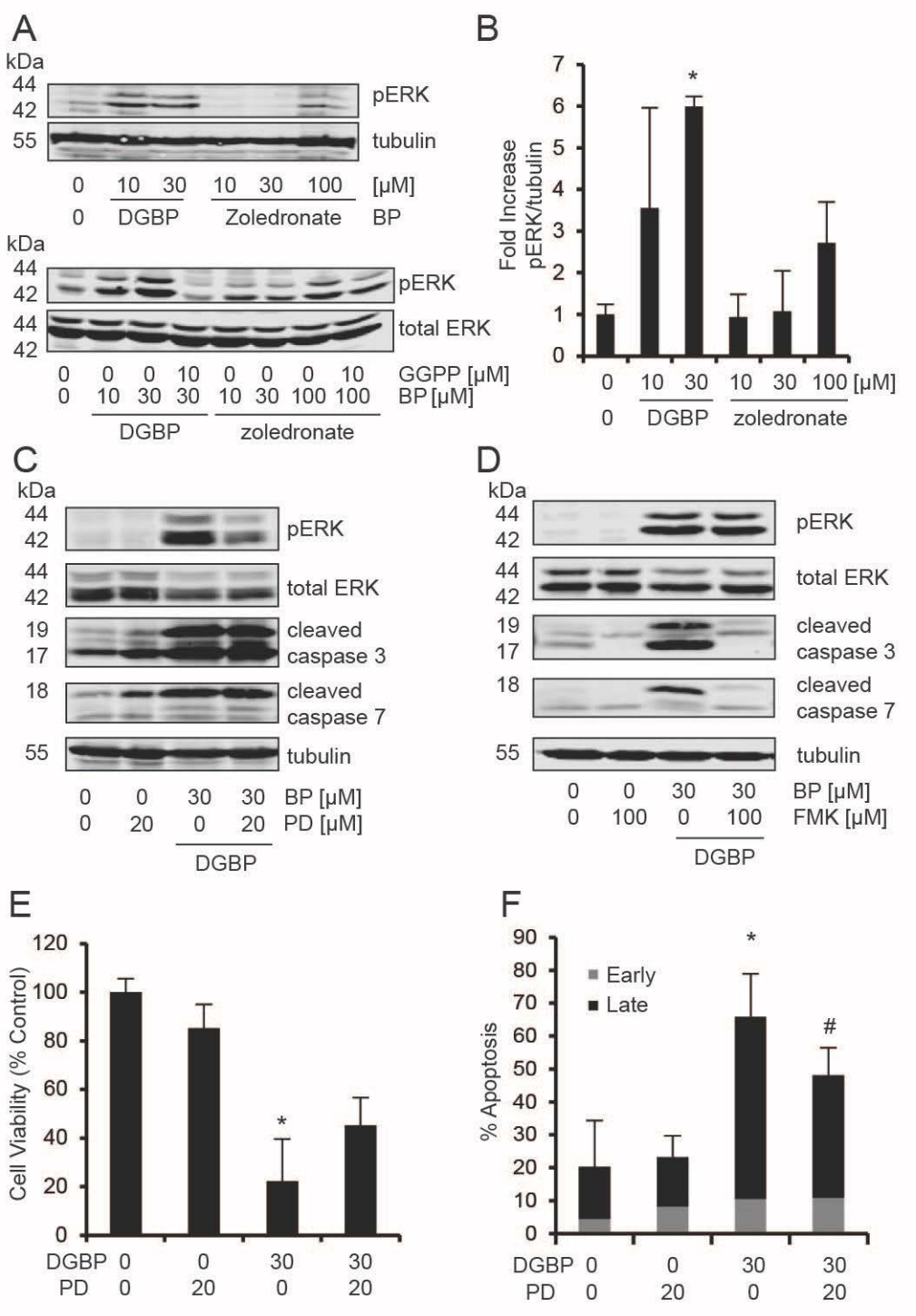

Figure 11. DGBP-mediated apoptosis is partially dependent on ERK.

A) Western blot showing ERK phosphorylation in Molt-4 cells treated with bisphosphonates. Data is representative of three independent experiments. B) ERK phosphorylation is dose-dependently increased by DGBP. The effect is greater with DGBP than with zoledronate. C) Western blot analysis of p-ERK, ERK, cleaved caspase 3 and 7 in response to DGBP and PD 98059. D) Western blot analysis of p-ERK, ERK, and cleaved caspase 3 and 7 in response to DGBP and zVAD-FMK treatment. E) Molt-4 proliferation with DGBP and PD 98059 (MEK inhibitor) treatment via viability assay. F) Molt-4 apoptosis with DGBP and PD 98059 treatment via flow cytometry. Annexin V+ and PI- represented by early apoptosis. Annexin V+ and PI+ represented by late apoptosis. All data in B, E, and F represented as mean ± SD, n=3. * indicates significant difference with respect to untreated control conditions. # indicates significant difference with respect to bisphosphonate-treated conditions. Statistical analysis done by ANOVA with Tukey's post-hoc analysis with $p<0.05$.

Tables

	IC_{50} (μM) (95% CI)			**Selectivity versus PBMC**	
	PBMC	Molt-4	Jurkat	**Molt-4**	**Jurkat**
DGBP	1200	15	30	**80**	**40**
	(480-3000)	(4.7-48)	(14-64)		
Zoledronate	63	52	81	**1.2**	**0.78**
	(32-120)	(37-74)	(46-140)		
Fold difference	*0.053*	*3.5*	*2.7*		

Table 1. Selectivity of DGBP and zoledronate for malignant versus primary cells.

DGBP (μM)	Zoledronate (μM)	CI
41	41	7.5
51	51	6.9
64	64	4.8
80	80	3.9
100	100	4.4

Table S1. Combination Index (CI) for experimental values of bisphosphonate combinations.

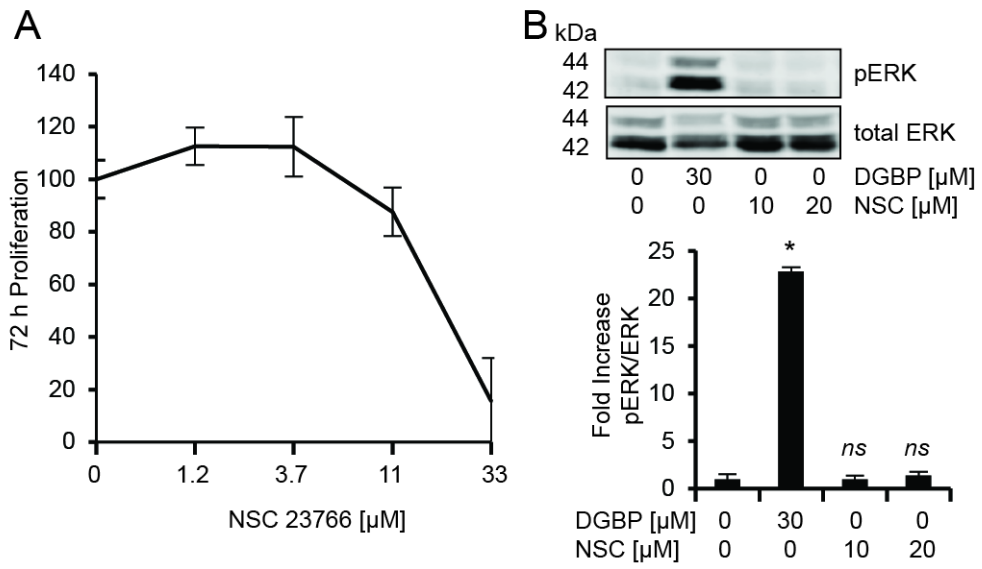

Figure S1. Rac inhibitor decreases proliferation but does not alter ERK phosphorylation.

A) Dose response of Rac inhibitor, NSC 23766, on proliferation of Molt-4 cells. Data is representative of five independent experiments B) Western blot analysis of p-ERK levels with NSC 23766 treatment. Data represents mean ± SD, n=3. * indicates significant difference with respect to untreated control conditions.

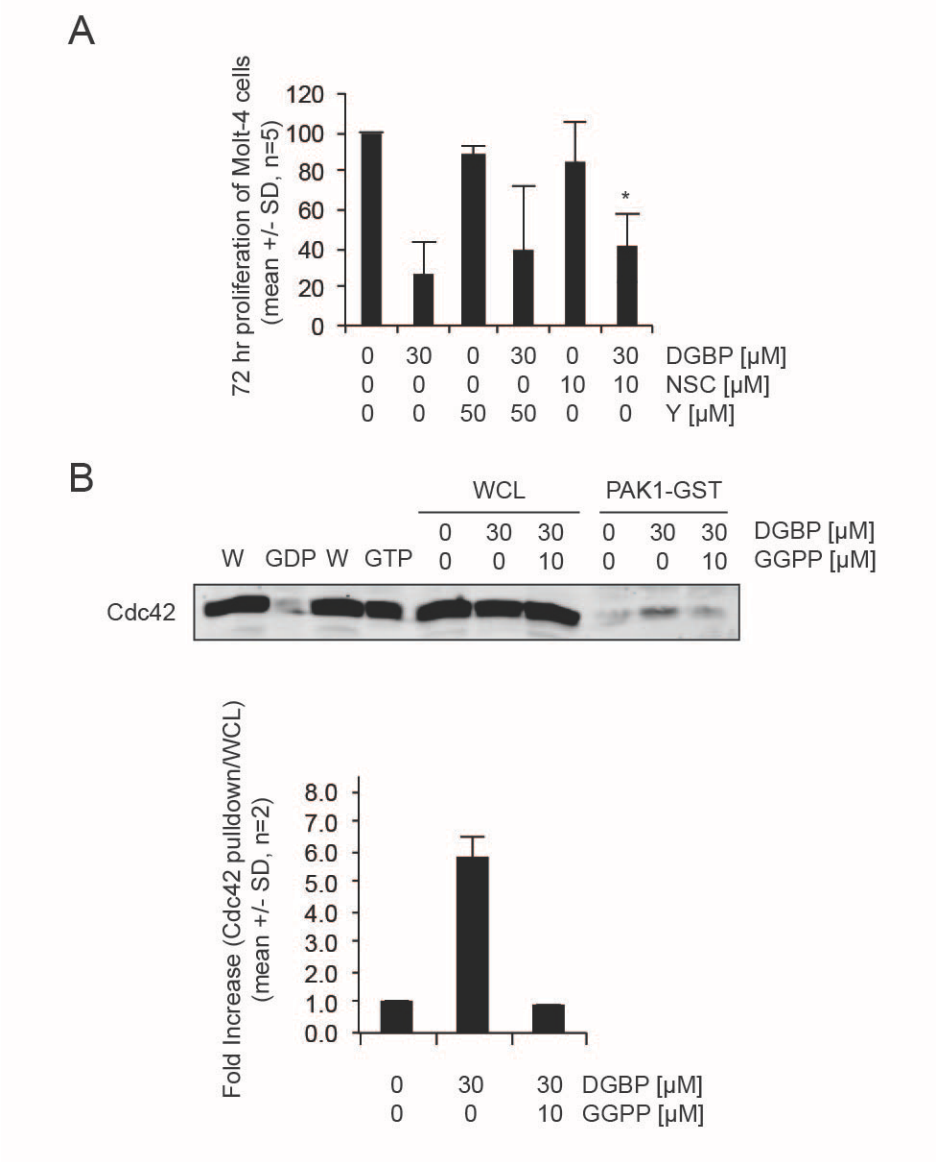

Figure S2. Rac1 inhibitor (NSC 23766) rescues the anti-proliferative effect of DGBP and DGBP increases levels of active cdc42.

A) Cells were treated with NSC 23766 alone, Y-27632 and in combination with DGBP for 72 hours. Proliferation is determined by CellQB assay. B) Western blot of PAK1-GST pull-down. "W" represents the whole cell lysate with GDP and GTP treated controls. "WCL" also represents the whole cell lysate input in treatment conditions. PAK1-GST represents pull-down conditions.

Quantification of pulldown shown below Western. *indicates significance with respect to bisphosphonate treatment.

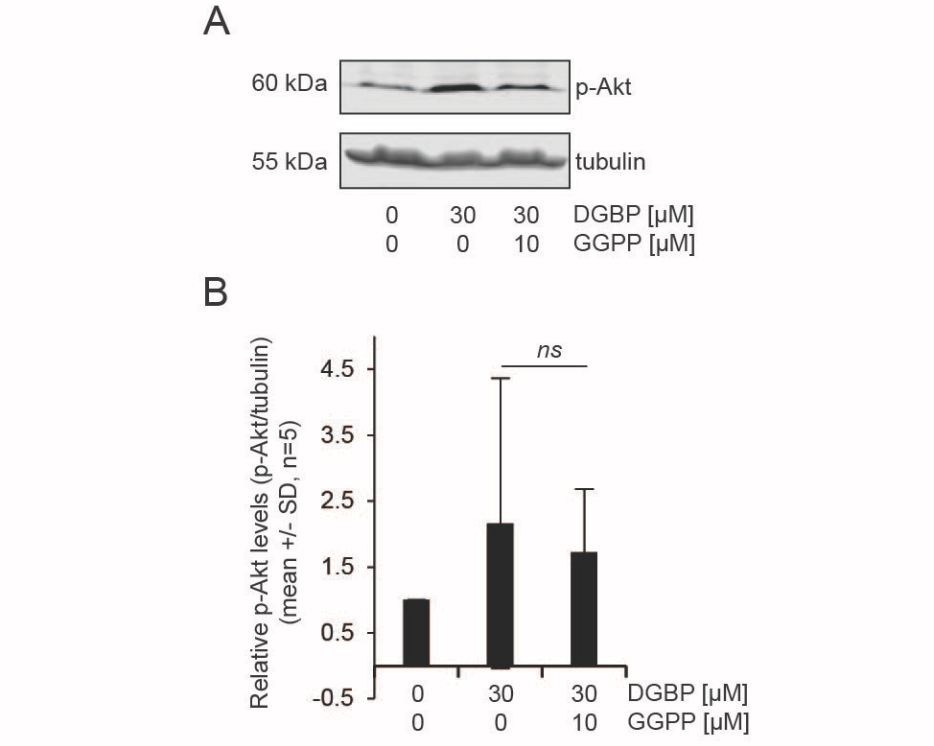

Figure S3. DGBP activates Akt.

A) Western blot analysis indicates increase in phosphorylated Akt upon treatment of DGBP (48 hours) which is partially rescued by addition of GGPP. B) Quantification of Western blot analyses.

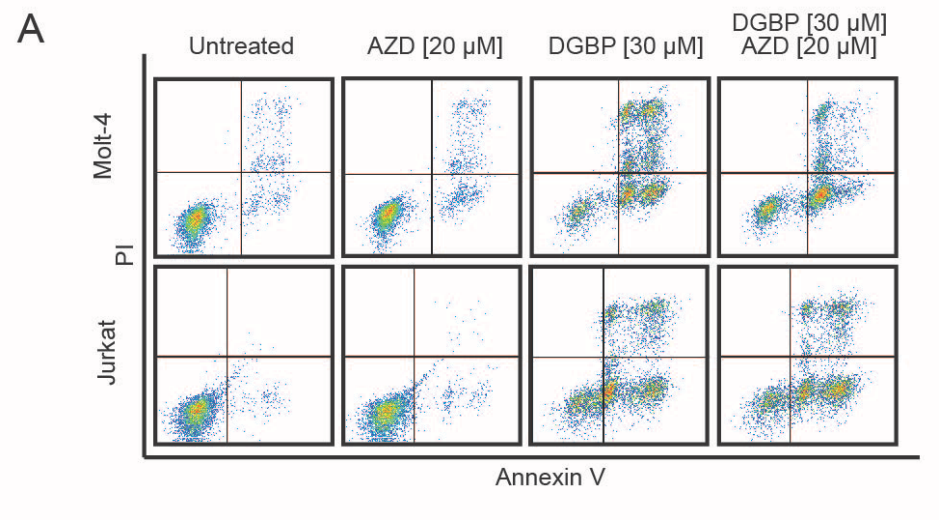

Figure S4. MEK/ERK 1 and 2 inhibitor, AZD-6244, rescues the effect of DGBP on apoptosis in Molt-4 cells.

A) Raw Annexin V and PI flow plots of Jurkat and Molt-4 cells treated for 72 hours with solvent control, AZD-6244, DGBP, and combination of AZD-6244 and DGBP.

CHAPTER 3. REGULATION OF THE NOTCH-ATM-ABL AXIS BY GERANYLGERANYL DIPHOSPHATE SYNTHASE INHIBITION

Abstract

Notch proteins drive oncogenesis of many cancers, most prominently in T-cell acute lymphoblastic leukemia (T-ALL). T-ALL, like many hematological malignancies, has high levels of DNA damage yet does not undergo DNA damage-induced apoptosis. We have identified and developed novel agents that induce apoptosis in T-ALL cells, which are selective inhibitors of the enzyme geranylgeranyl diphosphate synthase (GGDPS). Here, we show that GGDPS inhibition blocks Notch1 processing, preventing its transcriptional activity on c-myc and activating the DNA damage response. GGDPS inhibition circumvents the evasion of apoptosis through depletion of Notch1, activation of ataxia telangiectasia mutated kinase and of Abelson murine leukemia viral oncogene homolog 1 (ABL-1). Surprisingly, induction of apoptosis by GGDPS inhibition also is reduced by co-treatment with γ-secretase inhibitors. Inhibitors of γ-secretase and ataxia telangiectasia mutated, but not of GGDPS or ABL-1, promote Notch mRNA stability. Our results furthermore show that c-abl inhibitors reduce the cytotoxicity of DNA-damage inducing chemotherapy agents. These results provide a mechanism by which T-ALL cells use Notch1 to avoid DNA damage-induced apoptosis, which can be overcome by inhibition of GGDPS.

Introduction

T-cell acute lymphoblastic leukemia (T-ALL) is a rare but aggressive T-cell malignancy. T-ALL comprises approximately 15% of childhood and 25% of adult ALL cases (Pui et al., 2004). While the 5-year survival rate in children (80%) has improved significantly

due to advances in chemotherapy, survival in primary resistant and relapsed cases is still low (Sanchez-Martin et al., 2017), and many current therapies often cause toxicity in healthy cells. One of the most mutated genes in T-ALL is *NOTCH1*, which is altered in over 60% of T-ALL cases (Weng et al., 2004). Notch is also mutated in other types of cancer, such as breast, colon, lung and prostate cancer (Brzozowa-Zasada et al., 2017). However, its role in cancer is context dependent because Notch is oncogenic in some models but functions as a tumor suppressor in others (Radtke and Raj, 2003). Notch signaling is evolutionarily conserved and is required at multiple points in the developmental process and in particular in T-cell development (Andersson et al., 2011, Passaro et al., 2016). Notch is first processed in the Golgi by furin convertases (Brzozowa-Zasada et al., 2017). It is then transported to the plasma membrane where under normal circumstances it encounters its ligand (delta/serrate/LAG-2) (Olsauskas-Kuprys et al., 2013). Ligand binding promotes two cleavage events, one by Adam10 and the other by γ-secretase (Gordon et al., 2007). It has been proposed that Notch activation cannot occur without γ-secretase processing. Hydrolysis by γ-secretase processing releases the active form of Notch, the Notch internal domain (NICD), which can translocate to the nucleus, bind to transcription factors, and promote proliferation and differentiation (Sanchez-Martin and Ferrando, 2017).

Recent findings suggest a role for small GTPases in Notch processing. Court et al. showed a requirement of Rab7 and Rab8 in Notch1 signaling (Court et al., 2017), while Doi et al. found that Rap1 is essential in maturation of Adam10 (Doi et al., 2015). At the same time, we identified selective inhibitors of the enzyme geranylgeranyl diphosphate synthase (*GGPS1,* or GGDPS), which can be used to disrupt the function of these small GTPases (Wiemer et al., 2011, Wiemer et al., 2007, Agabiti et al., 2017, Shull et al., 2006, Wiemer et al., 2008a, Wiemer et al., 2008b). GGDPS is an enzyme in the isoprenoid biosynthesis pathway that produces

geranylgeranyl diphosphate (GGPP) whose lipid moiety is post-translationally attached to small GTPases such as Rab and Rap to promote membrane association (Agabiti et al., 2016). Thus, we hypothesized that disrupting small GTPase lipidation with a GGDPS inhibitor would affect Notch signaling and display beneficial growth inhibition in T-ALL. Because drugs such as statins and nitrogenous bisphosphonates deplete GGPP and are implicated as cancer therapeutics, it is important to understand the signaling pathways relevant to GGPP depletion. Throughout these studies we use an inhibitor of GGDPS, digeranyl bisphosphonate (DGBP), to directly deplete levels of GGPP. DGBP is not the most potent GGDPS inhibitor, as Haney et al. describes a GGDPS inhibitor with 30 nM cellular activity and Lacbay et al. with 0.14 μM activity against RPMI-8226 cells (Haney et al., 2018, Lacbay et al., 2018), DGBP has an IC_{50} of 200 nM and is well characterized making it useful for determining how GGPP depletion leads to apoptosis (Shull et al., 2006, Wiemer et al., 2007). Here, we describe the mechanism by which GGPP depletion downregulates Notch expression and function leading to apoptosis.

Results

Inhibition of GGDPS decreases expression of the Notch1 internal domain

A recent report demonstrated Rab GTPases regulate Notch processing (Court et al., 2017). Because Rab proteins are post-translationally geranylgeranylated, we asked whether or not geranylgeranylation inhibitors would affect Notch-dependent cells. We treated the T-ALL cell lines Molt-4 and Jurkat with the isoprenoid biosynthesis inhibitors lovastatin (HMG-CoA reductase), zoledronate (farnesyl diphosphate synthase), and digeranyl bisphosphonate or DGBP (Shull et al., 2006) (geranylgeranyl diphosphate synthase) to investigate the effect on cell viability. We also evaluated the γ-secretase inhibitor DAPT. Consistent with the literature (Rao et al., 2009, O'Neil et al., 2007), DAPT did not strongly impact cell viability (Figures 12A/B). In

contrast, both DGBP and lovastatin decreased cell viability with DGBP demonstrating the stronger effect. Zoledronate did not impact Molt-4 and Jurkat cell viability at concentrations up to 100 µM, even though it was more potent than DGBP in the osteosarcoma cell line U2OS, with activity at 10 µM (Supplementary Figure S5).

Because Notch is a critical oncogene, which drives proliferation of T-ALL cells, we evaluated these compounds in Western blots to determine the effect on Notch expression. Interestingly, of this panel only DGBP completely and dose-dependently decreased Notch1 protein expression and levels of the Notch1 NICD in Molt-4 cells (Figure 12C), although a slight reduction was observed following treatment with 10 µM of lovastatin. Increasing concentrations of DGBP also increased the amount of the unprocessed non-geranylgeranylated Rab7 GTPase as indicated by a slight upward shift in the apparent molecular weight (Figure 12C). These results were consistent in Jurkat cells (Figure 12D), though a slight decrease in NICD also was observed following treatment with 100 µM of zoledronate. Both cell lines were expected to be resistant to γ-secretase inhibition, and indeed no inhibitory effect was observed on the Notch1 NICD at concentrations up to 100 µM of DAPT in either cell line. But surprisingly, the addition of DAPT increased the levels of NICD, especially in the Jurkat cells. Taken together, inhibition of GGDPS by DGBP uniquely decreases Notch1 expression, prevents Rab processing, and impairs cell viability.

Notch depletion and cellular apoptosis induced by GGDPS inhibition are restored by γ-secretase inhibition

We had previously determined that co-incubation with the GGDPS product GGPP (immediate rescue) or the pan-caspase inhibitor Z-VAD-FMK (downstream rescue) could abrogate the effects of GGDPS inhibition on cell viability (Agabiti et al., 2017). Here we asked whether or not these two rescue agents would affect the ability of DGBP to decrease Notch

expression. Co-incubation of DGBP with GGPP abrogated the ability of DGBP to reduce Notch expression (Figure 13A). In contrast, co-incubation with Z-VAD-FMK did not impact the ability of DGBP to decrease NICD expression (Figure 13B), indicating that the impact of GGDPS inhibition on Notch expression is not a generalized nonspecific phenomenon downstream of caspase activation. In contrast, DGBP increased cleaved Notch4 and increased expression of the ectodomain shedding protease tumor necrosis factor-α-converting enzyme (TACE), an effect that also was dependent on GGPP (Supplementary Figure S6).

To determine whether or not GGDPS depletes Notch1 expression upstream or downstream of γ-secretase cleavage, we co-treated cells with the γ-secretase inhibitor (DAPT) in combination with DGBP. DAPT restored protein levels of Notch1 with DGBP co-incubation in both Molt4 (Figure 13C) and Jurkat cells (Figure 13D). Furthermore, both DAPT and a second γ-secretase inhibitor MK-0752 dose-dependently reduced the effect of DGBP on cell viability (Supplementary Figure S5). The effect of both γ-secretase inhibitors was more pronounced when cells were assessed for apoptosis using Annexin V staining (Figure 13E/F). Therefore, DGBP reduces Notch expression in a way that is dependent upon GGPP depletion and γ-secretase activity, but independent of caspase activation, and like GGPP and caspase inhibition, γ-secretase inhibitors reduce the effect of GGDPS inhibition on cell viability and apoptosis.

GGDPS inhibition decreases c-myc expression

We next sought to understand how reduced Notch expression caused by GGDPS inhibition would impact Notch signaling. Notch1 signaling affects transcription of a variety of genes, notably including c-myc (*MYC*), which promotes oncogenesis in T-cell leukemia (Sanchez-Martin and Ferrando, 2017, Weng et al., 2006). We treated Jurkat cells with DGBP and co-treated with GGPP or Z-VAD-FMK. GGDPS inhibition decreased levels of c-myc protein

expression, and co-treatment with GGPP restored the levels of c-myc (Figure 13G). Co-treatment with Z-VAD-FMK did not rescue the effect of DGBP on c-myc (Figure 13G), consistent with the pattern of activity that was observed with Notch1 expression. Co-treatment of DGBP with the proteasome inhibitor, MG132, did not rescue the effect of DGBP on c-myc depletion, consistent with transcriptional regulation of c-myc downstream of Notch1 rather than increased c-myc protein degradation (Figure 13G). Therefore, GGDPS-mediated Notch1 depletion reduces transcription of c-myc that is dependent on GGPP levels and is upstream or independent of cleaved caspases.

GGDPS inhibition increases the DNA damage response mediated by ATM

As c-myc transcription may not be the only underlying mechanism, we turned our attention to other consequences of Notch signaling. A recent report had demonstrated that Notch directly negatively regulates the DNA damage response (Vermezovic et al., 2015). The DNA damage response in Jurkat cells treated with DGBP is higher than that of primary T-cells treated with DGBP as demonstrated by phosphorylated histone H2A.X (Figure 14A). Because a well-constructed study by Vermezovic et al. found that Notch1 binds to the kinase regulatory domain of ataxia telangiectasia mutated (*ATM*), and prevents ATM activation (Vermezovic et al., 2015), we set out to determine if GGPP depletion regulates Notch1 to induce ATM activation and the DNA-damage response. We tested whether ATM was required for the apoptotic effects of GGDPS inhibition. Treatment of Molt-4 and Jurkat cells with Ku55933 (an ATM inhibitor) in combination with DGBP reduced the apoptosis induced by DGBP (Figure 14B). Therefore, GGDPS inhibition induces apoptosis via activation of the ATM-mediated DNA damage response.

c-abl mediates apoptosis induced by GGDPS inhibition in T-ALL

Because c-abl (*ABL-1*) is activated by ATM for DNA damage-induced apoptosis (Matt and Hofmann, 2016), we predicted that GGDPS inhibition would activate c-abl. To determine the role of c-abl in apoptosis induced by GGDPS inhibition, we co-treated cells with DGBP and the c-abl inhibitor imatinib and determined the degree of apoptosis by Annexin V staining. Interestingly, DGBP-induced apoptosis was blocked by imatinib (Figure 14C). An additional c-abl inhibitor, nilotinib, also reduced the apoptotic effect of DGBP in both the Molt-4 and Jurkat cells (Supplementary Figure S7). We knocked down c-abl expression using siRNA and treated cells with DGBP. Cells depleted of c-abl showed similar apoptosis with DGBP exposure as both non-transfected and scrambled cells exposed to DGBP (Figure 14D). Importantly, co-treatment with imatinib did not affect the ability of GGDPS inhibition to reduce Notch expression (Supplementary Figure S8), while co-treatment with DAPT did restore the effect of GGDPS inhibition on c-abl expression (Supplementary Figure S8), confirming that c-abl functions downstream of Notch in this system.

To determine how GGDPS inhibition affects c-abl protein expression, we treated Jurkat cells with DGBP and either GGPP, Z-VAD-FMK, or imatinib (Figure 15). DGBP treatment decreased the 120 kDa fraction of c-abl and increased expression of the active 60 kDa cleavage product of c-abl (Figure 16A-C). The effect on c-abl was rescued by co-treatment with GGPP (Figure 15A). Co-treatment with Z-VAD-FMK also reduced the effect of DGPB on c-abl expression, indicating that the effects on c-abl were dependent upon caspase activation (Figure 15B). While c-abl activation is thought to be upstream of cleaved caspases in some circumstances, cleaved caspases have been previously shown to at times cleave c-abl (Barila et al., 2003). Co-treatment with imatinib also restored expression of the 120 kDa form of abl and partially reduced expression of the 60 kDa form (Figure 15C). The pattern was also observed

with retinoblastoma protein (*RB1*) expression (Figure 15). The effect of DGBP on cleaved caspase 9 was fully rescued by GGPP and Z-VAD-FMK, but only partially rescued by imatinib co-treatment. The effect of DGBP on p-H2A.X was also rescued by GGPP, but not by Z-VAD-FMK or imatinib. Thus, DGBP allows for Jurkat cells to respond to DNA damage, leading to the phosphorylation of H2A.X, depletion of retinoblastoma protein, and stimulation of caspase-mediated c-abl cleavage.

c-abl is required for apoptosis induced by chemotherapy agents and DGBP

As c-abl is at the crux of DNA-damage response, we investigated the role of c-abl and imatinib in other common chemotherapies including: doxorubicin, cytarabine (AraC), and bortezomib. Both doxorubicin and cytarabine are used clinically for T-ALL therapy while bortezomib is a common chemotherapy that does not directly induce DNA damage. Both imatinib and nilotinib reduced the effects of DGBP in Jurkat and Molt-4 cells but not in Loucy cells (Figure 16). Additionally, imatinib and nilotinib reduced the effect of AraC on viability in all three cell lines. Imatinib and nilotinib did not rescue the effect of doxorubicin in Jurkat or Molt4 cells, but did reduce the impact of doxorubicin in Loucy cells. For bortezomib, imatinib and nilotinib rescued the effect on viability only in the Molt-4 cells. Taken together, in all of the cell line/c-abl inhibitor combinations tested, imatinib and nilotinib often reduced the effects of the chemotherapy agent and never increased their potency, supporting a role for c-abl in promoting cell death caused by these cytotoxic agents.

Secretase, ATM, and caspases, but not GGDPS or c-abl, control Notch mRNA degradation

Notch1 mRNA expression is regulated by miR-200 interaction with the Notch 3'UTR, which can be analyzed with a luciferase reporter construct that contains the luciferase gene flanked by the Notch1 3' UTR (Zhang et al., 2016). We assessed the ability of DGBP and its

viability rescue agents to affect the miR-200 mediated regulation of Notch1 mRNA degradation. Treatment with DGBP did not significantly alter Notch mRNA stability in this system (Figure 17A). However, treatment with DAPT, Ku55933, and to a lesser extent Z-VAD-FMK, decreased degradation of luciferase mRNA via the Notch 3' UTR leading to elevated luciferase activity. This data suggests that miR-200 not only regulates Notch, but also that miR-200 is itself regulated by ATM. No impact on luciferase expression was observed following treatment with imatinib.

GGDPS inhibition decreases expression of Notch1 in other hematological cell lines

To examine the relationship between GGDPS and the Notch-ATM-abl axis in patients, we analyzed publically available databases for these proteins. As expected, we observed that Notch mRNA expression is increased in T-ALL patients compared to bone marrow from healthy patients (Supplementary Figure S9) (Tang et al., 2017). Correlation was found between GGDPS and ATM normalized to Notch1 expression across different cancer populations (Supplementary Figure S9) (Tang et al., 2017). Also, Notch1 mutant cell lines displayed increased sensitivity to saracatinib, an abl kinase inhibitor, compared to wild-type cells, which further underscores the relationship between Notch1 and c-abl (Supplementary Figure S9) (Yang et al., 2013). Treatment with DGBP in various hematological cell lines revealed that DGBP reduces active Notch in cell lines expressing Notch (Figure 17B). In Loucy cells, there is reduced DGBP sensitivity (Figure 16), low Notch1 expression (Figure 6B), and no effect of DGBP on levels of active Notch (Figure 17B). RPMI-8226, HL-60, and K562 cells expressed active Notch1 which decreased with treatment of DGBP (Figure 17B). Daudi cells had no expression of Notch. Overall, even in non-T-ALL hematologic cell lines that express active Notch1, treatment with DGBP reduces Notch1 expression.

Discussion

Notch proteins are critical to development and progression of cancers including T-ALL, but disruption of Notch activity in T-ALL has been difficult to achieve. In this study, we demonstrate that inhibition of the enzyme GGDPS reduces expression of Notch and disrupts signaling through a Notch-ATM-abl pathway. DGBP is more potent than both DAPT and the other isoprenoid biosynthesis inhibitors at decreasing cell viability and levels of active Notch1 (Figure 12). These experiments provide evidence for conserved regulation of Notch by lipid synthesis, and disruption of this mechanism can impact Notch expression and viability of Notch dependent cells.

Because γ-secretase has been proposed as an anti-Notch target, we evaluated combinations of secretase inhibitors and DGBP to look for potential synergies. We surprisingly found that DAPT reduces the ability of DGBP to promote apoptosis and reduce NICD levels (Figure 13). Since Notch1 binds to the long range enhancer region to allow for the transcription of c-myc, and c-myc contributes to the oncogenicity of T-ALL, we tested whether DGBP would decrease c-myc levels. We found that DGBP decreased levels of c-myc in a manner than was not proteasome dependent, suggesting that DGBP decreases myc in a transcriptional manner (Figure 14). Because Notch1 also functions in ways that are non-transcriptional, we investigated the effect of Notch1 on DNA damage response and found that co-treatment with ATM and c-abl inhibitors rescued the effect of DGBP on apoptosis (Figure 14). Furthermore, DGBP activates ATM to induce DNA damage response which is upstream of cleaved caspase 9. Cleaved caspase 9 is upstream of retinoblastoma depletion and cleaved c-abl (Figure 15). Abl inhibitors mitigate the anti-proliferative effects, not only of DGBP, but also of relevant chemotherapy agents (Figure 16). Finally, we see that Notch1 mRNA degradation is regulated by DAPT and Ku55933

(Figure 17). But we do find that DGBP regulates Notch1 mRNA levels, therefore it is likely that DGBP alters Notch1 transcription (Supplementary figure S10). Further experiments are required to understand how DAPT plays a role in DGBP-mediated Notch1 transcriptional decrease and whether or not Notch1 regulates its own transciption. Ultimately, our results show that DGBP modulates the Notch1 signaling pathway to both regulate transcription of myc and initiate the ATM-dependent DNA damage response pathway to induce apoptosis.

Using GGDPS inhibitors to target Notch signaling may be a promising therapeutic strategy because small GTPases such as Rab are natively involved in Notch processing. While direct inhibitors of γ-secretase may prevent Notch signaling in some cases, certain mutations may confer insensitivity. While mutations in Molt-4 and Jurkat cells such as loss of PTEN are well known (Palomero et al., 2007), the finding that DAPT can reduce the impact of DGBP treatment is suggestive of the idea that it is not mutations in PTEN that confer lack of sensitivity but rather the binding conformation of the γ-secretase inhibitor to the γ-secretase complex. Because small GTPases such as Rab11, Rab7, Rab8, and Rap1 are involved in both normal and mutant Notch1 processing, disrupting small GTPase function via inhibition of GGDPS allows for Notch1 disruption even in the event of mutations to Notch1.

How then does GGDPS inhibition deplete active Notch while a γ-secretase inhibitor, DAPT, induces active Notch1 expression in Molt-4 and Jurkat cell lines? DAPT is a non-transition state inhibitor of the γ-secretase complex suggesting that it does not bind to the active site of the γ-secretase complex protease presenilin-1, but rather to an allosteric site within presenilin-1 (Olsauskas-Kuprys et al., 2013). Because there are mutations along the transmembrane region of Notch1 (Forbes et al., 2017), the binding conformation of the mutated alpha-helix may be different from the wild-type. Binding of DAPT in these cases may allow for

allosteric modulation rather than inhibition of the catalytic domain. Interestingly, there is overlap between the reported binding site of DAPT on presenilin-1 (aa372-467) (Dumanchin et al., 1999) and the binding site of Rab11 on presenilin-1 (aa374-400) (Morohashi et al., 2006). Perhaps binding of DAPT mimics binding of Rab to enable secretase processing of Notch1- though further experiments would be needed to confirm this hypothesis.

There is strong evidence in favor of the idea of repurposing isoprenoid biosynthesis inhibitors such as lovastatin and zoledronate for anti-cancer applications because zoledronate is currently used in the clinic for metastatic bone disease and because we and others have found that these inhibitors lead to apoptosis (Carter and Botteman, 2012, Fournier et al., 2008). Originally developed for non-cancer applications, these widely prescribed drugs have generated much interest for their potential anti-cancer properties. For example, a very recent article showed that statins could sensitize leukemia cells to venetoclax, a BCL-2 inhibitor, in a way that is dependent upon GGPP depletion (Lee et al., 2018). Interestingly, we observed GGDPS inhibition to affect Notch more strongly than the related clinical agents lovastatin and zoledronate, which target HMG-CoA reductase and farnesyl diphosphate synthase respectively (Pandyra et al., 2014, Wiemer et al., 2011). One potential explanation for this phenomenon is that, unlike GGDPS, both HMG-CoA reductase and farnesyl diphosphate synthase are under transcriptional control through cholesterol levels (Pandyra et al., 2015), which can mitigate the effects of these agents (Dudakovic et al., 2011, Brown and Goldstein, 1997). Alternatively, there may be a difference in rates of compound uptake, such as endocytosis, depending on cell line. As zoledronate has a higher charge:mass ratio than DGBP, its cellular entry is more likely to require endocytosis (Thompson et al., 2006).

Here, we show that DGBP targets Notch1 signaling with a two-fold effect: 1) decreased transcription of the c-myc oncogene, and 2) induction of the ATM mediated DNA damage response. C-myc is a well-known downstream target of Notch1 in T-ALL (Sanchez-Martin and Ferrando, 2017, Sharma et al., 2006, Weng et al., 2006). Because NICD binds to ATM and prevents its activation, Notch is directly involved in DNA damage response (Vermezovic et al., 2015). DGBP treatment depletes the Notch internal domain, which may free ATM to become activated. Active ATM phosphorylates H2A.X, a marker for DNA damage (Matt and Hofmann, 2016). We propose that GGPP depletion does not directly increase DNA damage, but rather allows for cells to recognize the level of DNA damage upon release of ATM inhibition by Notch. ATM ultimately activates cleaved caspases and initiates apoptosis (Korwek et al., 2012). Caspases will cleave retinoblastoma protein, which sits on the catalytic domain of c-abl and prevents its activation (Wang et al., 2001). There is some precedence for Notch involvement in retinoblastoma protein degradation as a γ-secretase inhibitor, which decreases active Notch, regulates retinoblastoma to exit the cell-cycle (Rao et al., 2009). Furthermore, lovastatin and nitrogenous bisphosphonates have been shown regulate retinoblastoma protein via induction of hypophosphorylation (Reszka et al., 2001). This reduction in retinoblastoma levels allows for caspases to cleave c-abl (Barila et al., 2003, Machuy et al., 2004), thereby depleting the 120 kDa c-abl protein. Since siRNA to c-abl did not rescue the effect of DGBP and since cleaved caspases deplete the 120 kDa c-abl, we predict that the 120 kDa c-abl is important to maintaining cell viability. While c-abl may be important in caspase initiated apoptosis, c-abl depletion in and of itself does not affect apoptosis. Perhaps this indicates the requirement of other signaling components such as retinoblastoma cleavage for c-abl to exert its effect.

Ultimately, these data indicate the connection between disruption of geranylgeranylation and induction of apoptosis in T-ALL.

While we have found that GGPP depletion regulates Notch1 expression and signaling, we found that GGPP depletion does not affect Notch1 mRNA degradation. miR-200 interacts with Notch signaling in cancer stem cells in breast cancer (Shimono et al., 2015) and pancreatic cancer (Xu et al., 2017). Interestingly, only DAPT and Ku55933 increase levels of Notch1 mRNA degradation. We predict that both of these inhibitors act through ATM inhibition. Ku55933 directly inhibits ATM, while DAPT indirectly decreases ATM activation by increasing active Notch1 and its subsequent binding to and inhibition of ATM. If ATM inhibition regulates Notch mRNA degradation, then it is not surprising that DGBP does not increase levels of Notch mRNA degradation because DGBP allows for the activation of ATM.

In summary, GGDPS inhibition provides an alternate means of depleting active Notch1 to activate DNA-damage induced apoptosis. The effect of GGDPS inhibition on Notch1 signaling can be restored by co-incubation with a γ-secretase inhibitor. GGPP depletion ultimately allows for the activation of ATM and the induction of DNA-damage induced apoptosis through cleaved caspases and cleaved c-abl.

Materials and Methods

Supplies and Materials

The cell lines Jurkat, Daudi, and HL-60 were obtained from ATCC (Manassas, VA, USA) prior to 2012. Molt-4 cells were obtained from ATCC in 2012. K562 cells were obtained from Sigma Aldrich (Saint Louis, MO) in 2012. RPMI-8226 cells were obtained from Coriell Institute (Camden, NJ) in 2013. U2OS cells were obtained from ATCC in 2014. Cells were cultured in media containing RPMI-1640, 10% FBS, and Pen/Strep. Loucy cells were obtained

from ATCC in 2017 and cultured in T-cell media (RPMI-1640, 10% FBS, penicillin/streptomycin, non-essential amino acids, sodium pyruvate, 0.0004% 2-mercaptoethanol, 10 mM HEPES pH 7.5). Cells were grown for at least two weeks after thawing before experimental use, and replaced with a fresh early passage stock after no more than three months. GGPP, DAPT, and coelenterazine were obtained from Cayman Chemical (Ann Arbor, MI, USA). DGBP was a generous gift from Dr. David Wiemer at the University of Iowa, Iowa City, IA. Z-VAD-FMK was obtained from ApexBio (Houston, TX, USA). Imatinib, nilotinib, and Ku55933 were obtained from LC laboratories (Woburn, MA, USA). Bortezomib was from Fisher. FITC-conjugated annexin V was obtained from Biolegend and propidium iodide was obtained from Fisher.

Retinoblastoma protein (C-2) and c-myc (C-33) antibodies came from Santa Cruz (Santa Cruz, CA, USA). Notch4 (A-12) and TACE (B-6) antibodies were obtained from Santa Cruz (Santa Cruz, CA, USA). Cleaved caspase 9 (Asp330) (D2D4) and p-H2A.X (S139) (20E3) antibodies were from Cell Signaling Technologies (Danvers, MA). β-actin (Poly 6221) and c-abl (8E9) antibodies were obtained from Biolegend (San Diego, CA, USA). The antibody for the Notch1 internal domain (bTAN20) was purchased from the Developmental Studies Hybridoma Bank (deposited by Artavanis-Tsakonas (Zagouras et al., 1995)). The antibody for actin (JLA20) was obtained from the Developmental Studies Hybridoma Bank (deposited by Lin, J.J. (Lin, 1981)).

The siRNA for c-abl and a negative control were obtained from Sigma. pCIneoRL-Notch1 3'UTR was purchased from Addgene (plasmid # 84595) (deposited by Yanan Yang (Zhang et al., 2016)).

Apoptosis analysis

Cells were seeded at 100,000 cells/mL and incubated for 72 hours. Cells were transferred to microcentrifuge tubes and centrifuged at 600 g for 3 minutes. After the supernatant was aspirated, cells were resuspended in 200 µL of binding buffer (10 mM HEPES, 150 mM NaCl, 1 mM $MgCl_2$, 5 mM KCl, and 1.8 mM $CaCl_2$, pH 7.4) and transferred to polystyrene test tubes. Two microliters of PI solution was used for each condition, while three microliters of annexin V were used for each condition. Cells were mixed by vortexing and data was acquired using a BD Fortessa and analyzed by FlowJo.

Cell Viability

Jurkat, Molt-4, and Loucy cells in log growth were seeded at 100,000 cells/mL in 96 well plates in 100 µL and incubated for 72 hours in the presence of compounds and fresh media. 10 µL of CellQuantiBlue reagent was added per well for 2 hours and scanned on a Victor5 Perkin Elmer (Waltham, MA, USA) plate reader (ex550/em600).

Electroporation

Jurkat cells were grown in RPMI + FBS media without antibiotics overnight and seeded at 10 x 10^6 cells/ mL. Cells were washed in RPMI and resuspended in RPMI media at 25 x 10^6 cells in 0.4 mL for each condition. Cells were incubated with DNA for 10 minutes before electroporation with a BioRad Gene Pulser Xcell at 316 V and 500 µF. Cuvettes were tapped 12 times and incubated at room temperature before adding to pre-warmed media. After 24 hours, cells were resuspended at 1x 10^5 and selection agent was added.

Luciferase assay

After electroporation, Jurkat cells were seeded at 1 x 10^5 in 24 well plates and treated with compounds. After 72 hours, cells were centrifuged at 600 x g for 3 minutes and washed

with PBS. Cells were lysed with Renilla lysis buffer (0.5x PBS, 0.025% NP-40, 1% EDTA (w/v), and freshly added 5 μM coelenterazine) and sonicated in a water bath and immediately read on Victor5 Perkin Elmer (Waltham, MA, USA) plate reader for counts per second. BCA assay was carried out to determine total protein concentration (Pierce).

Whole Cell Lysis

Cells were seeded at 250,000 cells/mL and incubated for 72 hours. Cells were transferred to conical tubes for centrifugation at 600 x g for 3 minutes. Cells were washed with PBS and lysed with Whole Cell Lysis buffer (50 mM Tris pH 8.0, 2% SDS, 150 mM NaCl) then sonicated in a water bath. Lysates were then heated at 95°C on heating block and passed through 27 ½ gauge syringe. Protein quantification was determined using a BCA assay (Pierce).

Western Blotting Analysis

Western blotting was performed as previously described. Briefly, cells were resuspended in media at 250,000 cells/mL for 72 hours with test compounds or solvent controls. Cells were then washed with PBS and lysed in RIPA buffer (25 mM Tris-HCl pH 7.6, 150 mM NaCl, 1% NP-40, 1% sodium deoxycholate, 0.1% SDS) or Lysis buffer without SDS (25 mM Tris-HCl pH 7.6, 150 mM NaCl, 1% NP-40, 1% sodium deoxycholate) either containing freshly added protease and phosphatase inhibitors including aprotinin (1 μg/mL), leupeptin (1 μg/mL), pepstatin (1 μg/mL), PMSF (200 μM), sodium vanadate (200 μM), sodium diphosphate (10 μM), sodium fluoride (50 μM), and glycerophosphoric acid (10 μM). Cells were lysed for 10 minutes on ice and centrifuged for 10 minutes at 4°C at 14,000 x g. The supernatant was taken out and quantified by BCA assay (Pierce, Waltham, MA, USA). 1X SDS was added to the sample and the sample was then heated for 4 min at 95°C with vortexing. Equivalent masses were loaded onto 7.5% or 12% bis-acrylamide gels depending on protein size. Proteins were transferred to

nitrocellulose membranes, blocked with BSA, and blotted with primary antibodies. Alexa-Fluor 680 goat-anti-mouse IgG and IRDye 800CW goat-anti-rabbit IgG were used as secondary antibodies.

Gene Database Correlation and Drug Sensitivity Analysis

The multiple gene correlation analysis for ATM and GGPS1 was obtained from the Gene Expression profiling Interactive Analysis (GEPIA) online database (http://gepia.cancer-pku.cn/) (Tang et al., 2017). ATM and GGPS1 expression were normalized to NOTCH1 expression. The data for these primary tumor samples and normal samples were acquired from The Cancer Genome Atlas (TCGA) and the Genotype-Tissue Expression (GTEx) data sets. The drug sensitivity data was derived from the Genomics of Drug Sensitivity in Cancer Project (https://www.cancerrxgene.org/) (Yang et al., 2013).

Real time RT Polymerase Chain reaction (RT-PCR)

Cells were seeded at 100,000 cells/ mL in 5 mL. Cells were incubated with appropriate compounds for 72 hours. Total RNA was isolated with the TRIZOL (Invitrogen) according to the manufacturer's protocol. The forward primer for Notch1 was: 5'AAT GCC TGC CTC ACC AA3'. The reverse primer for Notch1 was: 5' CCA CAC TCG TTG ACA TCC T3'. The forward primer for 18S was: 5' TAA GTC CCT GCC CTT TGT AAC ACA 3'. The 18S reverse primer was: 5' GAT CCG AGG GCC TCA CTA AC 3'. RNA levels were determined with Nanodrop and cDNA was made using MMLV reverse transcriptase according to the manufacturer's protocol. SYBR green protocol was used according to the manufacturer's protocol on a 7500 Applied Biosystems PCR machine. Relative mRNA levels were determined by $2^{-\Delta\Delta Ct}$ values.

Statistical Analysis

One-way ANOVA was used to determine statistical significance. Control conditions were compared to treatment conditions or between pairs of conditions indicated in the graphs. An α of 0.05 was used to establish significance. Bar and line graphs represent mean ± SD. Experiments were replicated at least 3 times as indicated n = 3).

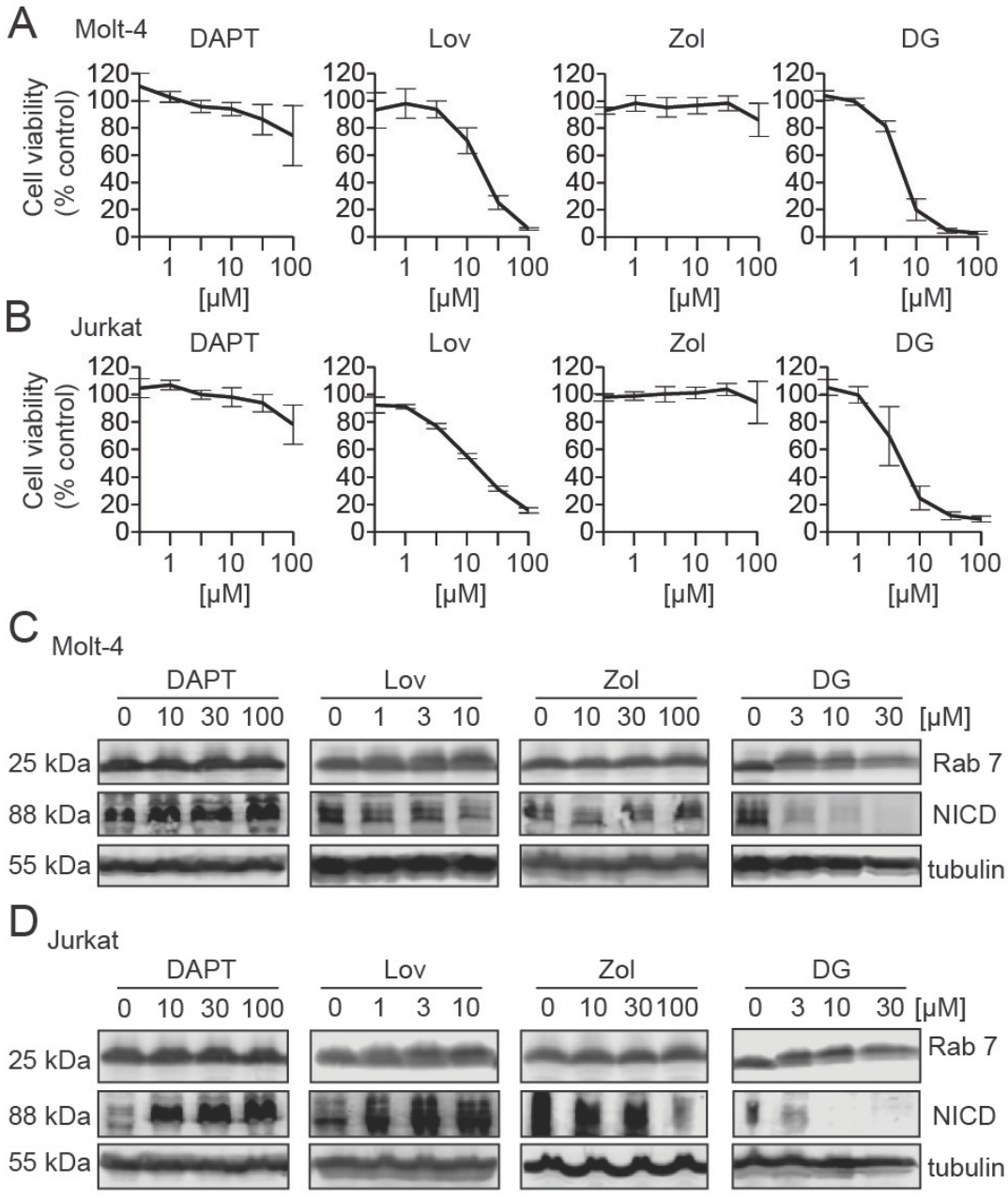

Figure 12. DGBP impacts Rab7 processing, decreases NICD protein levels and decreases cell viability.

A-B) Cell viability of Molt-4 (A) and Jurkat (B) cells after 72 hours treatment with DAPT, lovastatin, zoledronate, or DGBP. Graphs display means and standard deviations of three independent experiments for each compound and cell line. C-D) Western blots for Rab7 and

NICD after 72 hours treatment with various concentrations of the γ-secretase inhibitor DAPT (GSI), the HMG-CoA reductase inhibitor lovastatin (Lov), the farnesyl diphosphate synthase inhibitor zoledronate (Zol), and the geranylgeranyl diphosphate synthase inhibitor DGBP (DG) in Molt-4 (C) and Jurkat cells (D). Tubulin is shown as a loading control. Blots are representative of 3 independent experiments.

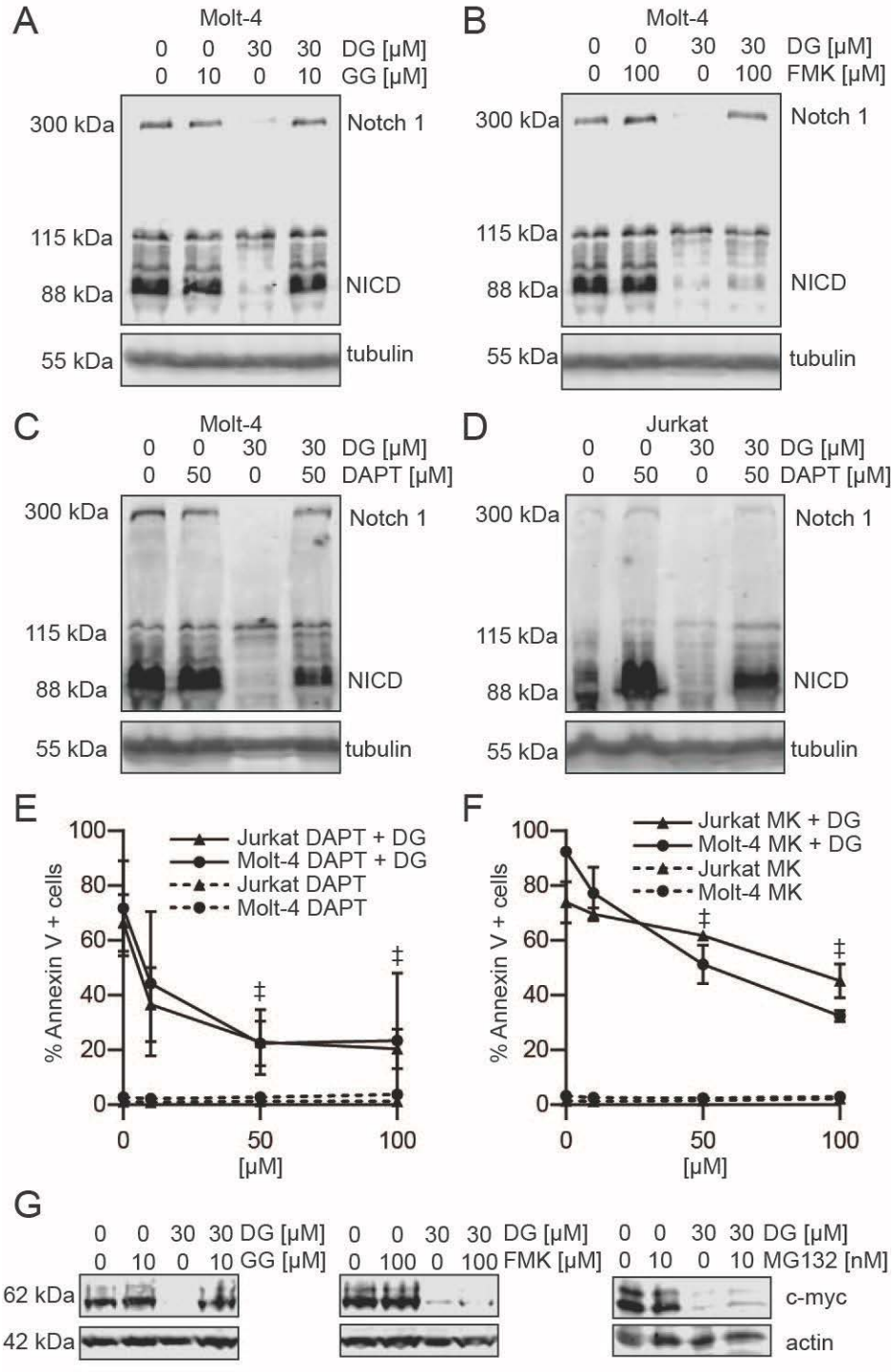

Figure 13. Secretase inhibitors rescue the effect of DGBP on NICD expression and apoptosis.

A-B) Western blot of full-length Notch1 and NICD in Molt-4 cells following 72 hour treatment with DGBP and co-treatment with or without either the GGDPS product GGPP (A) or the caspase inhibitor Z-VAD-FMK (B). Tubulin is shown as a loading control. C-D) Western blots of Notch1 and NICD after 72 hour treatment with DGBP and co-treatment with or without DAPT in Molt-4 (C) and Jurkat (D) cells. E-F) Annexin V staining of Molt-4 or Jurkat cells treated with DGBP and co-treated with or without (E) DAPT or (F) MK-0752 for 72 hours. G) Western blots showing c-myc with DGBP treatment and co-treatment of GGPP, Z-VAD-FMK, and MG1332. Actin is shown as a loading control. All Western blots are representative of three independent experiments. Graphs represent means and standard deviations of 3 independent experiments. Statistical significance was determined by ANOVA. *$p < 0.05$ versus untreated controls.‡$p < 0.05$ versus DGBP treated condition.

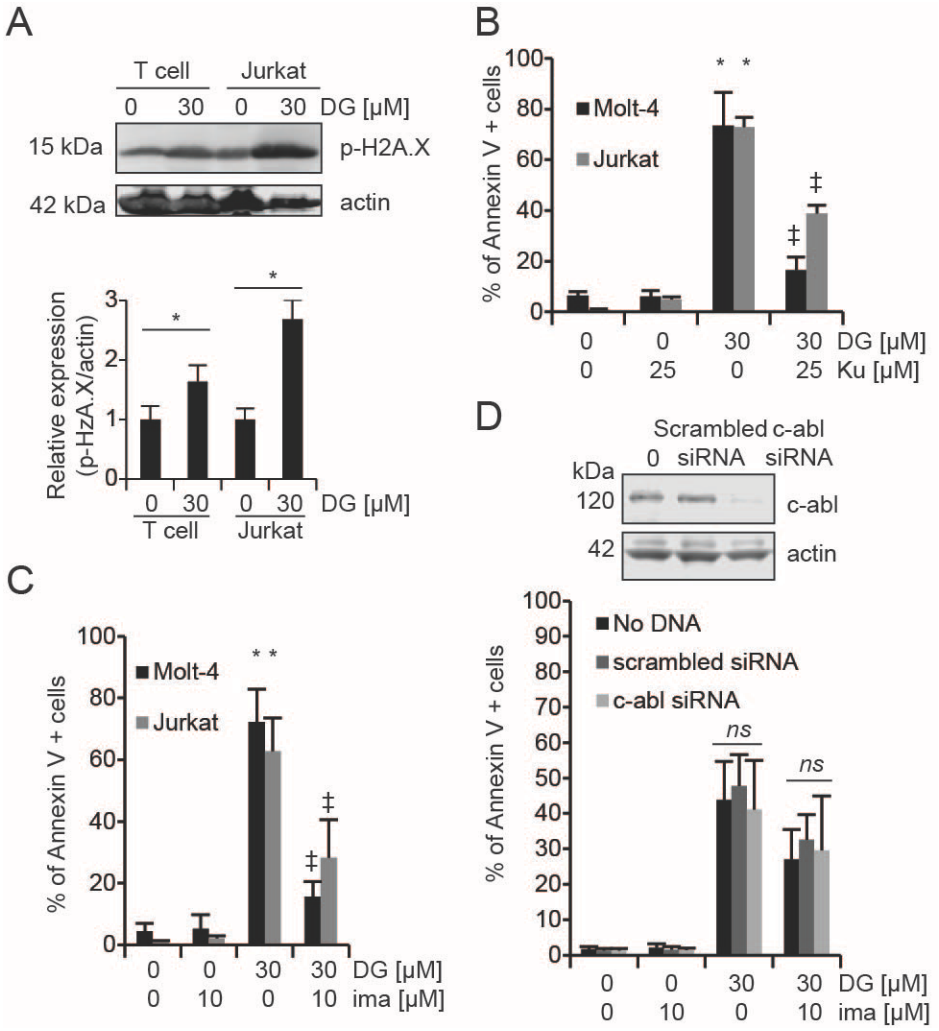

Figure 14. DGBP-induced apoptosis is mediated by ATM and c-abl downstream of Notch.

A) Western blot analysis of phosphorylated H2A.X in either expanded primary T-cells or Jurkat cells after 72 hours of treatment with DGBP, with actin shown as a loading control. B) Annexin V staining showing 72 hour DGBP treatment along with co-treatment with or without the ATM inhibitor Ku55955 in Molt-4 and Jurkat cells. C) Molt-4 or Jurkat cells were treated with DGBP with or without imatinib for 72 hours and assessed by Annexin V staining. Flow plots shown are representative of three independent experiments. D) Western blot of c-abl with electroporated

control with no DNA, scrambled siRNA and siRNA to c-abl. Annexin V staining for cells with electroporated without DNA, scrambled siRNA, and c-abl siRNA treated with imatinib, DGBP, or co-treatment with imatinib and DGBP. The bars represent means and standard deviations of three independent experiments (n=3). *$p < 0.05$ versus untreated controls. ‡$p < 0.05$ versus DGBP treated condition.

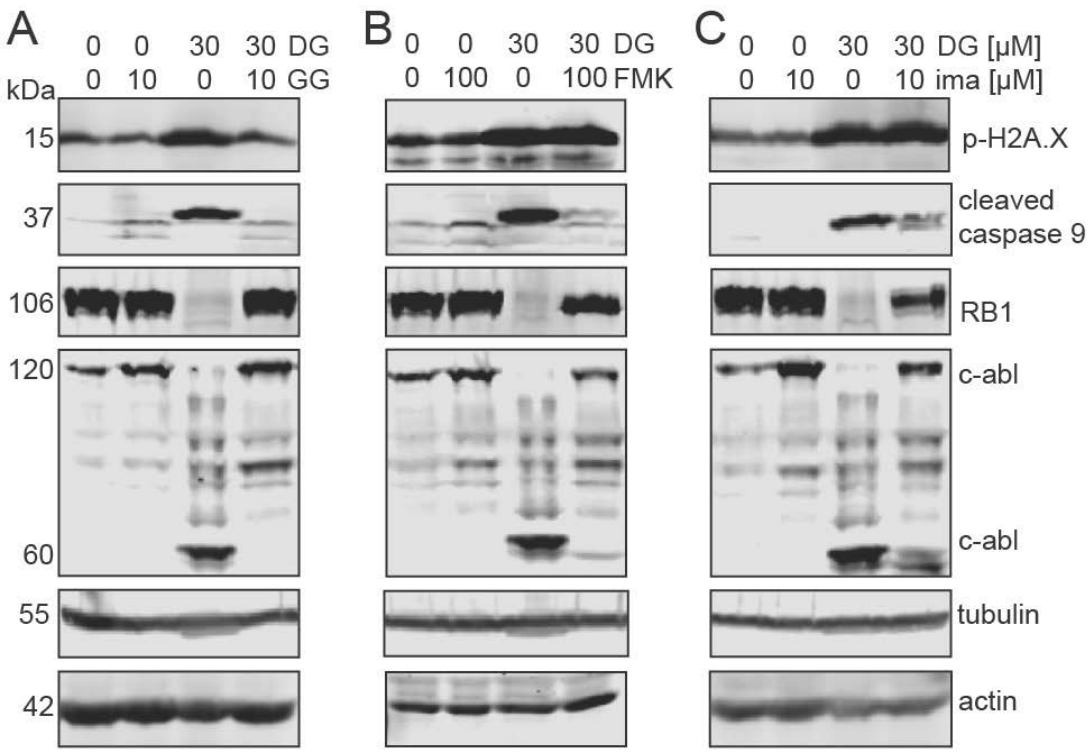

Figure 15. DGBP induces activation of caspases, which cleave retinoblastoma and c-abl.

A) Western blotting analysis of p-H2A.X, cleaved caspase 9, retinoblastoma, and c-abl. Tubulin and actin are shown as loading controls. Molt-4 cells were treated for 72 hours with DGBP in the presence or absence of GGPP, Z-VAD-FMK, or imatinib. Western blots are representative of three independent experiments.

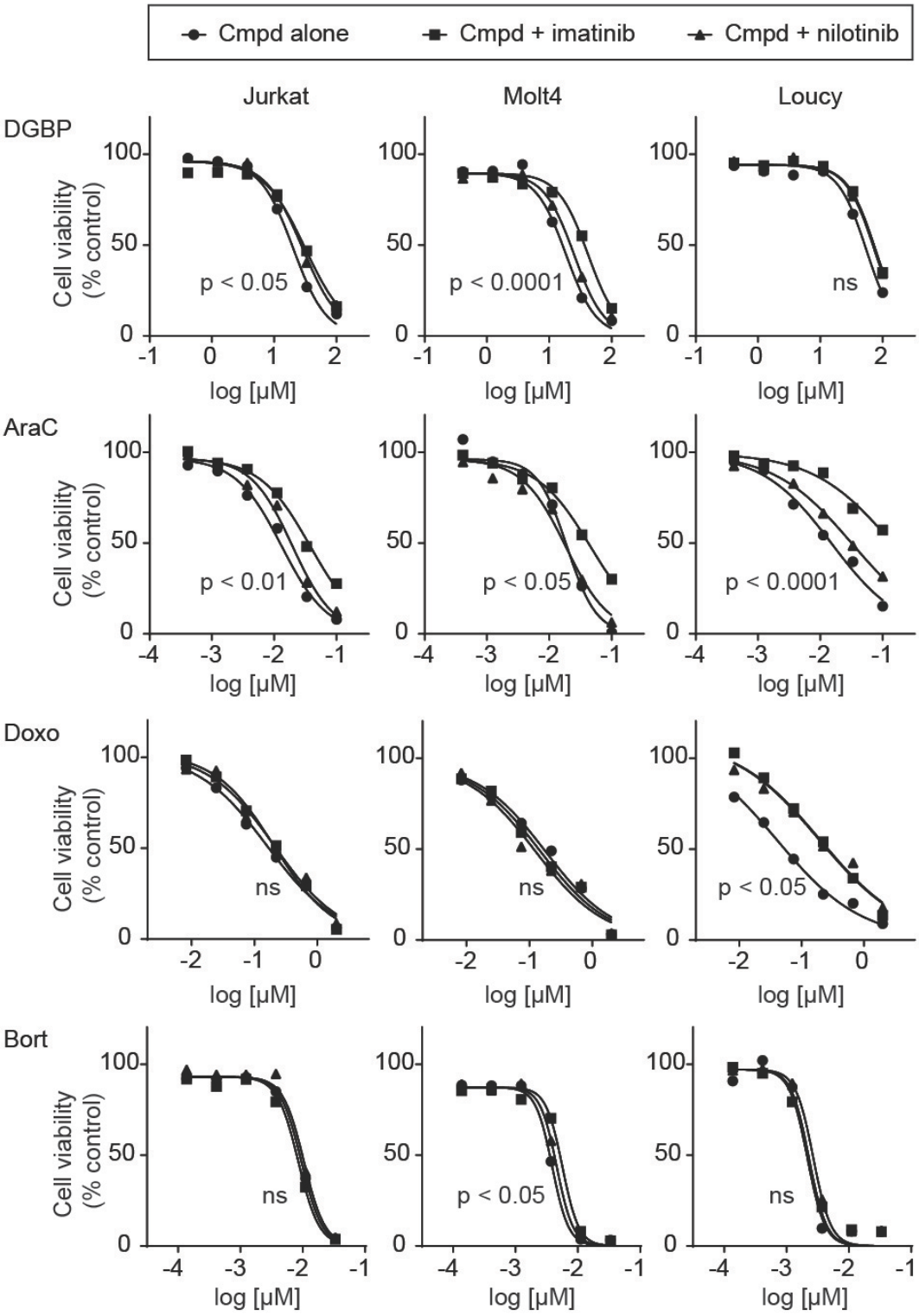

Figure 16. Inhibitors of c-abl are protective against apoptosis induce by chemotherapy agents.

Dose response of Molt-4, Jurkat, and Loucy cell viability with DGBP, cytarabine (AraC), doxorubicin, and bortezomib, and in combination with either 10 µM imatinib or 10 µM nilotinib for 72 hours.

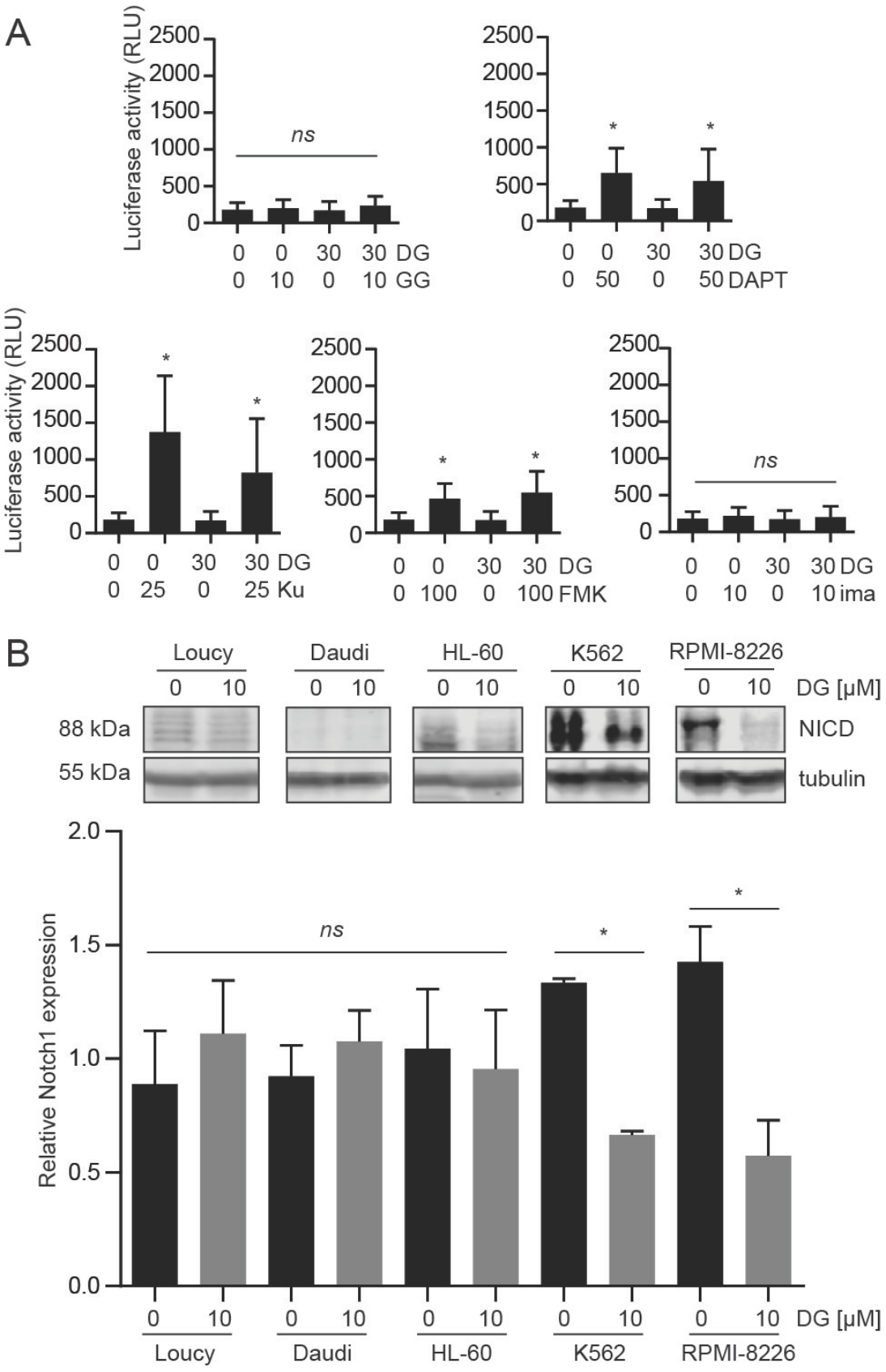

Figure 17. DGBP does not regulate mRNA degradation of Notch, but does regulate levels of active Notch in multiple hematological cell lines.

A) Luciferase activity in Jurkat cells transfected with Notch 3'UTR. Cells were treated with inhibitor alone or co-treated with DGBP for 72 hours. B) Western blot of active Notch (NICD) in Loucy, Daudi, HL-60, K562, and RPMI-8226 cell lines. All Western blots are representative of three independent experiments. In all graphs the bars represent means and standard deviations of three independent experiments (n=3). *$p < 0.05$ versus untreated controls.

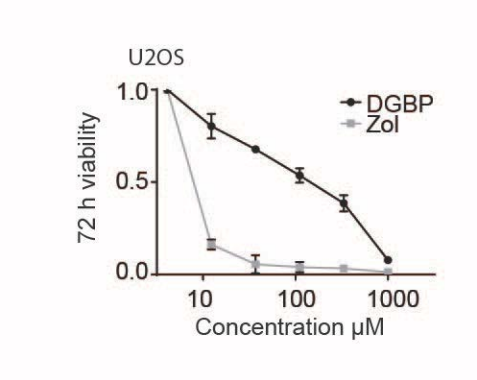

Supplementary figure S5.

Cell viability of U2OS cells treated with either DGBP or zoledronate for 72 hours.

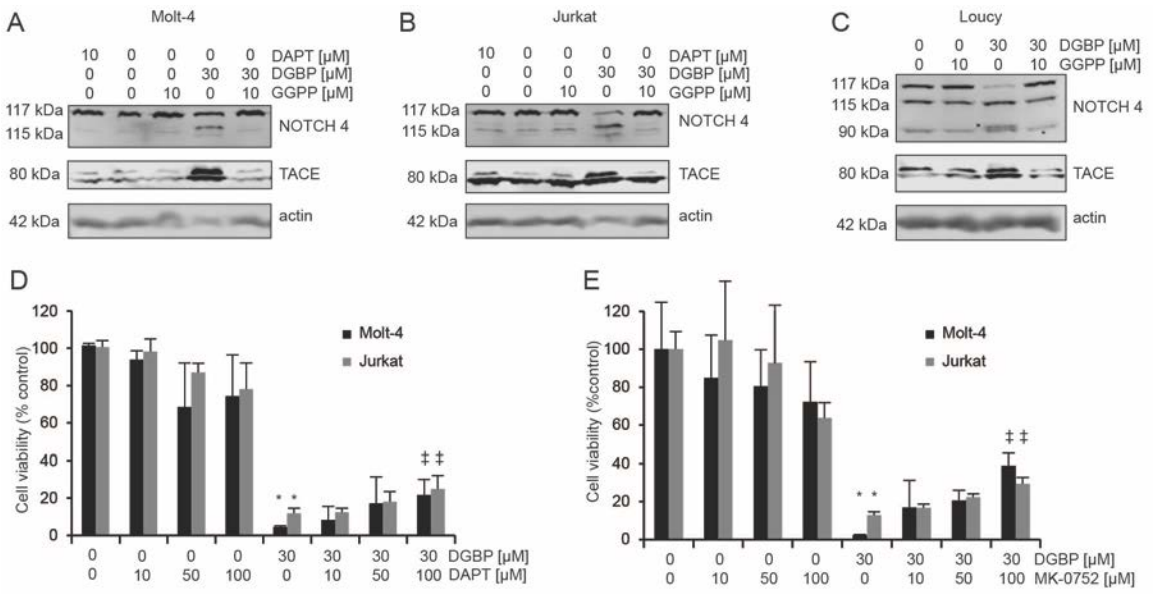

Supplementary figure S6. Notch signaling in T-ALL cell lines.

A-C) Western blots of Notch4 and TACE with DAPT, DGBP, and GGPP co-treatment in Molt-4 (A), Jurkat (B), and Loucy (C) cell lines. Cells were incubated for 72 hours then lysed for analysis. D-E) Cell viability of Molt-4 and Jurkat cells treated with γ-secretase inhibitor alone and with DGBP. D) Viability of cells with DAPT. E) Viability of cells with MK-0752. * denotes significant difference with respect to control, $p < 0.05$. ‡ represents $p<0.05$ significant different with respect to bisphosphonate-treated condition.

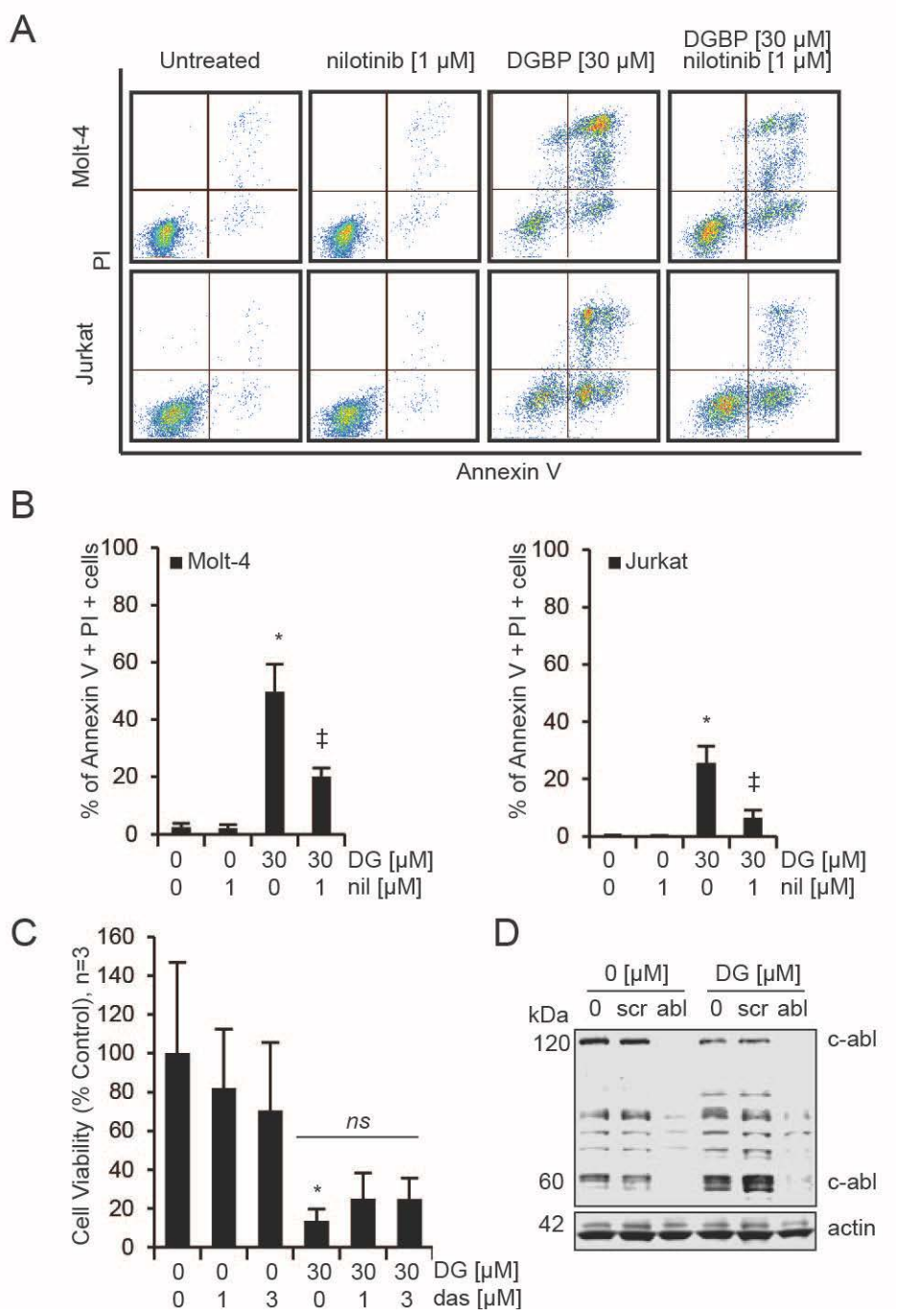

Supplementary figure S7. C-abl inhibition has varying effects on cell viability.

A) Annexin V/ PI staining of Jurkat and Molt-4 cells treated with DGBP and with nilotinib. B) Quantification of nilotinib rescues. C) Cell viability of Jurkat cells treated with DGBP and co-treated with dasatinib. D) Western blot of c-abl with Jurkat cells electroporated with media control (0), scrambled siRNA (scr), and c-abl siRNA (abl) and treated with solvent control and

DGBP. * denotes significant difference with respect to control, $p < 0.05$. ‡ represents $p < 0.05$ significant different with respect to bisphosphonate-treated condition.

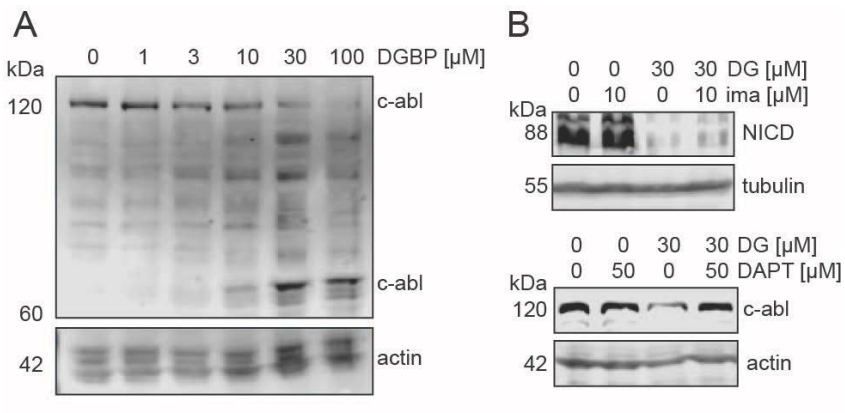

Supplementary figure S8. C-abl is dose dependently decreased by DGBP and is downstream of Notch signaling.

A) Western blot of c-abl and increasing concentration of DGBP in Jurkat cells. B) Western blot of Notch internal domain (NICD) and c-abl with DGBP and imatinib or DAPT co-treatment respectively.

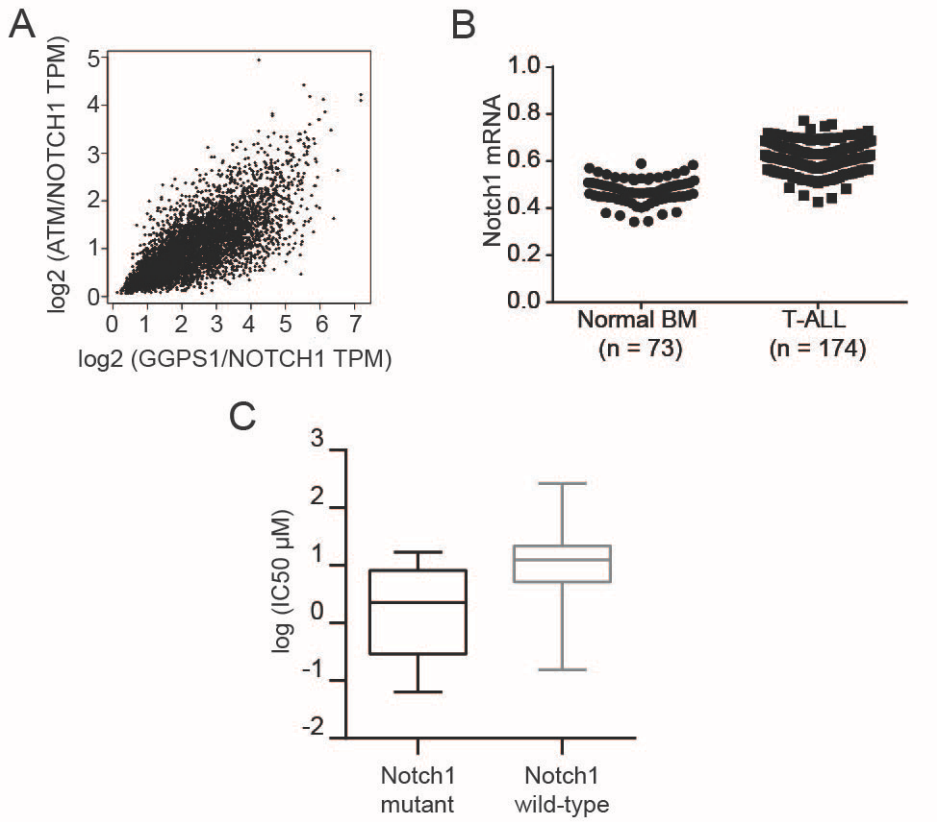

Supplementary figure S9. Notch expression is implicated in multiple cancer cell types.

A) Relationship between GGPS1 and ATM are correlated when compared to overall Notch1 levels across many cancer types and patient samples (BRCA, CESC, DLBC, GBM, HNSC, LAML, LUAD, OV, PAAD, PRAD, ULEC, UCS). B) Notch mRNA levels in normal patient bone marrow and in T-ALL patients. C) Sensitivity of Notch1 mutant cell lines and Notch1 wild-type cell lines to abl kinase inhibitor saracatinib.

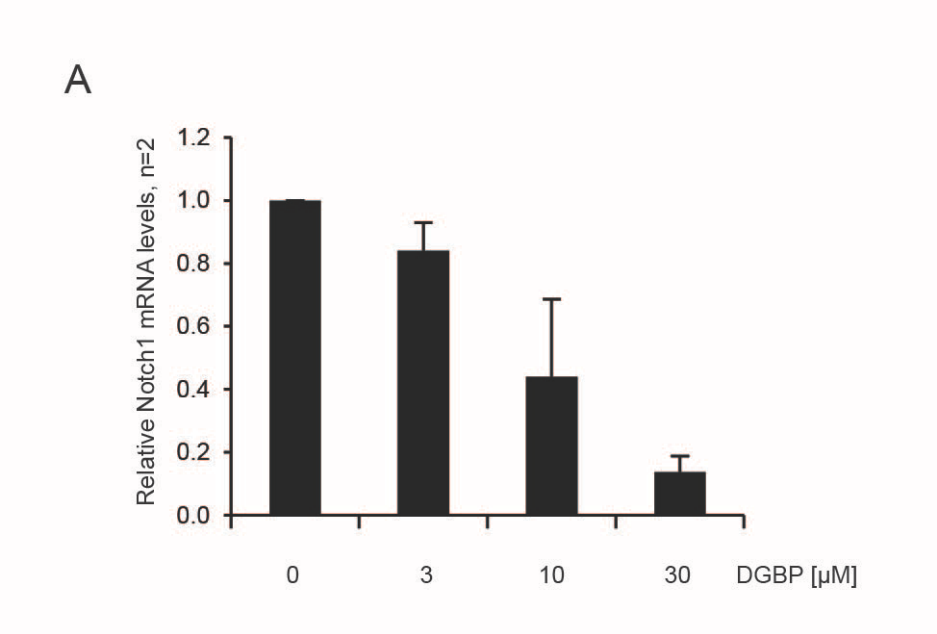

Supplementary figure S10. DGBP decreases Notch1 mRNA levels.

A) Relative mRNA levels of Notch1 with varying concentrations of DGBP. Molt-4 cells were treated for 72 hours with DGBP and then analyzed by qPCR. Mean ± SD, n=2.

CHAPTER4. GERANYLGERANYL DIPHOSPHATE SYNTHASE INHIBITION AFFECTS THE HIPPO PATHWAY.

Abstract

Cell growth and proliferation are regulated in part by geranylgeranylated small GTPases. As such, multiple signaling pathways be involved. Many cancers have genes mutated that play a role in cell development. One such pathway that may be dysregulated in T-ALL is the Hippo pathway. Because isoprenoid biosynthesis pathway inhibitors decrease activation of the Hippo pathway protein YAP, we predicted that DGBP will affect the activity of YAP. Here, we show that GGDPS inhibition affects Hippo pathway effector YAP activation and Hippo pathway mediator protein expression levels. DGBP dose-dependently decreases phosphorylation of YAP at Ser127, and decreases expression of LATS1 and MOB1. While still preliminary, we have seen cells transfected with mutant YAP is more resistant to DGBP compared to those transfected with WT-YAP. Lastly, DGBP affects YAP and BCR-ABL in Philadelphia chromosome positive K562 cells.

Introduction

Yap1 (Yes-associated protein-1), a member of the Hippo pathway, is a transcriptional co-activator involved in organ size control. Mouse models of inducible KRas indicated that in the absence of oncogenic KRas, the expression of Yap1 led to sustained tumors (Kapoor et al., 2014). In tumors of epithelial origin, Yap1 is highly expressed and is often oncogenic. In hematological cancers, however, Yap1 is downregulated or deleted altogether (Cottini et al., 2014). Many hematological cancers demonstrate a high level of DNA damage, but no apoptosis.

In down regulating Yap1, hematological cancers evade normal DNA damage response mechanisms leading to apoptosis.

YAP has been shown in the literature to be regulated by the isoprenoid biosynthesis pathway on multiple accounts. For example, Sorrentino et al demonstrated that zoledronate and a geranylgeranyl transferase inhibitor could prevent nuclear translocation of YAP/TAZ and mevalonate could not rescue this effect. But GGPP could rescue the presence of nuclear YAP/TAZ in cerivastatin-treated cells (Sorrentino et al., 2014). Moreover, constitutively active YAP transfected cells treated with increasing concentrations of cerivastatin were resistant to decreases in viability seen in the control (Sorrentino et al., 2014). Combination of an EGFR inhibitor and simvastatin reduced viability and YAP signaling while GGPP co-treatment restored viability and YAP activity (Liu et al., 2018). Finally, cerivastatin decreased p53 mediated transcription of cell cycle genes CCNB2 and CDK1 in a YAP-dependent manner (Di Agostino et al., 2016). Overall, these data suggest the link between YAP and geranylgeranyl diphosphate in controlling cell viability and provide a rationale for investigating the effects of DGBP on the Hippo pathway.

We have previously seen that GGPP depletion alters the function of RhoA and Rac wherein DGBP increases the cytosolic levels of RhoA and Rac. Notably, DGBP also decrease the membrane levels of Rac. As geranylgeranylated proteins have been found to affect Raf-1, also known as c-Raf, we suspect there is a connection between Raf-1 and the anti-proliferative phenotype seen with administration of DGBP. We have also previously seen that a MEK inhibitor partially rescues the apoptosis induced by DGBP. This indicates that downstream of Raf-1 there is an effector that is partially involved in DGBP-induced apoptosis. But what else is responsible for DGBP-induced apoptosis? According to O'Neill et al, Raf-1 also modulates

MST2, a component of the Hippo pathway, by inhibiting MST2 activation (O'Neill et al., 2004). Therefore, we predict a pathway in which GGDPS inhibition leads to MST1/2 inactivation, preventing LAT1/2 phosphorylation and thereby decreasing phospho-YAP at Ser127 (Figure 18). This would then allow for c-abl to phosphorylate YAP at Tyr357 and for YAP to translocate to the nucleus and bind to transcription factor p73 and c-abl to transcribe pro-apoptotic genes (Figure 18).

Results and Discussion

To begin assessing the effect of a GGDPS inhibitor on the Hippo pathway, we first asked whether DGBP affects the phosphorylation of one of the Hippo pathway's downstream effectors, Yes-associated protein (YAP). We treated Molt-4 and Jurkat cells with increasing concentrations of DGBP and found that DGBP dose-dependently decreased levels of phospho-YAP at Ser127 in both cell lines (Figure 19). Co-treatment of DGBP with GGPP also restored the effect of DGBP on levels of phospho-YAP Ser127 indicating that the effect shown on YAP is dependent on GGPP levels (Figure 19). When YAP is phosphorylated at Ser127 it is sequestered in the cytosol and is not transcriptionally active (Zhao et al., 2007). We show here that DGBP decreases levels of phosphor-YAP at Ser127, which can be rescued by addback of GGPP, suggesting that DGBP decreases levels of cytosolic YAP. YAP that is not phosphorylated at Ser127 is available to be phosphorylated by c-abl at Tyr537 and can translocate to the nucleus (Levy et al., 2008).

To further investigate this hypothesis that DGBP decreases levels of phosphorylated YAP at Ser127 and allows for the phosphorylation at Tyr357, we electroporated Jurkat cells with wild-type YAP and YAP-Y357F (Figure 20). The YAP-Y357F mutant cannot be phosphorylated by c-abl and thus cannot translocate to the nucleus. We hypothesized that cells electroporated with YAP-Y357F would be more resistant to the apoptotic effects of DGBP than cells electroporated

with WT-YAP. Notably, the process of electroporation had a harmful effect on the cells as the no-DNA electroporated control demonstrated high basal levels of apoptosis. Also, the empty vector control was toxic towards the cells as untreated controls had a high percentage of apoptosis (40%). But both no-DNA electroporated control and empty vector control showed little change with GGPP, increased in apoptosis with DGBP, which was then restored back to basal levels with GGPP addback. Interestingly, WT-YAP had an even higher level of basal apoptosis that did not change with any of the conditions. DGBP did not increase apoptosis of WT-YAP electroporated cells. YAP-Y357F had basal levels of apoptosis similar to that of the empty vector. These levels increased with GGPP alone but did not increase with the addition of DGBP. Compared to WT-YAP treated with DGBP, YAP-Y357F treated with DGBP had lower levels of apoptosis. While this data partially supports the hypothesis, the data is still preliminary and the unchanging levels of apoptosis in WT-YAP have yet to be explained.

YAP and TAZ (WW domain containing transcription regulator 1) are both transcriptional coactivators, have similar functions, and are considered redundant (Plouffe et al., 2018). Therefore, in addition to testing a YAP mutant, we also tested a TAZ mutant (Figure 20). In contrast to WT-YAP, WT-TAZ had apoptosis levels similar to that of vector control. Furthermore, treatment with DGBP increased WT-TAZ apoptotic cells. The corresponding phosphorylation site for TAZ to enter the nucleus is Ser89 (Piccolo et al., 2014). Interestingly, the TAZ-S89A mutant apoptosis levels did not change with treatment conditions. One potential experiment to further investigate this is to separate the nuclear and cytoplasmic fractions and blot for the different tags incorporated into each construct. Overall, the mutant and wild-type electroporated cells had different effects and these effects were opposite for YAP and TAZ. This

suggests that YAP and TAZ may have separate functions in Jurkat cells or that these mutants may function differently.

To further assess the role of GGDPS inhibition on the Hippo pathway, we blotted for proteins in within the pathway (Figure 21). We treated Jurkat cells with solvent control, with GGPP alone, with DGBP alone, and with DGBP and GGPP. LATS1, which is responsible for phosphorylating YAP at Ser127, decreases in expression with administration of DGBP. Addback of GGPP restored levels of LATS1. Interestingly, overall levels of YAP decreased with treatment of DGBP, which may be why DGBP decreased levels of phospho-YAP Ser127. But addback of GGPP only partially restored levels of total YAP. MOB1 is involved in stabilizing MST1/2 to allow MST1/2 to phosphorylate LATS1/2 (Meng et al., 2016). DGBP treatment decreased protein expression of MOB1 which was rescued with addback of GGPP. Most interestingly, however, DGBP led to a band at 60 kDa for c-abl. This band, as further investigated in Chapter 3, is still c-abl. C-abl has been shown to be involved in Hippo pathway mediated apoptosis (Cottini et al., 2014). Whether or not c-abl is involved via p53 or p73, remains to be elucidated.

As shown in Chapter 3, c-abl inhibitors such as imatinib can prevent apoptosis induced by DGBP. But this is not how c-abl inhibitors are typically used in the clinic as their original intention was to inhibit BCR-ABL activity. BCR-ABL is a fusion oncoprotein resulting from the reciprocal translocation of chromosome 9 and 22 making BCR-ABL a tyrosine kinase that is constitutively active (Rowley, 1973, Hantschel, 2012). BCR-ABL is the hallmark of chronic myelogenous leukemia and plays an important role in its malignancy (Lugo et al., 1990, Deininger et al., 2000). Here we investigate how DGBP affects phospho-Yap Ser127 in a chronic myelogenous leukemia cell line K562 that expresses BCR-ABL. DGBP decreases levels of

phospho-YAP dose dependently (Figure 22). Lovastatin at 30 μM had a more pronounced decrease than DGBP at 30 μM. Dasatinib also decreased levels of phospho-YAP at 1 nM. This is interesting because dasatinib prevents activation of c-abl and would prevent activation of phospho-YAP at Tyr357. The fact that dasatinib has this effect indicates that BCR-ABL may also regulate levels of phospho-YAP Ser127. Thus, we also assess whether c-abl inhibitors could rescue the apoptotic effect of DGBP in the BCR-ABL mutant context. We found that imatinib rescued the effect of DGBP while nilotinib co-incubation increased apoptosis. Furthermore, the K562 cells were very sensitive to dasatinib, even though proliferation data showed that cells were still viable at 0.2 nM (Figure). The combination of dasatinib and DGBP lead to an even greater increase in apoptosis. This suggests that the effect of c-abl inhibitors on cancer cell viability is a structural matter, or that inhibition of off-target kinases such as Src by dasatinib may complicate interpretation. Interestingly, in the BCR-ABL context, imatinib and nilotinib have opposite effects suggesting that the rescue effect may be dependent on binding conformation.

Materials and Methods

Molt-4, Jurkat, and K562 cells were obtained from ATCC (Manassas, VA, USA). Cells were cultured in 10% FBS serum with penicillin and streptomycin. GGPP and XMU-MP-1 were obtained from Cayman Chemical (Ann Arbor, MI, USA). Imatinib, nilotinib and dasatinib were obtained from LC laboratories (Woburn, MA, USA). LATS1 (C66B5), MOB1 (E1N90), phosphor-YAP Ser127 (D9W21), and YAP/TAZ (D24E4) were obtained from Cell Signaling Technologies (Danvers, MA, USA). HA-TAZ (Addgene plasmid # 32839) and HA-TAZ-S89A (Addgene plasmid # 32840) were gifts from Kunliang Guan (Lei et al., 2008). pcDNA Flag Yap1

(Addgene plasmid # 18881) and pcDNA Flag Yap1 Y357F (Addgene plasmid # 18882) were gifts from Yosef Shaul (Levy et al., 2008).

Western blotting

Cells were seeded at 100,000 cells/ mL and cultured with indicated compounds for 72 hours. Cells were washed with PBS and lysed with 25 mM Tris-HCl pH 7.6, 150 mM NaCl, 1% NP-40, 1% sodium deoxycholate) either containing freshly added protease and phosphatase inhibitors including aprotinin (1 μg/mL), leupeptin (1 μg/mL), pepstatin (1 μg/mL), PMSF (200 μM), sodium vanadate (200 μM), sodium diphosphate (10 μM), sodium fluoride (50 μM), and glycerophosphoric acid (10 μM) and incubated for 10 minutes of sonication in a water bath. Total protein levels were quantified by BCA Assay (Pierce) and equivalent masses were loaded onto 5% or 7.5% bis-acrylamide gels for separation. Proteins were transferred onto nitrocellulose membranes and blocked with 5% BSA. Antibodies against Hippo pathway proteins were incubated with 5% BSA overnight on rotator at 4 C. Blots were visualized using Licor Odyssey.

Electroporation

Jurkat cells were allowed to grow overnight in antibiotic-free media. Cells were washed once with RPMI-1640 and resuspended at 25 x 10^6 cells/ mL. 0.4 mL of cells was added to 20 μg of DNA in electroporation cuvettes. This mixture was incubated for 10 minutes at room temperature prior to electroporation. Electroporation was conducted on a Biorad GenePulser XL according to the exponential protocol at 316 V and 500 μF and allowed to rest at room temperature for 15 minutes before being transferred to 6 well plates. After 24 hours, cells were counted and resuspended in fresh media with antibiotics and seeded for flow cytometry.

Flow cytometry

Cells were seeded at 100,000 cells/ mL. After 72 hour incubation with compounds, cells were washed with PBS and resuspended in 200 µL of 1x Binding Buffer (10 mM HEPES, 150 mM NaCl, 1 mM $MgCl_2$, 5 mM KCl, and 1.8 mM $CaCl_2$, pH 7.4) then transferred to polystyrene flow tubes. 2.5 µL of FITC Annexin V (Biolegend) solution were added to the tubes. 2 µL of PI (Sigma-Aldrich, St. Louis, MO) 50 µg/mL solution were added to the tubes. Samples were gently vortexed and read on a BD LSR Fortessa X-20 (BD Biosciences, Franklin Lakes, NJ).

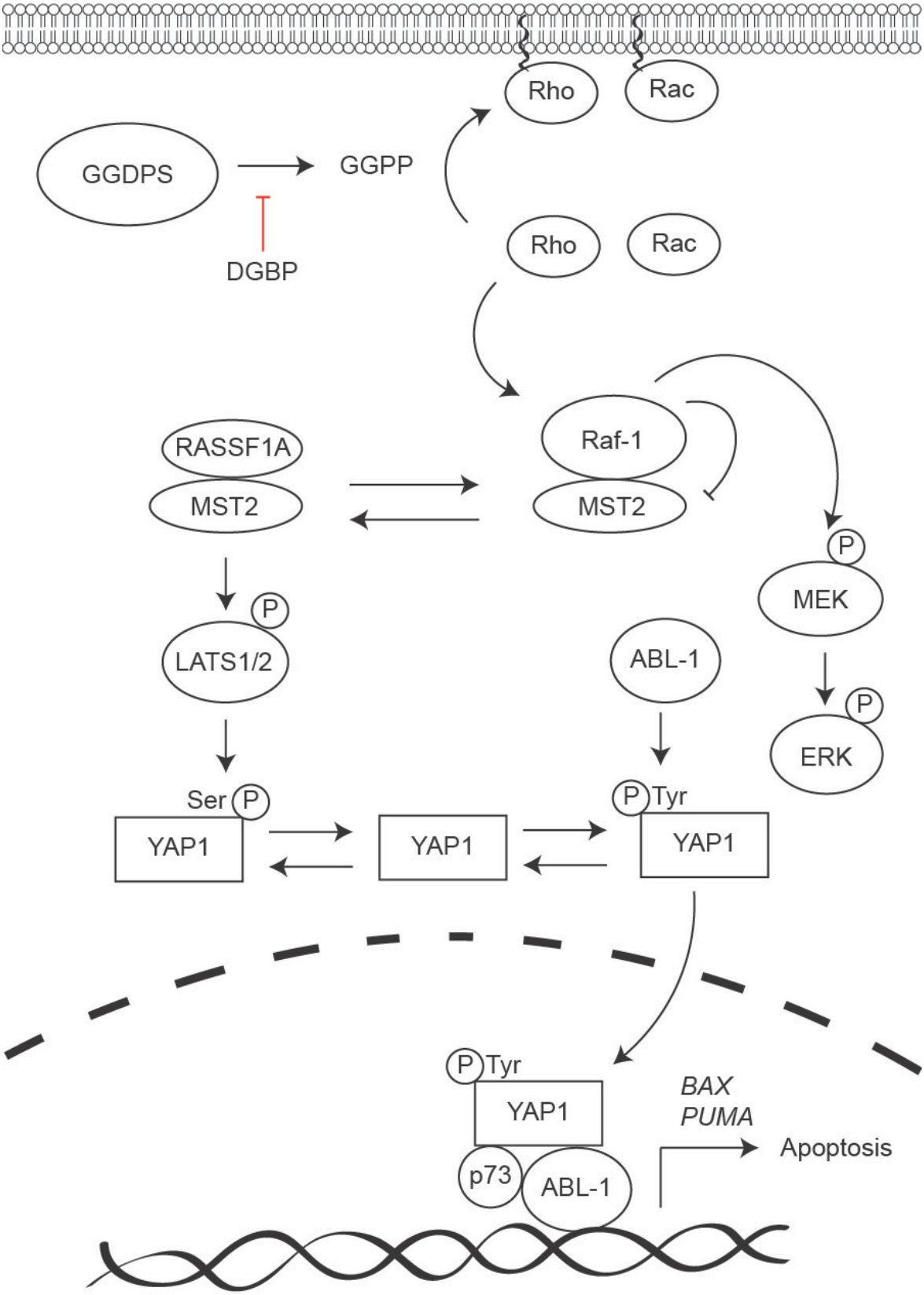

Figure 18. Proposed pathway of how GGDPS inhibition affects the Hippo pathway to induce apoptosis in T-ALL.

GGDPS biosynthesizes GGPP, which can be inhibited by DGBP. GGPP allows for small GTPases such as Rho and Rac to be membrane-associated. Inhibition of GGDPS depletes GGPP, which prevents these GTPases from being membrane-associated and allows them to interact with Raf-1, which then inhibits MST2 and activates MEK1/2 and ERK1/2. If MST2 is not inhibited by Raf-1, it associates with RASSF1A, which activates LATS1/2. LATS1/2 then phosphorylates YAP at Ser127 preventing it from translocating to the nucleus. If Raf-1 inhibits MST2, then LATS1/2 does not phosphorylate YAP at Ser127 allowing it to be phosphorylated by Abl-1 or c-abl at Tyr357. This phosphorylation event allows YAP to translocate to the nucleus and bind to transcription factors p73 and c-abl to transcribe pro-apoptotic genes.

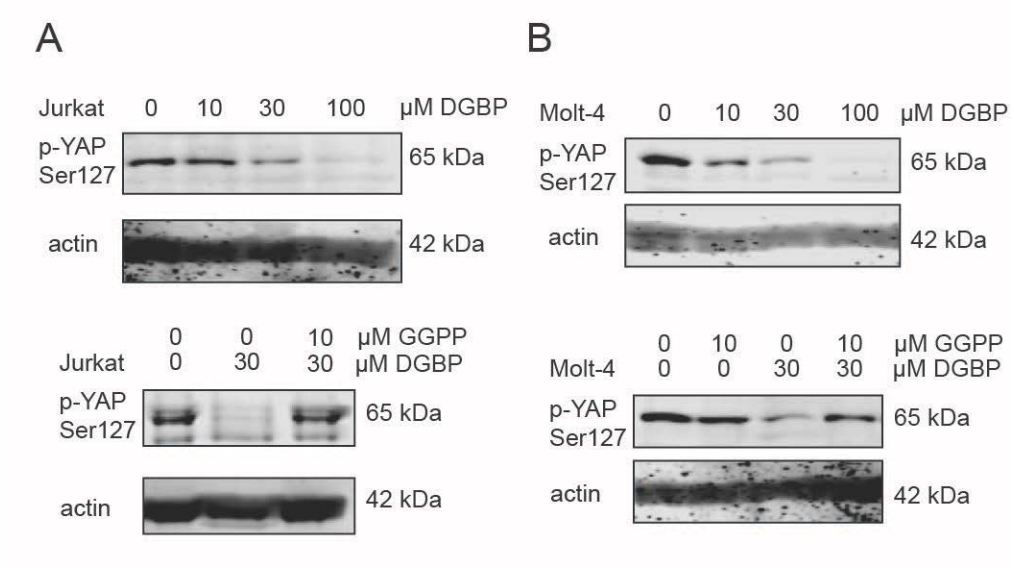

Figure 19. GGDPS inhibition decreases levels of phospho-YAP Ser127.

A) Western blots showing phospho-YAP levels in Jurkat cells with dose response of DGBP (top) and addback of GGPP (bottom). B) Western blots showing phospho-YAP levels in Molt-4 cells with dose response of DGBP (top) and addback of GGPP (bottom). For all blots shown, n=1.

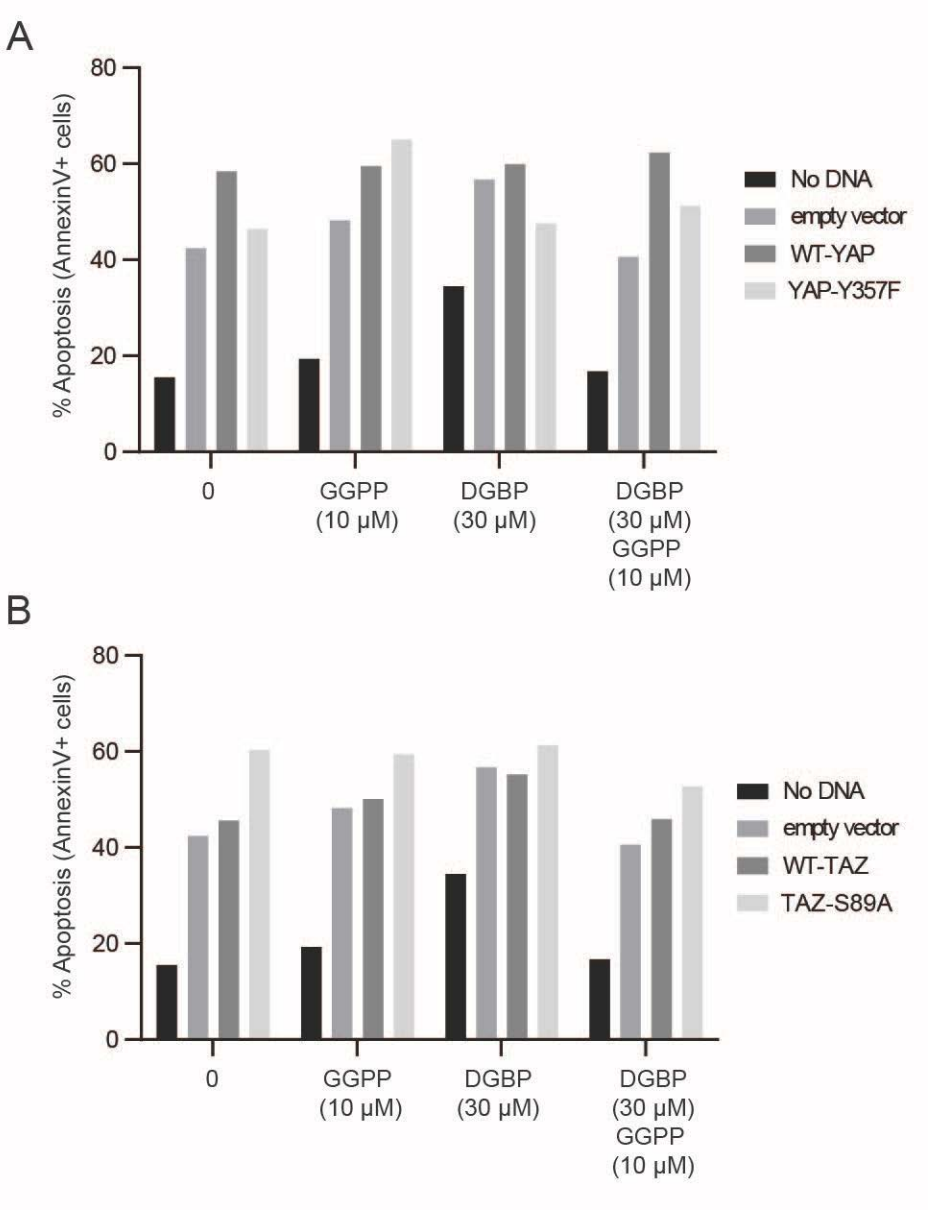

Figure 20. YAP and TAZ transfected mutants have different responses to DGBP.

A) Annexin V staining as determined by flow cytometry of Jurkat cells transfected with WT-YAP and YAP-Y357F. B) Annexin V staining as determined by flow cytometry of Jurkat cells transfected with WT-TAZ and TAZ-S89A. Cells were treated with compounds for 72 hours; n=1.

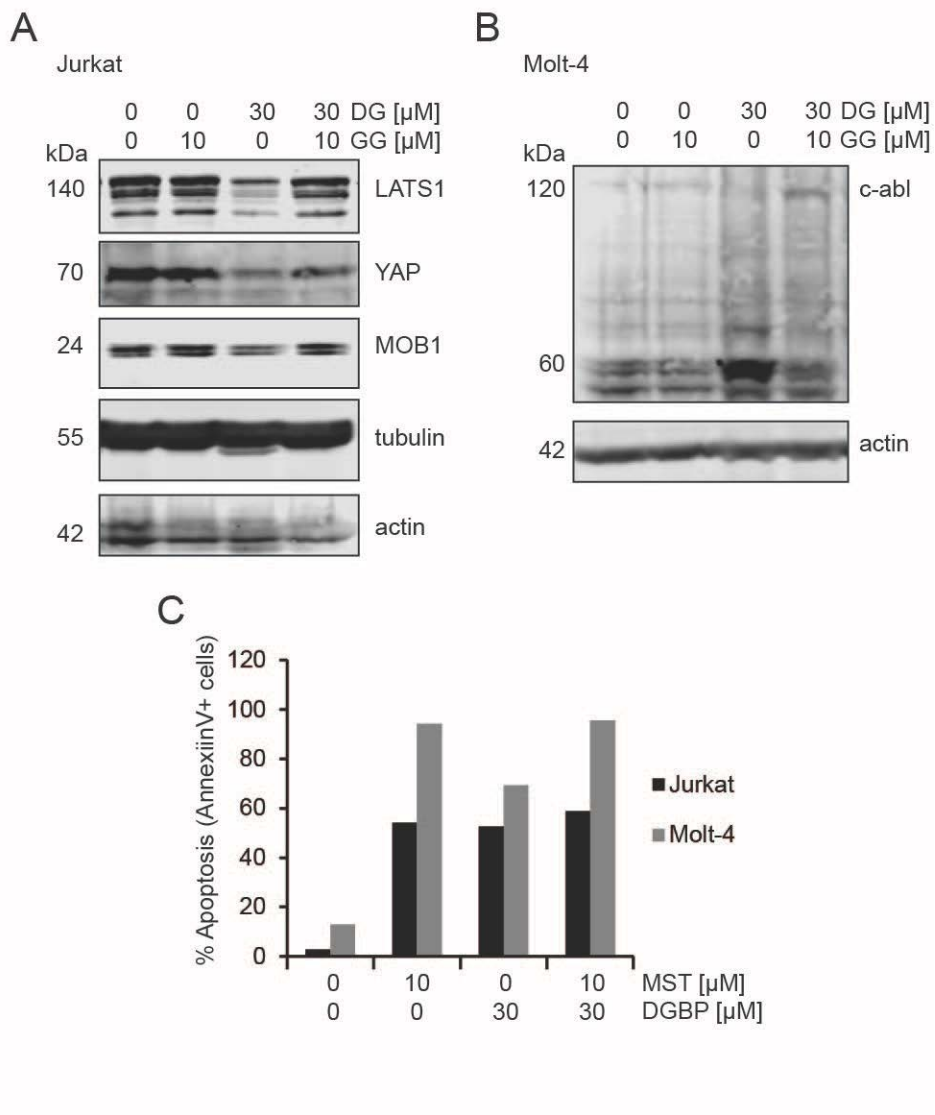

Figure 21. DGBP decreases expression of Hippo pathway proteins.

A) Western blots of various Hippo pathway proteins in Jurkat cells treated with DGBP and co-treated with GGPP. B) Western blots of c-abl or Abl-1 in Molt-4 cells. Cells were treated with DGBP for 72 hours. C) Annexin V/ PI staining as determined by flow cytometry of Jurkat and Molt-4 cells treated with XMU-MP-1 an MST1/2 inhibitor. Cells were treated for 72 hours prior to analysis of flow cytometry. N=1 for experiments depicted in this figure.

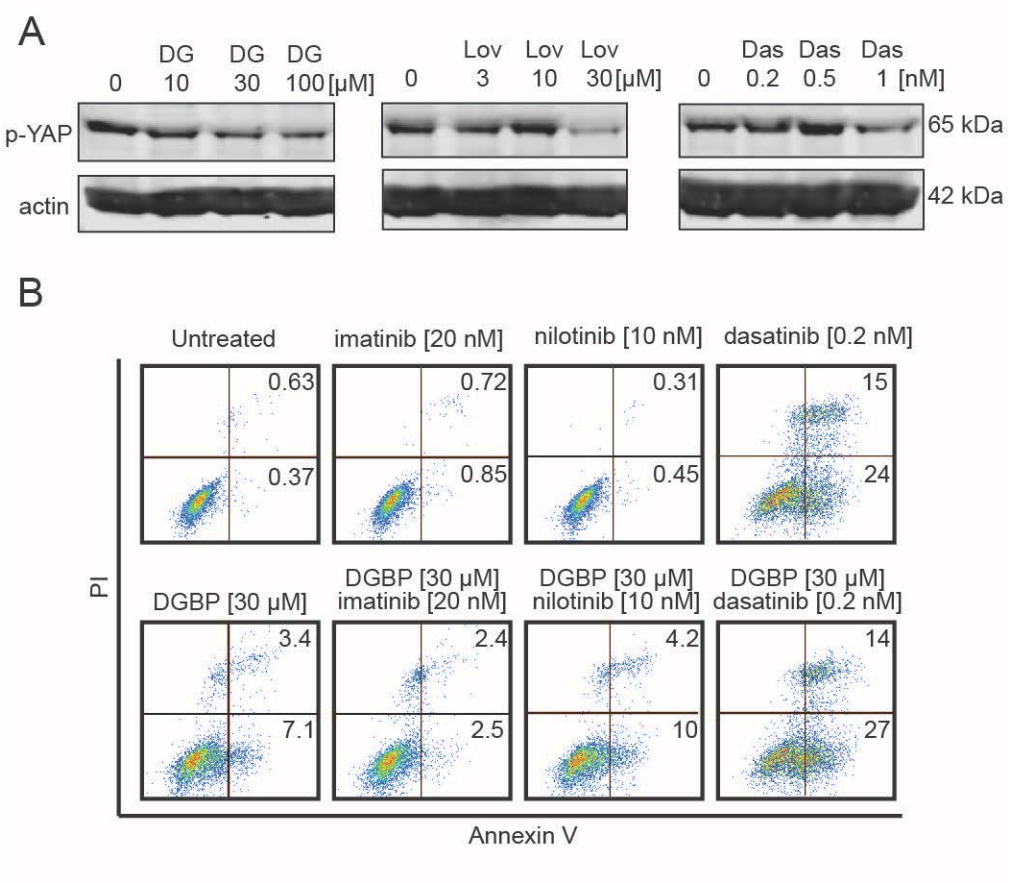

Figure 22. Isoprenoid biosynthesis pathway inhibitors and c-abl inhibitors in K562 cells.

A) Western blots of phospho-YAP Ser127 in K562 cells after treatment with varing concentrations of DGBP, lovastatin, and dasatinib. B) Raw Annexin V/ PI staining flow cytometry plots of DGBP-treated K562 cells and co-treatment with c-abl inhibitors: imatinib, nilotinib, and dasatinib. N=1 for Westerns and flow cytometry experiments shown in this figure.

CHAPTER 5: ASSESSING THE ROLE OF ISOPRENOID BIOSYNTHESIS PATHWAY INHIBITORS IN RPMI-8226 CELLS.

Abstract

DGBP affects multiple pathways that ultimately decrease cell viability and induce apoptosis. DGBP induces cleaved caspases, activates ERK, depletes levels of active Notch1, and activates ATM and other DNA damage-response pathway components in T-ALL cell lines. But does GGDPS inhibition affect other pathways and how does it act in other cellular contexts compared to other isoprenoid biosynthesis pathway inhibitors? In this chapter, I explore the effects of DGBP in a different cellular context that differed from the T-ALL lines that we investigated previously. Here I examine the RPMI-8226 multiple myeloma cell line. RPMI-8226 has been shown previously to respond to geranylgeranyl diphosphate synthase inhibitors (Zhou et al., 2014). In this chapter, we investigated the role of isoprenoid biosynthesis inhibitors on VEGF cytokine levels, Rab3A mRNA levels, and on Rab GTPase localization in RPMI-8226 cells. Because isoprenoid biosynthesis pathway inhibitors have differential effects on sterol levels, we predicted that they would differentially effect Rab GTPase expression and levels of cytokine secretion. The results showed that lovastatin and DGBP differentially affected mRNA levels and VEGF levels, but they did not differently affect Rab5A and Rab9A expression or localization.

Introduction

The RPMI-8226 cell line provides a good model for study of geranylgeranyl diphosphate synthase inhibition for several reasons. RPMI-8226 cells are interesting because zoledronate,

another bisphosphonate, is already clinically approved for multiple myeloma. Another rationale for investigating the role of GGDPS inhibitors in RPMI-8226 is that RPMI-8226, unlike the T-ALL lines explored here thus far, are KRas mutated (Ramakrishnan et al., 2012). This mutation allows for increased signaling through the Ras/MAPK signaling pathway. It has been thought that targeting Ras/MAPK will prevent proliferation of KRas mutant cells. Indeed, inhibition of ERK has been shown to induce senescence in KRas mutant pancreatic cancer (Hayes et al., 2016). Due to the clinical relevance and KRas role, we proposed that using an inhibitor to farnesyl transferase in combination with DGBP would result in synergistic anti-proliferative activity.

Multiple myeloma is partially driven by its microenvironment. The bone marrow microenvironment allows for the secretion of growth factors and initiates angiogenesis, ultimately supporting the growth of the tumor. Vascular endothelial growth factor (VEGF) is a cytokine responsible for initiating angiogenesis by stimulating endothelial sprouting and vascular permeability in nearby blood vessels (Rini, 2005). As most cytokines are subject to vesicular trafficking and Rab GTPases play an important role in vesicular trafficking, we hypothesized that GGDPS inhibition would decrease VEGF levels. Because the bone marrow microenvironment is important in T-ALL relapse as relapsed T-ALL bone is particularly resistant to standard treatment, it is important to investigate the cytokines involved in the bone marrow microenvironment.

The isoprenoid biosynthesis pathway is partially regulated by sterol levels as cholesterol depletion and FPP depletion lead to increased transcription of isoprenoid biosynthesis enzymes such as HMG-CoA reductase via SREBPs. It has also been shown that statin treatment can affect levels of small GTPases. In this chapter, we determine how DGBP and lovastatin affect small

GTPase mRNA levels. We predict that because lovastatin controls sterol levels that this decreased sterol level will activate SREBPs and increase transcription of Rab GTPases.

Results and Discussion

We started this study by investigating the effects of multiple isoprenoid biosynthesis pathway inhibitors on RPMI-8226 cell viability. Interestingly, tipifarnib, an inhibitor of farnesyl transferase, was most potent of these compounds with an IC_{50} of 0.15 μM (Figure 23A-D). Lovastatin was next at 2.1 μM and DGBP had an IC_{50} of 8.0 μM. Zoledronate had the highest IC_{50} of these compounds (33 μM) despite being the only one approved for clinical anti-myeloma use. These data suggest that there is potential for the use of other isoprenoid biosynthesis inhibitors in multiple myeloma contexts.

While the use of one of these inhibitors indicated promising effects, we hypothesized that the use of multiple inhibitors would be antagonistic if combined with zoledronate. We tested the combination of zoledronate with DGBP and zoledronate with tipifarnib. We also tested tipifarnib with DGBP. We predicted that the combination of DGBP with tipifarnib would be synergistic because the GGPP was not likely under SREBP control and inhibiting farnesylation would likely decrease Ras activity. Preventing the membrane association of both geranylgeranylated proteins and farnesylated proteins such as KRas will likely decrease viability of cells compared to preventing the membrane association of either group alone as both are involved in cell proliferation. The combination of tipifarnib and zoledronate are slightly antagonistic (Figure 23E). Interestingly, DGBP and tipifarnib are only slightly synergistic (Figure 23F). The combination of DGBP and zoledronate are strongly antagonistic (Figure 23G), which was similar to what we demonstrated in Molt-4 cells.

In order to investigate how isoprenoid biosynthesis pathway inhibitors affect VEGF levels, we treated RPMI-8226 cells with lovastatin alone, lovastatin with GGPP, DGBP alone, and DGBP with GGPP and then measured levels of VEGF-A in the media. We predicted that both lovastatin and DGBP would decrease VEGF. Lovastatin decreased levels of VEGF by approximately half while DGBP decreased VEGF levels minimally (Figure 24). Co-incubation of GGPP restored the effect of lovastatin. In contrast, co-incubation of GGPP with DGBP increased VEGF levels by two-fold compared to the control. Overall, we found that lovastatin decreased VEGF levels but DGBP did not. These results were surprising because DGBP had a minimal effect. We proposed that because GGDPS is closer in the isoprenoid biosynthesis pathway to Rab GTPases in comparison to HMG-CoA reductase that DGBP would be more potent in regulating Rab GTPases and therefore be more potent in regulating levels of VEGF. Interestingly, the fact that lovastatin could be rescued by addition of GGPP. Perhaps increased GGPP levels increase active geranylgeranylated GTPases and increase levels of VEGF. While the effects of lovastatin were interesting, we chose not to continue these assays as VEGF is primarily involved in paracrine functions and would best be investigated with a microenvironment model where other cell types are present (Dankbar et al., 2000).

We hypothesized that isoprenoid biosynthesis pathway inhibitors may regulate the mRNA levels of GTPases. To test this, we treated cells with lovastatin alone, lovastatin with GGPP, DGBP along, and lovastatin with GGPP. We found that lovastatin treatment decreased Rab3A mRNA levels while DGBP increased Rab3A mRNA levels (Figure 25). Simultaneously, GGPP co-incubation with lovastatin partially rescued the effect of lovastatin. And addback of GGPP to DGBP-treated cells also restored the effect of DGBP. These data suggest that SREBPs are involved in regulating not only isoprenoid pathway enzyme levels but also in regulating

small GTPases. To further test this in the future, we would use a knock-down model of SREBPs and determine whether the same effect is seen with other small GTPases. We also investigated the protein levels of Rab3A and found that they were low compared to both tubulin and unprenylated Rap1a (Figure 25C). Unprenylated Rap1a was used as a positive control to determine whether or not lovastatin and DGBP were preventing prenylation. Because the protein levels of Rab3A are low (Figure 25B), the effects on mRNA levels may not have large consequences on overall cell signaling. Therefore, we chose to explore the effects of isoprenoid biosynthesis pathway inhibitors on Rab protein expression and membrane localization.

While Rab3A had low protein expression, other Rab GTPases were better expressed in the RPMI-8226 cells. We compare the effects of an untreated/solvent control, DGBP, risedronate, lovastatin, as well as a co-incubation condition with GGPP for each compound, on protein expression and membrane localization. Rab5A had low levels of expression, but demonstrated high membrane localization without treatment (Figure 26). Treatment with DGBP, risedronate and lovastatin all increased the cytosolic levels and decreased the membrane levels. Also, co-incubation with GGPP restored these levels. Rab9A had high levels of basal expression with high membrane levels. Rab9A was affected by the isoprenoid biosynthesis pathway inhibitors in the same fashion as Rab 5A. Most interestingly with Rab9A, the co-incubation with GGPP decreased the overall expression levels suggesting that elevated levels of GGPP may decrease Rab9A expression. Rab11A was also more cytosolic than membrane localized with DGBP treatment. In contrast to the other GTPases, however, Rab11A decreased in overall expression with DGBP treatment, which was partially rescued by addback of GGPP. Overall, these data suggest that these inhibitors act similarly on GTPase membrane localization, and the levels of GGPP may affect expression levels. One future experiment that could be done to further

explore this idea is determining the mRNA levels of Rab9A and Rab11A and treating with similar conditions along with GGPP alone at different concentrations.

Materials and Methods

RPMI-8226 cells were obtained from ATCC and grown according to ATCC's recommendation in 10% FBS media. Rab 11 (D4F5), Rab9 (D52G8), and Rab5 (C8B1) were obtained from Cell Signaling (Danvers, MA, USA). Rab3A (K-15) and Rap1a (C-17) antibody was obtained from Santa Cruz Biotechnology (Santa Cruz, CA, USA). E7 tubulin was deposited to the DSHB by Michael Klymkowsky (DSHB Hybridoma Product E7) (Chu and Klymkowsky, 1989). The VEGF-A ELISA kit was obtained from Thermo Fisher (Waltham, MA, USA).

Cell Viability

Cells were cultured and seeded in fresh media at 100,000 cells/mL in 100 µL in 96 well plates. Cells were incubated with the appropriate compounds for 72 hours. 10 µL of CellQuantiblue reagent was added to each well and incubated at 37°C for 2 hours before reading on Victor V plate reader (Perkin Elmer). Combinatorial effects were calculated using Calcusyn Software (Biosoft, Cambridge, UK). Combination Index values were calculated according to the Chou and Talalay method (Chou and Talalay, 1984). Isobolograms were generated for combinations using 80% dilutions of each compound based on their individual IC_{50} values.

VEGF-A ELISA

RPMI-8226 cells were seeded and cultured in 48-well plates for 48 hours. 96 well plates were coated with VEGF-A capturing antibody and blocked 24 hours before 48-hour time point. Media was transferred to microcentrifuge tubes and centrifuged for 3 minutes at 600 x g. Media was then added to coated plates and the manufacturer's protocol was followed for VEGF-A standard

curve and the rest of the protocol. Absorbance at 450 nm and 550 nm were read on a Victor V plate reader (Perkin Elmer).

Real time RT Polymerase Chain reaction (RT-PCR)

Cells were seeded at 100,000 cells/ mL in 5 mL. Cells were incubated with appropriate compounds for 48 hours. Total RNA was isolated with the TRIZOL (Invitrogen) according to the manufacturer's protocol. The forward primer for Rab3A was: 5'ATC AAG CTG CAG ATC TGG GAC ACA 3'. The reverse primer for Rab3A was: 5' AAG AAC TCG AAC CCA AGG TGG TCA 3'. The forward primer for 18S was: 5' TAA GTC CCT GCC CTT TGT AAC ACA 3'. The 18S reverse primer was: 5' GAT CCG AGG GCC TCA CTA AC 3'. RNA levels were determined with Nanodrop and cDNA was made using MMLV reverse transcriptase according to the manufacturer's protocol. SYBR green protocol was used according to the manufacturer's protocol on a 7500 Applied Biosystems PCR machine. Relative mRNA levels were determined by $2^{-\Delta\Delta Ct}$ values.

Triton X-114 phase separation and Western blot

Membrane and cytosolic fractions were isolated using Triton X-114. Cells were resuspended at a concentration of 750,000 cells/mL and cultured for 48 hours. Cells were washed with PBS and resuspended in 4°C Triton X-114 lysis buffer (20 mM Tris pH 7.5, 150 mM NaCl, 1% Triton X-114) with freshly added protease inhibitors. Lysate was passed through a 27 gauge ½ inch needle until homogenous and centrifuged for 15 minute at 12,000 x g at 4°C. 40 µL of this supernatant was reserved to determine whole cell lysate protein levels. The supernatant is transferred to a new microcentrifuge tube and incubated in a 37°C water bath for 10 minutes. The supernatant was then centrifuged at room temperature at 12,000 x g for 2 minutes. The resulting aqueous phase (upper) and detergent phase (lower) were then separated and diluted. A BCA assay was

used to determine total protein concentration. Western blot analysis was performed as described previously (Agabiti et al., 2017).

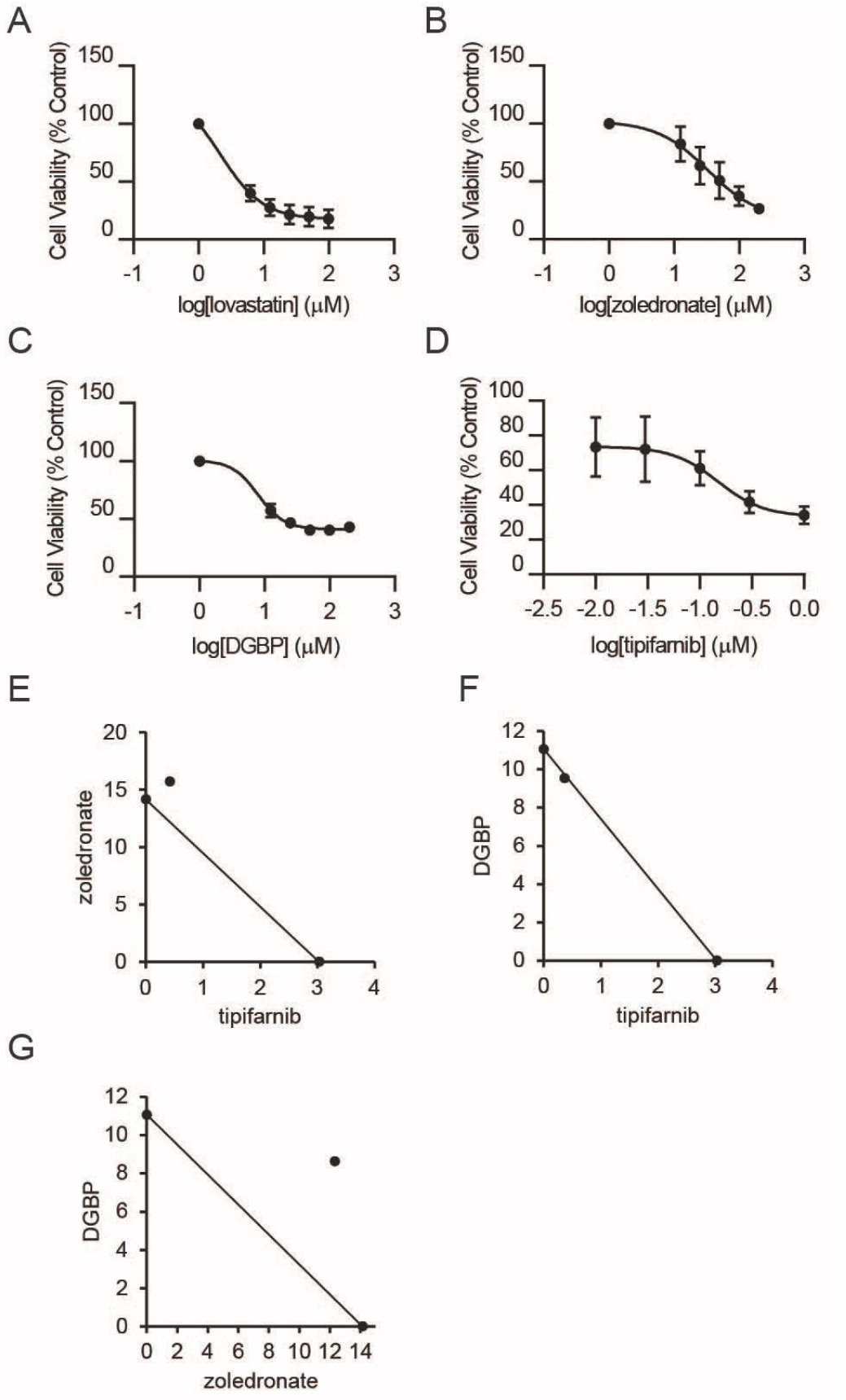

Figure 23. Isoprenoid biosynthesis pathway inhibitors decrease cell viability in RPMI-8226 cells.

A) Dose response of lovastatin. B) Dose response of zoledronate. C) Dose response of DGBP. D) Dose response of tipifarnib. For A-D, n=3 mean ± SD. E) Isobologram of zoledronate and tipifarnib, n=1. F) Isobologram of DGBP and tipifarnib, n=1. G) Isobologram of DGBP and zoledronate, n=1. EC_{75} values were used to calculate isobologram data. Cells were incubated for 72 hours with compound to determine cell viability.

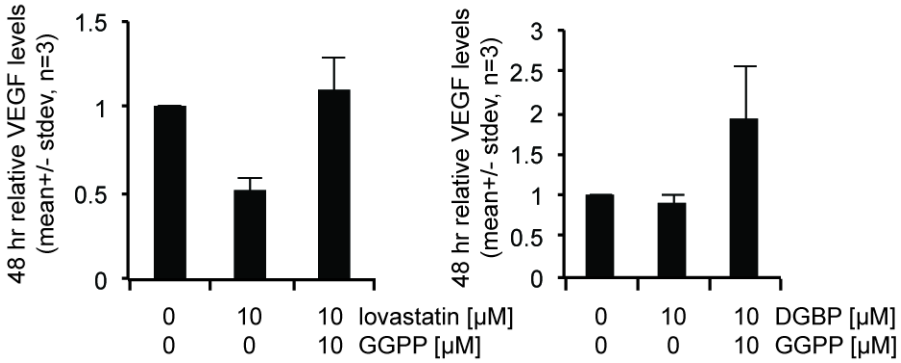

Figure 24. Lovastatin decreases relative VEGF-A levels in RPMI-8226 cells.

Relative VEGF-A levels of RPMI-8226 cell media as determined by ELISA. Left: Cells were treated with lovastatin and co-treatment with GGPP. Right: Cells were treated with DGBP and co-treatment with GGPP.

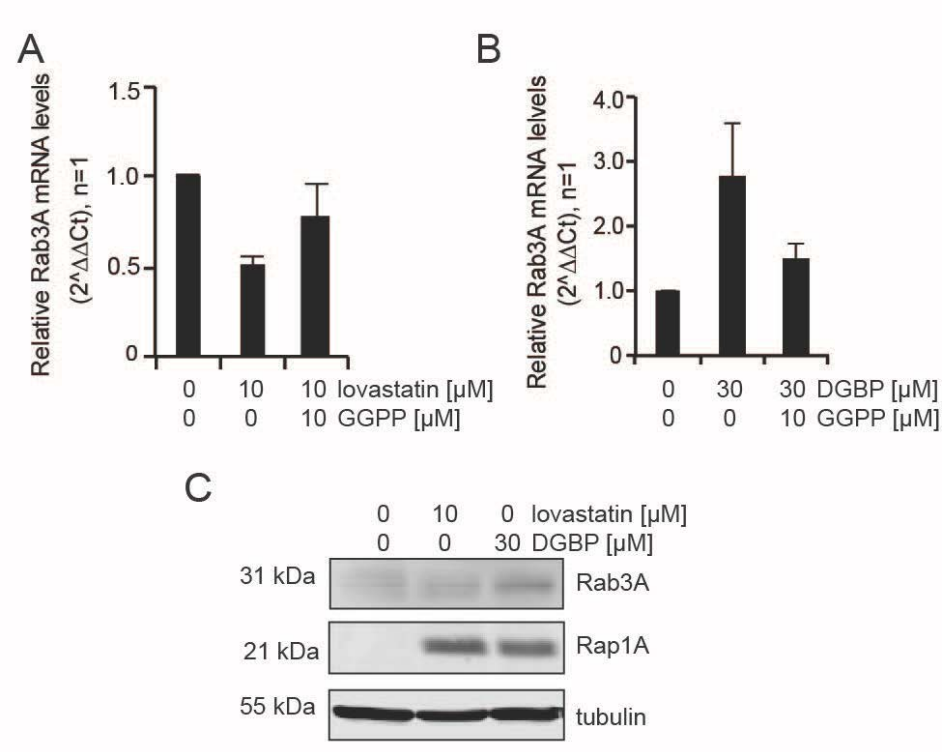

Figure 25. Isoprenoid biosynthesis pathway inhibitors affect the expression of Rab3A.

A) Relative mRNA levels of Rab3A in RPMI-8226 cells with treatment of lovastatin and co-treatment with GGPP. B) Relative mRNA levels of Rab3A in RPMI-8226 cells with treatment of DGBP and addback of GGPP. C) Western blot of Rab3A and Rap1A protein expression levels in RPMI-8226 cells with lovastatin and DGBP treatment. n = 1 for these experiments.

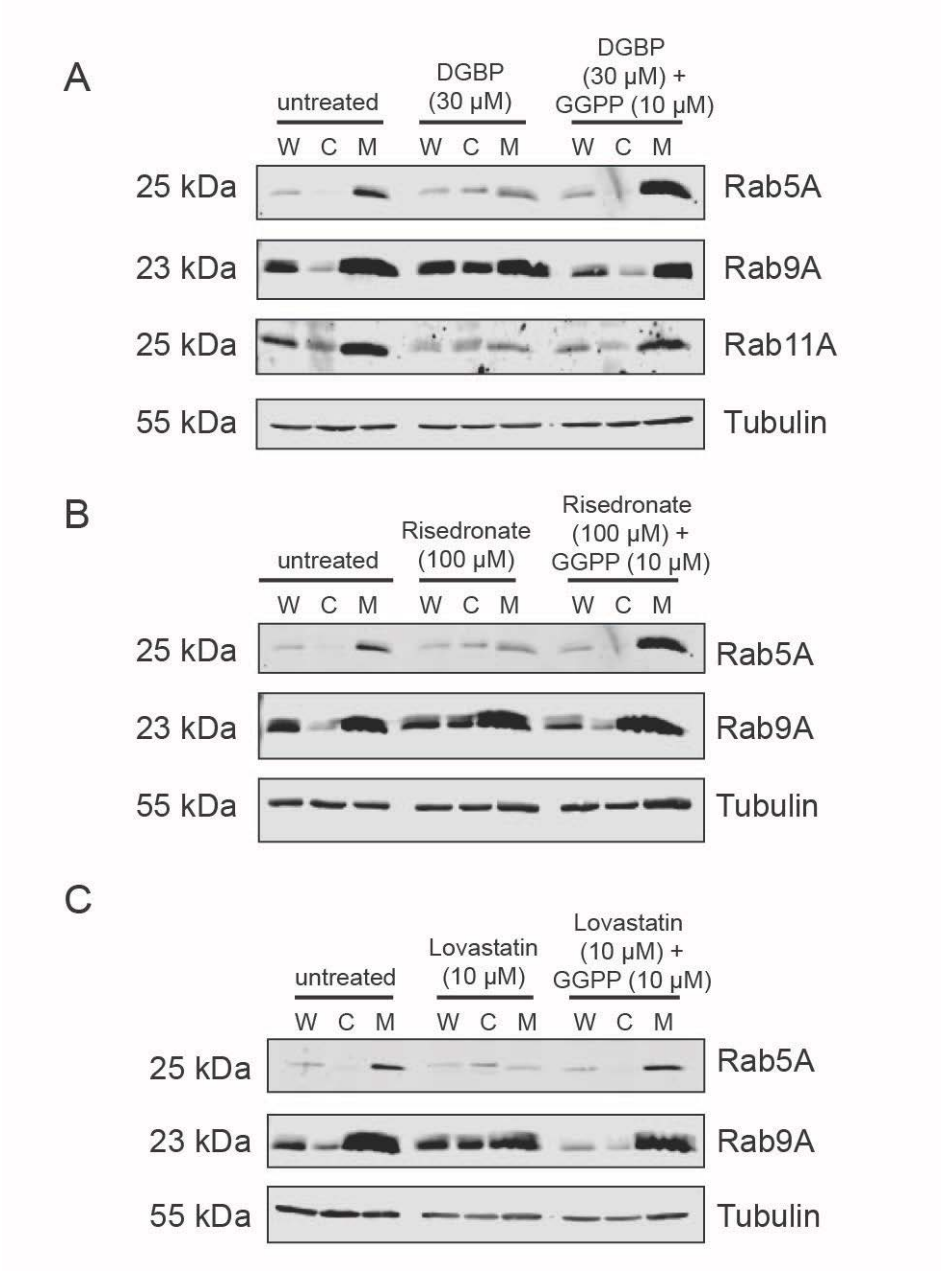

Figure 26. Isoprenoid biosynthesis pathway inhibitors change the localization of Rab GTPases in RPMI-8226 cells.

"W" represents whole cell lysate. "C" represents the cytosolic fraction. "M" represents the membrane fraction. A) Western blot of Rab5A, Rab9A, Rab11A showing whole cell, cytosolic, and membrane fractions separated using the TritonX-114 protocol. RPMI-8226 cell were treated

with DGBP and co-treated with GGPP. B) Western blot of Rab5A and Rab9A showing whole cell, cytosolic, and membrane fractions separated using the TritonX-114 protocol. RPMI-8226 cell were treated with risedronate and co-treated with GGPP. C) Western blot of Rab5A and Rab9A showing whole cell, cytosolic, and membrane fractions separated using the TritonX-114 protocol. RPMI-8226 cell were treated with lovastatin and co-treated with GGPP. N = 1 for the depicted experiments.

Chapter 6: Conclusions

Introduction

The isoprenoid biosynthesis pathway has a history of being a target for anti-cancer therapies (Dewick, 2002). Inhibitors for multiple enzymes have been targeted suggesting the importance of understanding this pathway and its downstream signaling effects (Figure 27). Nitrogenous bisphosphonates have been successfully used as inhibitors to farnesyl diphosphate synthase (FDPS) in osteoporosis to prevent bone resorption (Hamdy, 2010). Zoledronate, a bisphosphonate that inhibits FDPS, has been repurposed for multiple myeloma and is successful in the clinic (Terpos et al., 2013). Another group of isoprenoid biosynthesis pathway inhibitors that has been suggested for anti-cancer therapy is the statins. Statins have recently been implicated in decreasing proliferation of cell line models (Jiang et al., 2014). Interestingly, GGPP co-incubation can often rescue the effect of statins, and geranylgeranyl transferase inhibitors often recapitulate the effect of statins (Kotamraju et al., 2007, Gbelcova et al., 2017, Lee et al., 2018). Thus, the effect of statins and nitrogenous bisphosphonates is thought to be due to inhibition of prenylation, and in many cases, specific to geranylgeranylation.

The prenyltransferases are further downstream in the isoprenoid biosynthesis pathway and pharmaceutical efforts were poured into their preclinical development (Appels et al., 2005). Farnesyl transferases have been targeted mainly due to the established role of KRas as a cancer driver (Brunner et al., 2003). But these inhibitors were not shown to be clinically effective, in large part due to alternative geranylgeranylation of KRas under conditions of farnesyltransferase inhibition (Appels et al., 2005, Whyte et al., 1997). Geranylgeranyl transferase inhibitors are potentially good therapeutic agents because of their close proximity within the pathway to small

GTPases (Figure 27). But because there are two primary transferases and there may be some redundancy amongst the small GTPases, it is possible for other small GTPases to compensate for the inhibited GTPases. While it would be ideal to identify the small GTPase responsible for the maintaining viability, there are many geranylgeranylated small GTPases and a combination of them may be responsible since they thought to act as a class rather than as single entities (Hentschel et al., 2016, Mullen et al., 2016). Therefore, geranylgeranyl diphosphate synthase (GGDPS) is an attractive target because it is uniquely poised to prevent the membrane association of multiple small GTPases.

Depletion of a metabolite or inhibition of a signaling pathway?

While impaired prenylation is thought to be the source of the decrease in viability observed following isoprenoid depletion, the fact that GGPP rescues the viability may suggest that this may be due to depletion of a metabolite derived from GGPP. There are downstream metabolites that are made from GGPP such as menquinone-4 (Figure 27). UBIAD1 has been identified as a prenyltransferase that adds GGPP to the napthoquinone to form menaquinone-4, a vitamin K2 homolog (Nakagawa et al., 2010). UBIAD1 has been shown to be involved in non-mitochondrial biosynthesis of ubiquinone (Mugoni et al., 2013). Whether or not this requires GGPP, however, is not known. But because UBIAD1 is involved in zebrafish (Mugoni et al., 2013) and UBIAD1 has a GGPP binding site, it is possible for UBIAD1 to add GGPP to form co-enzyme Q10. Recently, Yu et al. used a variety of mutant and myrisytolated GTPases to show that the effect of statins could be uncoupled from prenylation (Yu et al., 2018). This prompted them to suggest that while the effects of statins could be rescued by GGPP co-incubation, that the effect of GGPP was due to depletion of a downstream metabolite such as dolichol or ubiquinone. While they tested substrates of GGTase I, they did not test substrates of GGTase II

nor did they evaluate a GGTase II inhibitor. Therefore, the effect of statins could still go through GGTase II modified small GTPases such as Rab. Nevertheless, it is important to investigate whether or not the effect of GGPP is due to downstream depletion of isoprenoid biosynthesis pathway metabolites. While it is possible that the effects of isoprenoid biosynthesis pathway inhibitors are due to depletion of metabolites downstream of GGPP, the fact that geranylgeranyl transferase inhibitors can recapitulate the effect of the statins (van de Donk et al., 2003), nitrogenous bisphosphonates (Wilke et al., 2014, Hasmim et al., 2007), and geranylgeranyl diphosphate synthase inhibitors (Dudakovic et al., 2011), suggests that this effect is due to geranylgeranylation and not depletion of a downstream metabolite.

In addition to discussion of whether prenylation is responsible, there is also discussion of whether or not GGPP itself is necessary for maintaining viability. In chapter 2 we discuss that GGPP not FPP robustly rescues the decrease on viability of bisphosphonates DGBP and zoledronate. Furthermore, GGPP is a better rescue agent than FPP in bisphosphonate-mediated apoptosis in T-ALL. Yu et al. has also found that GGPP not FPP rescues the effect of statins in breast cancer cell lines. Despite these findings, Malwal et al. argues that because Mitrofan et al. (Mitrofan et al., 2009) found that zoledronate treatment and GGOH co-treatment resulted in very low levels of IPP, that GGOH also inhibits mevalonate kinase and prevents isoprenoid biosynthesis through IPP depletion (Hinson et al., 1997, Malwal et al., 2018). Henneman et al. noted that non-sterol isoprenoids can be detected using HPLC-MS/MS showing that inhibiting FDPS with pamidronate increases IPP/DMAPP (there is also a slight increase in GPP) in a time-dependent manner, and leaving little to no GGPP or FPP (Henneman et al., 2008). Further studies are necessary to determine whether the effect of GGDPS inhibition and GGPP addback has any effect of levels of upstream metabolites.

GGPP also regulates the isoprenoid biosynthesis pathway upstream of GGDPS by aiding in the degradation of HMG-CoA reductase. Interestingly, insig-dependent and sterol-stimulated degradation of HMG-CoA reductase is augmented by GGOH, but not by FOH (Sever et al., 2003). UBIAD1-mediated degradation of HMGCR is regulated by a geranylgeranylated protein as GGTI-298 prevents the ubiquitylation of HMGal, a chimeric protein containing the membrane region of HMGCR that is sufficient to drive endoplasmic-reticulum-associated degradation (Leichner et al., 2011). Further studies are necessary to determine whether GGPP-mediated degradation of HMG-CoA reductase regulates transcription of isoprenoid biosynthesis enzymes.

New findings in geranylgeranyl diphosphate synthase inhibition

GGDPS is gaining traction as a target for cancer. Recently, Lacbay et al. identified several new potent GGDPS inhibitors. These inhibitors are thienopyrimide-based bisphosphonates with EC_{50} toward RPMI-8226 cell proliferation less than 1 μM. Enzymatic inhibition with compound 10 and 11 analogs demonstrated IC_{50} values ranging from 42 nM to 100 nM (Figure 28). Even more, Lacbay et al. found that 11c increased phosphorylation of ERK1/2 and decreased phosphorylated Akt, which corroborates our results shown in Chapter 2. Overall, this new type of GGDPS inhibitor showed IC_{50} values comparable to that of VSW1198 described in Chapter 1, induced apoptosis across multiple cancer cell lines and decreased serum mouse immunoglobulin in a mouse multiple-myeloma model. Pre-clinical studies have also recently been performed for the E/Z mixture of VSW1198. VSW1198 was found in the bone marrow, brain, liver, spleen and kidney. VSW1198 prevented Rap1 geranylgeranylation in the liver, spleen and kidney. Interestingly, the Z-isomer was more prevalent in the bone marrow (Haney et al., 2018). In clinical models, overexpression of GGDPS in lung carcinoma patients correlated with decreased overall survival. But this effect is likely more related to migration and

metastasis than apoptosis as decreased GGDPS via siRNA decreased migration and invasion while addback of GGPP restored the effect of the GGDPS knock-down (Wang et al., 2018). In conclusion, there is increased interest in GGDPS as a target both in inhibitor development and in pre-clinical studies.

DNA damage and geranylgeranylation

Throughout chapters 2 and 3, we demonstrate that GGDPS inhibition activates DNA-damage response induced apoptosis (Figure 29). In Chapter 2, we discuss how DGBP increases phosphorylated ERK to increase apoptosis. Interestingly, the most prominent effects of activated ERK in apoptosis is shown in cisplatin-treated cells suggesting that ERK is involved in DNA-damage response. Moreover, an ATM inhibitor could rescue the effects of etoposide on ERK activation. Thus, indicating the role of ERK in DNA damage response. In Chapter 3, we found that DGBP decreased active Notch1 levels and a Notch1 processing inhibitor could rescue the effects. Furthermore, an ATM inhibitor and c-abl inhibitors could rescue the apoptotic effect of DGBP. But this is not the first association of geranylgeranylation and DNA damage because Sun et al. found that GGTI-298 induced hypophosphorylation of RB1 in lung carcinoma cell line Calu-1 (Sun et al., 1999). More studies are required to understand how DNA damage response occurs in GGDPS inhibited cells. ATM phosphorylates PIDD1 at Thr788 which is crucial for caspase-2-PIDDosome formation, which promotes Mdm2 cleavage (Ando et al., 2012). Ku55933 prevents cisplatin-induced Mdm2 cleavage (Terry et al., 2015). This ultimately suggests a role for cleaved caspase 2, Mdm2, and p53. More importantly, it is crucial to understand how GGDPS inhibition leads to changes in transcription. DGBP decreased Notch1 mRNA levels dose-dependently. How this happens is unclear, but one potential mechanism is through p53. Ral1B GTPase silencing activates and stabilizes p53 (Tecleab et al., 2014). P53 targets Notch1

transcription in skin fibroblasts (Lefort et al., 2007). Finally, Weissenrieder et al. found that DGBP decreases androgen receptor target gene transcription in prostate cancer cell lines (Weissenrieder et al., 2018). There is likely a role of geranylgeranylation in regulating transcription and in DNA-damage response.

As both the Notch1 pathway and the Hippo pathway converge on c-abl (figure 29), one must ask if small GTPases interact with c-abl directly. It is possible for small GTPases to affect c-abl or BCR-ABL directly. BCR-ABL has a Rac binding site (Diekmann et al., 1991). Thus, it would be interesting to test c-abl inhibitors with a Rac GTPase inhibitor. This would be interesting because imatinib and farnesyl transferase inhibitors showed synergism when combined in both imatinib-resistant and imatinib-sensitive CML cell lines suggesting a role of farnesylated GTPases (Radujkovic et al., 2006). Overall, small GTPases may have a direct role on c-abl kinases and affect DNA damage-induced apoptosis through c-abl direct interaction.

Conclusions

Overall, we demonstrate that DGBP induces apoptosis through the DNA-damage response pathway in T-ALL cell lines. We show that GGPP can robustly rescue the pro-apoptotic effect of zoledronate and DGBP. We also demonstrate that GGPP depletion increases levels of phosphorylated ERK. This we predict is related to DNA-damage response as well. The role of Notch1 as a driver for T-ALL is well established. We discovered that GGDPS inhibition decreased levels of Notch1. We also found that the anti-apoptotic effects of DGBP could be ameliorated by co-treatment with an ATM inhibitor and c-abl inhibitors. This result that indicates an isoprenoid biosynthesis pathway inhibitor can regulate apoptosis by the DNA-damage response pathway is surprising and warrants further research.

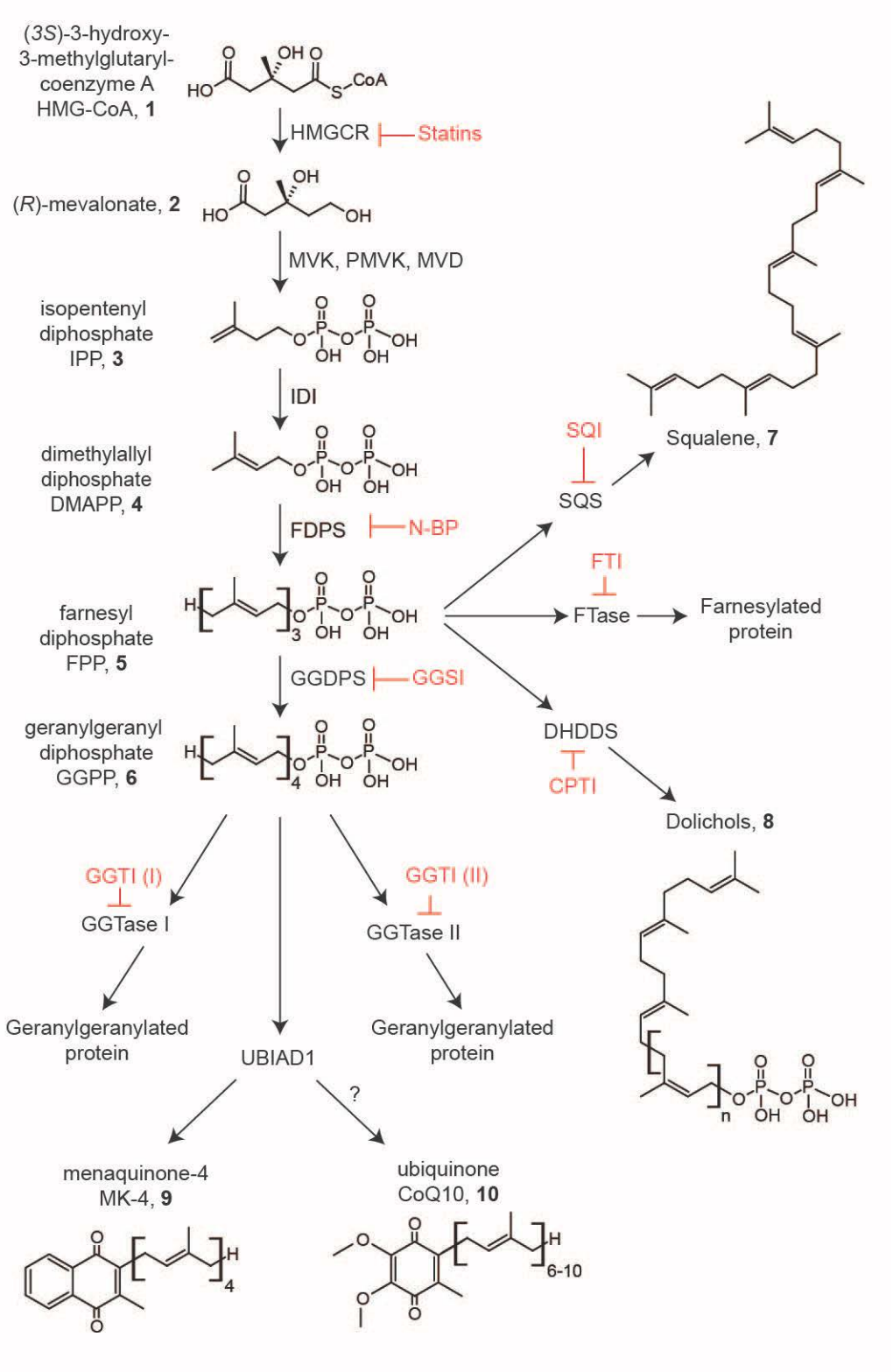

Figure 27. The isoprenoid biosynthesis pathway including FPP, GGPP and downstream effectors.

HMG-CoA, **1**, is used by HMG-CoA reductase (HMGCR) to biosynthesize mevalonate, **2**. This step can be inhibited by statins. Mevalonate kinase (MVK), phosphomevalonate kinase (PMVK), and mevalonate diphosphodecarboxylase (MVD), convert mevalonate to isopentenyl diphosphate (IPP), **3**. IPP is isomerized by isopentenyl-diphosphate delta isomerase (IDI) to form dimethylallyl diphosphate (DMAPP), **4**. Farnesyl diphosphate synthase (FDPS) then uses DMAPP to biosynthesize farnesyl diphosphate (FPP), **5**. This step can be inhibited by the nitrogenous bisphosphonates (N-BP). Geranylgeranyl diphosphate synthase then uses FPP and IPP to biosynthesize geranylgeranyl diphosphate (GGPP), **6**. This step can be inhibited by geranylgeranyl diphosphate synthase inhibitors (GGSI). FPP is also used by squalene synthase, which can be inhibited by squalene synthase inhibitors (SQI), to biosynthesize squalene, **7**. Farnesyl transferase (FTase) uses FPP to farnesylate small GTPases such as KRas and laminA. This step can be inhibited by farnesyl transferase inhibitors (FTI). Dehydrodolichyl diphosphate synthase (DHDDS) uses FPP and IPP to biosynthesize dolichols, **8**. This step can be inhibited by the *cis* prenyltransferase inhibitors (CPTI). GGPP is also used by geranylgeranyl transferase I (GGTase I) to geranylgeranylate proteins such as RhoA, Rap1A, and Ral1. This step can be inhibited by geranylgeranyl transferase I inhibitors (GGTI (I)). Geranylgeranyl transferase II also uses GGPP to geranylgeranylate other small GTPase proteins such as Rab3A and Rab5A. This can be inhibited by geranylgeranyl transferase II inhibitors (GGTI (II)). UBIAD1 uses GGPP to add a geranylgeranyl group to menaquinone-4, **9**, and ubiquinone, **10**.

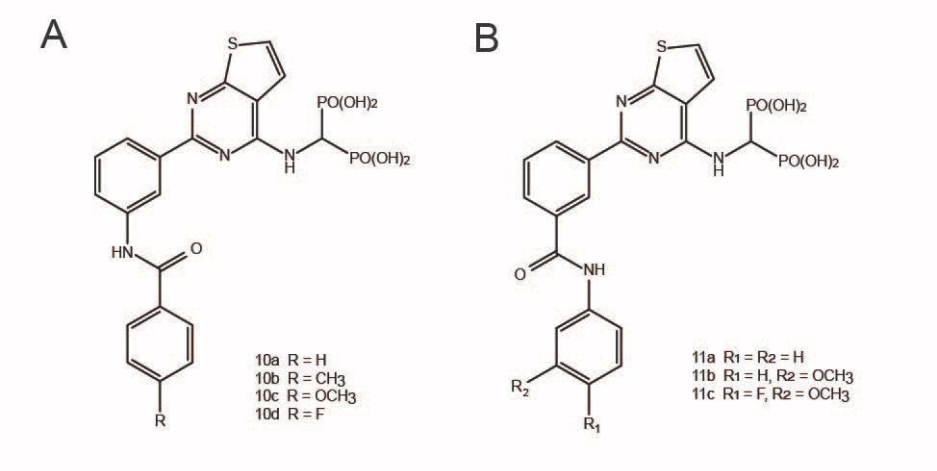

Figure 28. Novel thienopyrimide-based geranylgeranyl diphosphate synthase inhibitors (Lacbay et al., 2018).

A) Structure of compound 10 B) Structure of compound 11.

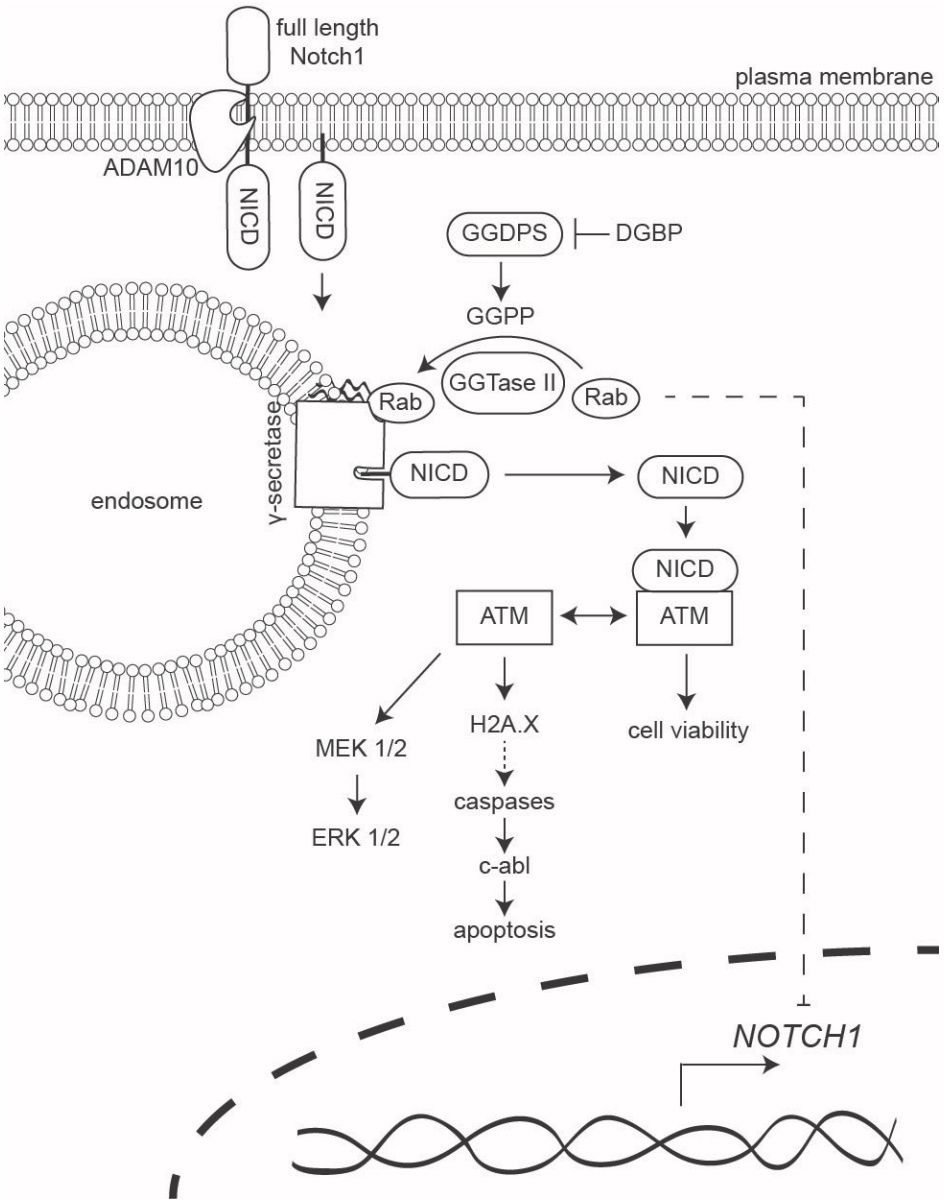

Figure 29. Thesis Summary.

Adam10 cleaves full-length Notch1 which is then transported to the endosome to be cleaved by γ-secretase. GGDPS biosynthesizes GGPP which is then used by geranylgeranyl transferase II (GGTase II) to geranylgeranylate Rab GTPases. Rab GTPases can then localize to the endosome membrane and exert their function at the γ-secretase complex. This then allows for γ-secretase to cleave Notch and release NICD. NICD binds to ATM, preventing its activation. With GGDPS inhibition, however, GGPP is depleted preventing Rab from localizing to the endosome

membrane and preventing γ-secretase from cleaving Notch1. This also decreases transcription of Notch1. This then depletes NICD and allows for ATM activation leading to DNA damage response and apoptosis. ATM activation also activates MEK1/2 and ERK.

References

ADNANE, J., BIZOUARN, F. A., QIAN, Y., HAMILTON, A. D. & SEBTI, S. M. 1998. p21wafi/cipi Is Upregulated by the Geranylgeranyltransferase I Inhibitor GGTI-298 through a Transforming Growth Factor b- and Sp1-Responsive Element: Involvement of the Small GTPase RhoA. *Molecular and cellular biology,* 18**,** 6962-6970.

AGABITI, S. S., LI, J. & WIEMER, A. J. 2017. Geranylgeranyl diphosphate synthase inhibition induces apoptosis that is dependent upon GGPP depletion, ERK phosphorylation and caspase activation. *Cell Death Dis,* 8**,** e2678.

AGABITI, S. S., LIANG, Y. & WIEMER, A. J. 2016. Molecular mechanisms linking geranylgeranyl diphosphate synthase to cell survival and proliferation. *Mol Membr Biol***,** 1-11.

ALAN, J. K. & LUNDQUIST, E. A. 2013. Mutationally activated Rho GTPases in cancer. *Small GTPases,* 4**,** 159-63.

ALLAL, C., FAVRE, G., COUDERC, B., SALICIO, S., SIXOU, S., HAMILTON, A. D., SEBTI, S. M., LAJOIE-MAZENC, I. & PRADINES, A. 2000. RhoA prenylation is required for promotion of cell growth and transformation and cytoskeleton organization but not for induction of serum response element transcription. *J Biol Chem,* 275**,** 31001-8.

ALLAL, C., PRADINES, A., HAMILTON, A. D., SEBTI, S. M. & FAVRE, G. 2002. Farnesylated RhoB prevents cell cycle arrest and actin cytoskeleton disruption caused by the geranylgeranyltransferase I inhibitor GGTI-298. *Cell Cycle,* 1**,** 430-7.

AMIN, D., CORNELL, S. A., GUSTAFSON, S. K., NEEDLE, S. J., ULLRICH, J. W., BILDER, G. E. & PERRONE, M. H. 1992. Bisphosphonates used for the treatment of bone disorders inhibit squalene synthase and cholesterol biosynthesis. *J Lipid Res,* 33**,** 1657-1663.

ANDERSSON, E. R., SANDBERG, R. & LENDAHL, U. 2011. Notch signaling: simplicity in design, versatility in function. *Development,* 138**,** 3593-612.

ANDO, K., KERNAN, J. L., LIU, P. H., SANDA, T., LOGETTE, E., TSCHOPP, J., LOOK, A. T., WANG, J., BOUCHIER-HAYES, L. & SIDI, S. 2012. PIDD death-domain phosphorylation by ATM controls prodeath versus prosurvival PIDDosome signaling. *Mol Cell,* 47**,** 681-93.

APARICIO, A., GARDNER, A., TU, Y., SAVAGE, A., BERENSON, J. & LICHTENSTEIN, A. 1998. In vitro cytoreductive effects on multiple myeloma cells induced by bisphosphonates. *Leukemia,* 12**,** 220-9.

APPELS, N. M., BEIJNEN, J. H. & SCHELLENS, J. H. 2005. Development of farnesyl transferase inhibitors: a review. *Oncologist,* 10**,** 565-78.

BABA, T. T., NEMOTO, T. K., MIYAZAKI, T. & OIDA, S. 2008. Simvastatin suppresses the differentiation of C2C12 myoblast cells via a Rac pathway. *J Muscle Res Cell Motil,* 29**,** 127-34.

BARILA, D., RUFINI, A., CONDO, I., VENTURA, N., DOREY, K., SUPERTI-FURGA, G. & TESTI, R. 2003. Caspase-dependent cleavage of c-Abl contributes to apoptosis. *Mol Cell Biol,* 23**,** 2790-9.

BARNEY, R. J., WASKO, B. M., DUDAKOVIC, A., HOHL, R. J. & WIEMER, D. F. 2010. Synthesis and biological evaluation of a series of aromatic bisphosphonates. *Bioorg Med Chem,* 18**,** 7212-20.

BAULCH-BROWN, C., MOLLOY, T. J., YEH, S. L., MA, D. & SPENCER, A. 2007. Inhibitors of the mevalonate pathway as potential therapeutic agents in multiple myeloma. *Leuk Res,* 31**,** 341-52.

BENFORD, H. L., FRITH, J. C., AURIOLA, S., MONKKONEN, J. & ROGERS, M. J. 1999. Farnesol and geranylgeraniol prevent activation of caspases by aminobisphosphonates: biochemical evidence for two distinct pharmacological classes of bisphosphonate drugs. *Mol Pharmacol,* 56**,** 131-40.

BENNIS, F., FAVRE, G., LE GAILLARD, F. & SOULA, G. 1993. Importance of mevalonate-derived products in the control of HMG-CoA reductase activity and growth of human lung adenocarcinoma cell line A549. *Int J Cancer,* 55**,** 640-5.

BERGSTROM, J. D., BOSTEDOR, R. G., MASARACHIA, P. J., RESZKA, A. A. & RODAN, G. 2000. Alendronate is a specific, nanomolar inhibitor of farnesyl diphosphate synthase. *Arch Biochem Biophys,* 373**,** 231-241.

BERNDT, N., HAMILTON, A. D. & SEBTI, S. M. 2011. Targeting protein prenylation for cancer therapy. *Nat Rev Cancer,* 11**,** 775-91.

BLANCO-COLIO, L. M., VILLA, A., ORTEGO, M., HERNANDEZ-PRESA, M. A., PASCUAL, A., PLAZA, J. J. & EGIDO, J. 2002. 3-Hydroxy-3-methyl-glutaryl coenzyme A reductase inhibitors, atorvastatin and simvastatin, induce apoptosis of vascular smooth muscle cells by downregulation of Bcl-2 expression and Rho A prenylation. *Atherosclerosis,* 161**,** 17-26.

BODY, J. J. 2006. Bisphosphonates for malignancy-related bone disease: current status, future developments. *Support Care Cancer,* 14**,** 408-18.

BORDIER, C. 1981. Phase separation of integral membrane proteins in Triton X-114 solution. *J Biol Chem,* 256**,** 1604-7.

BRINKKOETTER, P. T., GOTTMANN, U., SCHULTE, J., VAN DER WOUDE, F. J., BRAUN, C. & YARD, B. A. 2006. Atorvastatin interferes with activation of human CD4(+) T cells via inhibition of small guanosine triphosphatase (GTPase) activity and caspase-independent apoptosis. *Clin Exp Immunol,* 146**,** 524-32.

BROWN, M. S. & GOLDSTEIN, J. L. 1980. Multivalent feedback regulation of HMG CoA reductase, a control mechanism coordinating isoprenoid synthesis and cell growth. *J Lipid Res,* 21**,** 505-17.

BROWN, M. S. & GOLDSTEIN, J. L. 1997. The SREBP pathway: regulation of cholesterol metabolism by proteolysis of a membrane-bound transcription factor. *Cell,* 89**,** 331-40.

BROWN, M. S. & GOLDSTEIN, J. L. 2009. Cholesterol feedback: from Schoenheimer's bottle to Scap's MELADL. *J Lipid Res,* 50 Suppl**,** S15-27.

BRUNNER, T. B., HAHN, S. M., GUPTA, A. K., MUSCHEL, R. J., MCKENNA, W. G. & BERNHARD, E. J. 2003. Farnesyltransferase inhibitors: an overview of the results of preclinical and clinical investigations. *Cancer Res,* 63**,** 5656-68.

BRZOZOWA-ZASADA, M., PIECUCH, A., MICHALSKI, M., SEGIET, O., KUREK, J., HARABIN-SLOWINSKA, M. & WOJNICZ, R. 2017. Notch and its oncogenic activity in human malignancies. *Eur Surg,* 49**,** 199-209.

CARTER, J. A. & BOTTEMAN, M. F. 2012. Health-economic review of zoledronic acid for the management of skeletal-related events in bone-metastatic prostate cancer. *Expert Rev Pharmacoecon Outcomes Res,* 12**,** 425-37.

CHAPLET, M. L., DETRY, D., DEROANNE, C., FISHER, L. W., CASTRONOVO, V. & BELLAHCENE, A. 2004. Zoledronic acid up-regulates bone sialoprotein expression in osteoblastic cells through Rho GTPase inhibition. *Biochemical Journal,* 384**,** 591-598.
CHEN, C. K.-M., HUDOCK, M. P., ZHANG, Y., GUO, R. T., CAO, R., NO, J. H., LIANG, P. H., KO, T. P., CHANG, T. H., CHANG, S. C., SONG, Y., AXELSON, J., KUMAR, A., WANG, A. H. & OLDFIELD, E. 2008. Inhibition of geranylgeranyl diphosphate synthase by bisphosphonates: a crystallographic and computational investigation. *J Med Chem,* 51**,** 5594-607.
CHEN, S. H., LIN, S. W., LIN, S. R., LIANG, P. H. & YANG, J. M. 2013. Moiety-linkage map reveals selective nonbisphosphonate inhibitors of human geranylgeranyl diphosphate synthase. *J Chem Inf Model,* 53**,** 2299-311.
CHENG, F. & OLDFIELD, E. 2004. Inhibition of isoprene biosynthesis pathway enzymes by phosphonates, bisphosphonates, and diphosphates. *J Med Chem,* 47**,** 5149-58.
CHOU, T. C. & TALALAY, P. 1984. Quantitative analysis of dose-effect relationships: the combined effects of multiple drugs or enzyme inhibitors. *Adv Enzyme Regul,* 22**,** 27-55.
CHU, D. T. & KLYMKOWSKY, M. W. 1989. The appearance of acetylated alpha-tubulin during early development and cellular differentiation in Xenopus. *Dev Biol,* 136**,** 104-17.
CHUAH, C., BARNES, D. J., KWOK, M., CORBIN, A., DEININGER, M. W., DRUKER, B. J. & MELO, J. V. 2005. Zoledronate inhibits proliferation and induces apoptosis of imatinib-resistant chronic myeloid leukaemia cells. *Leukemia,* 19**,** 1896-904.
CIOSEK, C. P., JR., MAGNIN, D. R., HARRITY, T. W., LOGAN, J. V., DICKSON, J. K., JR., GORDON, E. M., HAMILTON, K. A., JOLIBOIS, K. G., KUNSELMAN, L. K., LAWRENCE, R. M. & ET AL. 1993. Lipophilic 1,1-bisphosphonates are potent squalene synthase inhibitors and orally active cholesterol lowering agents in vivo. *J Biol Chem,* 268**,** 24832-7.
CLENDENING, J. W., PANDYRA, A., BOUTROS, P. C., EL GHAMRASNI, S., KHOSRAVI, F., TRENTIN, G. A., MARTIROSYAN, A., HAKEM, A., HAKEM, R., JURISICA, I. & PENN, L. Z. 2010. Dysregulation of the mevalonate pathway promotes transformation. *Proc Natl Acad Sci U S A,* 107**,** 15051-6.
CLEZARDIN, P., BENZAID, I. & CROUCHER, P. I. 2011. Bisphosphonates in preclinical bone oncology. *Bone,* 49**,** 66-70.
COTTINI, F., HIDESHIMA, T., XU, C., SATTLER, M., DORI, M., AGNELLI, L., TEN HACKEN, E., BERTILACCIO, M. T., ANTONINI, E., NERI, A., PONZONI, M., MARCATTI, M., RICHARDSON, P. G., CARRASCO, R., KIMMELMAN, A. C., WONG, K. K., CALIGARIS-CAPPIO, F., BLANDINO, G., KUEHL, W. M., ANDERSON, K. C. & TONON, G. 2014. Rescue of Hippo coactivator YAP1 triggers DNA damage-induced apoptosis in hematological cancers. *Nat Med,* 20**,** 599-606.
COURT, H., AHEARN, I. M., AMOYEL, M., BACH, E. A. & PHILIPS, M. R. 2017. Regulation of NOTCH signaling by RAB7 and RAB8 requires carboxyl methylation by ICMT. *J Cell Biol,* 216**,** 4165-4182.
COX, A. D., DER, C. J. & PHILIPS, M. R. 2015. Targeting RAS Membrane Association: Back to the Future for Anti-RAS Drug Discovery? *Clin Cancer Res,* 21**,** 1819-27.
DAI, Y., KHANNA, P., CHEN, S., PEI, X. Y., DENT, P. & GRANT, S. 2007. Statins synergistically potentiate 7-hydroxystaurosporine (UCN-01) lethality in human leukemia and myeloma cells by disrupting Ras farnesylation and activation. *Blood,* 109**,** 4415-23.

DANKBAR, B., PADRO, T., LEO, R., FELDMANN, B., KROPFF, M., MESTERS, R. M., SERVE, H., BERDEL, W. E. & KIENAST, J. 2000. Vascular endothelial growth factor and interleukin-6 in paracrine tumor-stromal cell interactions in multiple myeloma. *Blood,* 95**,** 2630-6.

DEININGER, M. W., GOLDMAN, J. M. & MELO, J. V. 2000. The molecular biology of chronic myeloid leukemia. *Blood,* 96**,** 3343-56.

DENOYELLE, C., HONG, L., VANNIER, J. P., SORIA, J. & SORIA, C. 2003. New insights into the actions of bisphosphonate zoledronic acid in breast cancer cells by dual RhoA-dependent and -independent effects. *British journal of cancer,* 88**,** 1631-1640.

DEWICK, P. M. 2002. The biosynthesis of C5-C25 terpenoid compounds. *Nat Prod Rep,* 19**,** 181-222.

DI AGOSTINO, S., SORRENTINO, G., INGALLINA, E., VALENTI, F., FERRAIUOLO, M., BICCIATO, S., PIAZZA, S., STRANO, S., DEL SAL, G. & BLANDINO, G. 2016. YAP enhances the pro-proliferative transcriptional activity of mutant p53 proteins. *EMBO Rep,* 17**,** 188-201.

DIEKMANN, D., BRILL, S., GARRETT, M. D., TOTTY, N., HSUAN, J., MONFRIES, C., HALL, C., LIM, L. & HALL, A. 1991. Bcr encodes a GTPase-activating protein for p21rac. *Nature,* 351**,** 400-2.

DOI, K., IMAI, T., KRESSLER, C., YAGITA, H., AGATA, Y., VOOIJS, M., HAMAZAKI, Y., INOUE, J. & MINATO, N. 2015. Crucial role of the Rap G protein signal in Notch activation and leukemogenicity of T-cell acute lymphoblastic leukemia. *Sci Rep,* 5**,** 7978.

DUDAKOVIC, A., TONG, H. & HOHL, R. J. 2011. Geranylgeranyl diphosphate depletion inhibits breast cancer cell migration. *Invest New Drugs,* 29**,** 912-20.

DUDAKOVIC, A., WIEMER, A. J., LAMB, K. M., VONNAHME, L. A., DIETZ, S. E. & HOHL, R. J. 2008. Inhibition of geranylgeranyl diphosphate synthase induces apoptosis through multiple mechanisms and displays synergy with inhibition of other isoprenoid biosynthetic enzymes. *J Pharmacol Exp Ther,* 324**,** 1028-1036.

DUMANCHIN, C., CZECH, C., CAMPION, D., CUIF, M. H., POYOT, T., MARTIN, C., CHARBONNIER, F., GOUD, B., PRADIER, L. & FREBOURG, T. 1999. Presenilins interact with Rab11, a small GTPase involved in the regulation of vesicular transport. *Hum Mol Genet,* 8**,** 1263-9.

DUNFORD, J. E., ROGERS, M. J., EBETINO, F. H., PHIPPS, R. J. & COXON, F. P. 2006. Inhibition of protein prenylation by bisphosphonates causes sustained activation of Rac, Cdc42, and Rho GTPases. *J Bone Miner Res,* 21**,** 684-94.

DYKSTRA, K. M., ALLEN, C., BORN, E. J., TONG, H. & HOLSTEIN, S. A. 2015. Mechanisms for autophagy modulation by isoprenoid biosynthetic pathway inhibitors in multiple myeloma cells. *Oncotarget,* 6**,** 41535-49.

EBETINO, F. H., HOGAN, A. M., SUN, S., TSOUMPRA, M. K., DUAN, X., TRIFFITT, J. T., KWAASI, A. A., DUNFORD, J. E., BARNETT, B. L., OPPERMANN, U., LUNDY, M. W., BOYDE, A., KASHEMIROV, B. A., MCKENNA, C. E. & RUSSELL, R. G. 2011. The relationship between the chemistry and biological activity of the bisphosphonates. *Bone,* 49**,** 20-33.

FALSETTI, S. C., WANG, D. A., PENG, H., CARRICO, D., COX, A. D., DER, C. J., HAMILTON, A. D. & SEBTI, S. M. 2007. Geranylgeranyltransferase I inhibitors target RalB to inhibit anchorage-dependent growth and induce apoptosis and RalA to inhibit anchorage-independent growth. *Mol Cell Biol,* 27**,** 8003-14.

FORBES, S. A., BEARE, D., BOUTSELAKIS, H., BAMFORD, S., BINDAL, N., TATE, J., COLE, C. G., WARD, S., DAWSON, E., PONTING, L., STEFANCSIK, R., HARSHA, B., KOK, C. Y., JIA, M., JUBB, H., SONDKA, Z., THOMPSON, S., DE, T. & CAMPBELL, P. J. 2017. COSMIC: somatic cancer genetics at high-resolution. *Nucleic Acids Res,* 45**,** D777-D783.

FOURNIER, P. G., DAUBINE, F., LUNDY, M. W., ROGERS, M. J., EBETINO, F. H. & CLEZARDIN, P. 2008. Lowering bone mineral affinity of bisphosphonates as a therapeutic strategy to optimize skeletal tumor growth inhibition in vivo. *Cancer Res,* 68**,** 8945-53.

FOURNIER, P. G., STRESING, V., EBETINO, F. H. & CLÉZARDIN, P. 2010. How Do Bisphosphonates Inhibit Bone Metastasis In Vivo? *Neoplasia (New York, N.Y.),* 12**,** 571-578.

FREED-PASTOR, W. A., MIZUNO, H., ZHAO, X., LANGEROD, A., MOON, S. H., RODRIGUEZ-BARRUECO, R., BARSOTTI, A., CHICAS, A., LI, W., POLOTSKAIA, A., BISSELL, M. J., OSBORNE, T. F., TIAN, B., LOWE, S. W., SILVA, J. M., BORRESEN-DALE, A. L., LEVINE, A. J., BARGONETTI, J. & PRIVES, C. 2012. Mutant p53 disrupts mammary tissue architecture via the mevalonate pathway. *Cell,* 148**,** 244-58.

FROMIGUE, O., HAY, E., MODROWSKI, D., BOUVET, S., JACQUEL, A., AUBERGER, P. & MARIE, P. J. 2006. RhoA GTPase inactivation by statins induces osteosarcoma cell apoptosis by inhibiting p42/p44-MAPKs-Bcl-2 signaling independently of BMP-2 and cell differentiation. *Cell Death Differ,* 13**,** 1845-56.

GBELCOVA, H., RIMPELOVA, S., KNEJZLIK, Z., SACHOVA, J., KOLAR, M., STRNAD, H., REPISKA, V., D'ACUNTO, W. C., RUML, T. & VITEK, L. 2017. Isoprenoids responsible for protein prenylation modulate the biological effects of statins on pancreatic cancer cells. *Lipids Health Dis,* 16**,** 250.

GHOSH, P. M., GHOSH-CHOUDHURY, N., MOYER, M. L., MOTT, G. E., THOMAS, C. A., FOSTER, B. A., GREENBERG, N. M. & KREISBERG, J. I. 1999. Role of RhoA activation in the growth and morphology of a murine prostate tumor cell line. *Oncogene,* 18**,** 4120-30.

GNANT, M. 2012. Adjuvant bisphosphonates: a new standard of care? *Curr Opin Oncol,* 24**,** 635-42.

GOKEY, N. G., LOPEZ-ANIDO, C., GILLIAN-DANIEL, A. L. & SVAREN, J. 2011. Early growth response 1 (Egr1) regulates cholesterol biosynthetic gene expression. *J Biol Chem,* 286**,** 29501-10.

GORDON, W. R., VARDAR-ULU, D., HISTEN, G., SANCHEZ-IRIZARRY, C., ASTER, J. C. & BLACKLOW, S. C. 2007. Structural basis for autoinhibition of Notch. *Nat Struct Mol Biol,* 14**,** 295-300.

GUENTHER, A., GORDON, S., TIEMANN, M., BURGER, R., BAKKER, F., GREEN, J. R., BAUM, W., ROELOFS, A. J., ROGERS, M. J. & GRAMATZKI, M. 2010. The bisphosphonate zoledronic acid has antimyeloma activity in vivo by inhibition of protein prenylation. *Int J Cancer,* 126**,** 239-46.

GUO, R. T., CAO, R., LIANG, P. H., KO, T. P., CHANG, T. H., HUDOCK, M. P., JENG, W. Y., CHEN, C. K., ZHANG, Y., SONG, Y., KUO, C. J., YIN, F., OLDFIELD, E. & WANG, A. H. 2007. Bisphosphonates target multiple sites in both cis- and trans-prenyltransferases. *Proc Natl Acad Sci U S A,* 104**,** 10022-10027.

HAHNE, K., VERVACKE, J. S., SHRESTHA, L., DONELSON, J. L., GIBBS, R. A., DISTEFANO, M. D. & HRYCYNA, C. A. 2012. Evaluation of substrate and inhibitor binding to yeast and human isoprenylcysteine carboxyl methyltransferases (Icmts) using biotinylated benzophenone-containing photoaffinity probes. *Biochem Biophys Res Commun,* 423**,** 98-103.

HAMDY, R. C. 2010. Zoledronic acid: clinical utility and patient considerations in osteoporosis and low bone mass. *Drug Des Devel Ther,* 4**,** 321-35.

HANEY, S. L., CHHONKER, Y. S., VARNEY, M. L., TALMON, G., MURRY, D. J. & HOLSTEIN, S. A. 2018. Preclinical investigation of a potent geranylgeranyl diphosphate synthase inhibitor. *Invest New Drugs*.

HANTSCHEL, O. 2012. Structure, regulation, signaling, and targeting of abl kinases in cancer. *Genes Cancer,* 3**,** 436-46.

HASMIM, M., BIELER, G. & RUEGG, C. 2007. Zoledronate inhibits endothelial cell adhesion, migration and survival through the suppression of multiple, prenylation-dependent signaling pathways. *J Thromb Haemost,* 5**,** 166-73.

HAYES, T. K., NEEL, N. F., HU, C., GAUTAM, P., CHENARD, M., LONG, B., AZIZ, M., KASSNER, M., BRYANT, K. L., PIEROBON, M., MARAYATI, R., KHER, S., GEORGE, S. D., XU, M., WANG-GILLAM, A., SAMATAR, A. A., MAITRA, A., WENNERBERG, K., PETRICOIN, E. F., 3RD, YIN, H. H., NELKIN, B., COX, A. D., YEH, J. J. & DER, C. J. 2016. Long-Term ERK Inhibition in KRAS-Mutant Pancreatic Cancer Is Associated with MYC Degradation and Senescence-like Growth Suppression. *Cancer Cell,* 29**,** 75-89.

HENDRIX, A., MAYNARD, D., PAUWELS, P., BRAEMS, G., DENYS, H., VAN DEN BROECKE, R., LAMBERT, J., VAN BELLE, S., COCQUYT, V., GESPACH, C., BRACKE, M., SEABRA, M. C., GAHL, W. A., DE WEVER, O. & WESTBROEK, W. 2010. Effect of the secretory small GTPase Rab27B on breast cancer growth, invasion, and metastasis. *J Natl Cancer Inst,* 102**,** 866-80.

HENNEMAN, L., VAN CRUCHTEN, A. G., DENIS, S. W., AMOLINS, M. W., PLACZEK, A. T., GIBBS, R. A., KULIK, W. & WATERHAM, H. R. 2008. Detection of nonsterol isoprenoids by HPLC-MS/MS. *Anal Biochem,* 383**,** 18-24.

HENTSCHEL, A., ZAHEDI, R. P. & AHRENDS, R. 2016. Protein lipid modifications--More than just a greasy ballast. *Proteomics,* 16**,** 759-82.

HINSON, D. D., CHAMBLISS, K. L., TOTH, M. J., TANAKA, R. D. & GIBSON, K. M. 1997. Post-translational regulation of mevalonate kinase by intermediates of the cholesterol and nonsterol isoprene biosynthetic pathways. *J Lipid Res,* 38**,** 2216-23.

HIRAI, A., NAKAMURA, S., NOGUCHI, Y., YASUDA, T., KITAGAWA, M., TATSUNO, I., OEDA, T., TAHARA, K., TERANO, T., NARUMIYA, S., KOHN, L. D. & SAITO, Y. 1997. Geranylgeranylated rho small GTPase(s) are essential for the degradation of p27Kip1 and facilitate the progression from G1 to S phase in growth-stimulated rat FRTL-5 cells. *J Biol Chem,* 272**,** 13-6.

HOTTMAN, D. A. & LI, L. 2014. Protein prenylation and synaptic plasticity: implications for Alzheimer's disease. *Mol Neurobiol,* 50**,** 177-85.

HOUGLAND, J. L., LAMPHEAR, C. L., SCOTT, S. A., GIBBS, R. A. & FIERKE, C. A. 2009. Context-dependent substrate recognition by protein farnesyltransferase. *Biochemistry,* 48**,** 1691-701.

HSIAO, C. H., LIN, X., BARNEY, R. J., SHIPPY, R. R., LI, J., VINOGRADOVA, O., WIEMER, D. F. & WIEMER, A. J. 2014. Synthesis of a phosphoantigen prodrug that potently activates Vgamma9Vdelta2 T-lymphocytes. *Chem Biol,* 21**,** 945-54.

HUA, X., YOKOYAMA, C., WU, J., BRIGGS, M. R., BROWN, M. S., GOLDSTEIN, J. L. & WANG, X. 1993. SREBP-2, a second basic-helix-loop-helix-leucine zipper protein that stimulates transcription by binding to a sterol regulatory element. *Proc Natl Acad Sci U S A,* 90**,** 11603-7.

IBRAHIM, A., SCHER, N., WILLIAMS, G., SRIDHARA, R., LI, N., CHEN, G., LEIGHTON, J., BOOTH, B., GOBBURU, J. V., RAHMAN, A., HSIEH, Y., WOOD, R., VAUSE, D. & PAZDUR, R. 2003. Approval summary for zoledronic acid for treatment of multiple myeloma and cancer bone metastases. *Clin Cancer Res,* 9**,** 2394-9.

INOUE, R., MATSUKI, N. A., JING, G., KANEMATSU, T., ABE, K. & HIRATA, M. 2005. The inhibitory effect of alendronate, a nitrogen-containing bisphosphonate on the PI3K-Akt-NFkappaB pathway in osteosarcoma cells. *Br J Pharmacol,* 146**,** 633-41.

ISHIKAWA, C., MATSUDA, T., OKUDAIRA, T., TOMITA, M., KAWAKAMI, H., TANAKA, Y., MASUDA, M., OHSHIRO, K., OHTA, T. & MORI, N. 2007. Bisphosphonate incadronate inhibits growth of human T-cell leukaemia virus type I-infected T-cell lines and primary adult T-cell leukaemia cells by interfering with the mevalonate pathway. *Br J Haematol,* 136**,** 424-32.

JIANG, P., MUKTHAVARAM, R., CHAO, Y., NOMURA, N., BHARATI, I. S., FOGAL, V., PASTORINO, S., TENG, D., CONG, X., PINGLE, S. C., KAPOOR, S., SHETTY, K., AGGRAWAL, A., VALI, S., ABBASI, T., CHIEN, S. & KESARI, S. 2014. In vitro and in vivo anticancer effects of mevalonate pathway modulation on human cancer cells. *Br J Cancer,* 111**,** 1562-71.

KAPOOR, A., YAO, W., YING, H., HUA, S., LIEWEN, A., WANG, Q., ZHONG, Y., WU, C. J., SADANANDAM, A., HU, B., CHANG, Q., CHU, G. C., AL-KHALIL, R., JIANG, S., XIA, H., FLETCHER-SANANIKONE, E., LIM, C., HORWITZ, G. I., VIALE, A., PETTAZZONI, P., SANCHEZ, N., WANG, H., PROTOPOPOV, A., ZHANG, J., HEFFERNAN, T., JOHNSON, R. L., CHIN, L., WANG, Y. A., DRAETTA, G. & DEPINHO, R. A. 2014. Yap1 activation enables bypass of oncogenic Kras addiction in pancreatic cancer. *Cell,* 158**,** 185-97.

KAVANAGH, K. L., DUNFORD, J. E., BUNKOCZI, G., RUSSELL, R. G. & OPPERMANN, U. 2006a. The crystal structure of human geranylgeranyl pyrophosphate synthase reveals a novel hexameric arrangement and inhibitory product binding. *J Biol Chem,* 281**,** 22004-12.

KAVANAGH, K. L., GUO, K., DUNFORD, J. E., WU, X., KNAPP, S., EBETINO, F. H., ROGERS, M. J., RUSSELL, R. G. & OPPERMANN, U. 2006b. The molecular mechanism of nitrogen-containing bisphosphonates as antiosteoporosis drugs. *Proc Natl Acad Sci U S A,* 103**,** 7829-7834.

KIMURA, S. K. J., SEGAWA, H., SATO, K., NOGAWA, M., YUASA, T. O. K. & MAEKAWA, T. 2004. Antiproliferative efficacy of the third-generation bisphosphonate, zoledronic acid, combined with other anticancer drugs in leukemia cell lines. *International journal of hematology,* 79**,** 37-43.

KIYOKAWA, T., YAMAGUCHI, K., TAKEYA, M., TAKAHASHI, K., WATANABE, T., MATSUMOTO, T., LEE, S. Y. & TAKATSUKI, K. 1987. Hypercalcemia and osteoclast proliferation in adult T-cell leukemia. *Cancer,* 59**,** 1187-91.

KORWEK, Z., SEWASTIANIK, T., BIELAK-ZMIJEWSKA, A., MOSIENIAK, G., ALSTER, O., MORENO-VILLANUEVA, M., BURKLE, A. & SIKORA, E. 2012. Inhibition of ATM blocks the etoposide-induced DNA damage response and apoptosis of resting human T cells. *DNA Repair (Amst),* 11**,** 864-73.

KOTAMRAJU, S., WILLIAMS, C. L. & KALYANARAMAN, B. 2007. Statin-induced breast cancer cell death: role of inducible nitric oxide and arginase-dependent pathways. *Cancer Res,* 67**,** 7386-94.

KUZUGUCHI, T., MORITA, Y., SAGAMI, I., SAGAMI, H. & OGURA, K. 1999. Human geranylgeranyl diphosphate synthase. cDNA cloning and expression. *J Biol Chem,* 274**,** 5888-94.

LACBAY, C. M., WALLER, D. D., PARK, J., GOMEZ PALOU, M., VINCENT, F., HUANG, X. F., TA, V., BERGHUIS, A. M., SEBAG, M. & TSANTRIZOS, Y. S. 2018. Unraveling the Prenylation-Cancer Paradox in Multiple Myeloma with Novel Geranylgeranyl Pyrophosphate Synthase (GGPPS) Inhibitors. *J Med Chem*.

LEE, J. S., ROBERTS, A., JUAREZ, D., VO, T. T., BHATT, S., HERZOG, L. O., MALLYA, S., BELLIN, R. J., AGARWAL, S. K., SALEM, A. H., XU, T., JIA, J., LI, L., HANNA, J. R., DAVIDS, M. S., FLEISCHMAN, A. G., O'BRIEN, S., LAM, L. T., LEVERSON, J. D., LETAI, A., SCHATZ, J. H. & FRUMAN, D. A. 2018. Statins enhance efficacy of venetoclax in blood cancers. *Sci Transl Med,* 10.

LEFORT, K., MANDINOVA, A., OSTANO, P., KOLEV, V., CALPINI, V., KOLFSCHOTEN, I., DEVGAN, V., LIEB, J., RAFFOUL, W., HOHL, D., NEEL, V., GARLICK, J., CHIORINO, G. & DOTTO, G. P. 2007. Notch1 is a p53 target gene involved in human keratinocyte tumor suppression through negative regulation of ROCK1/2 and MRCKalpha kinases. *Genes Dev,* 21**,** 562-77.

LEI, Q. Y., ZHANG, H., ZHAO, B., ZHA, Z. Y., BAI, F., PEI, X. H., ZHAO, S., XIONG, Y. & GUAN, K. L. 2008. TAZ promotes cell proliferation and epithelial-mesenchymal transition and is inhibited by the hippo pathway. *Mol Cell Biol,* 28**,** 2426-36.

LEICHNER, G. S., AVNER, R., HARATS, D. & ROITELMAN, J. 2011. Metabolically regulated endoplasmic reticulum-associated degradation of 3-hydroxy-3-methylglutaryl-CoA reductase: evidence for requirement of a geranylgeranylated protein. *J Biol Chem,* 286**,** 32150-61.

LEVY, D., ADAMOVICH, Y., REUVEN, N. & SHAUL, Y. 2008. Yap1 phosphorylation by c-Abl is a critical step in selective activation of proapoptotic genes in response to DNA damage. *Mol Cell,* 29**,** 350-61.

LI, J., FALCONE, E. R., HOLSTEIN, S. A., ANDERSON, A. C., WRIGHT, D. L. & WIEMER, A. J. 2016. Novel alpha-substituted tropolones promote potent and selective caspase-dependent leukemia cell apoptosis. *Pharmacol Res,* 113**,** 438-448.

LI, X., LIU, L., TUPPER, J. C., BANNERMAN, D. D., WINN, R. K., SEBTI, S. M., HAMILTON, A. D. & HARLAN, J. M. 2002. Inhibition of protein geranylgeranylation and RhoA/RhoA kinase pathway induces apoptosis in human endothelial cells. *J Biol Chem,* 277**,** 15309-16.

LICATA, A. A. 2005. Discovery, clinical development, and therapeutic uses of bisphosphonates. *Ann Pharmacother,* 39**,** 668-77.

LIN, J. J. 1981. Monoclonal antibodies against myofibrillar components of rat skeletal muscle decorate the intermediate filaments of cultured cells. *Proc Natl Acad Sci U S A,* 78**,** 2335-9.

LIU, B. S., XIA, H. W., ZHOU, S., LIU, Q., TANG, Q. L., BI, N. X., ZHOU, J. T., GONG, Q. Y., NIE, Y. Z. & BI, F. 2018. Inhibition of YAP reverses primary resistance to EGFR inhibitors in colorectal cancer cells. *Oncol Rep,* 40**,** 2171-2182.

LOBELL, R. B., OMER, C. A., ABRAMS, M. T., BHIMNATHWALA, H. G., BRUCKER, M. J., BUSER, C. A., DAVIDE, J. P., DESOLMS, S. J., DINSMORE, C. J., ELLIS-HUTCHINGS, M. S., KRAL, A. M., LIU, D., LUMMA, W. C., MACHOTKA, S. V., RANDS, E., WILLIAMS, T. M., GRAHAM, S. L., HARTMAN, G. D., OLIFF, A. I., HEIMBROOK, D. C. & KOHL, N. E. 2001. Evaluation of farnesyl:protein transferase and geranylgeranyl:protein transferase inhibitor combinations in preclinical models. *Cancer Res,* 61**,** 8758-68.

LUCKMAN, S. P., HUGHES, D. E., COXON, F. P., GRAHAM, R., RUSSELL, G. & ROGERS, M. J. 1998. Nitrogen-containing bisphosphonates inhibit the mevalonate pathway and prevent post-translational prenylation of GTP-binding proteins, including Ras. *J Bone Miner Res,* 13**,** 581-9.

LUGO, T. G., PENDERGAST, A. M., MULLER, A. J. & WITTE, O. N. 1990. Tyrosine kinase activity and transformation potency of bcr-abl oncogene products. *Science,* 247**,** 1079-82.

MACHUY, N., RAJALINGAM, K. & RUDEL, T. 2004. Requirement of caspase-mediated cleavage of c-Abl during stress-induced apoptosis. *Cell Death Differ,* 11**,** 290-300.

MAEDA, A., YANO, T., ITOH, Y., KAKUMORI, M., KUBOTA, T., EGASHIRA, N. & OISHI, R. 2010. Down-regulation of RhoA is involved in the cytotoxic action of lipophilic statins in HepG2 cells. *Atherosclerosis,* 208**,** 112-8.

MALWAL, S. R., O'DOWD, B., FENG, X., TURHANEN, P., SHIN, C., YAO, J., KIM, B. K., BAIG, N., ZHOU, T., BANSAL, S., KHADE, R. L., ZHANG, Y. & OLDFIELD, E. 2018. Bisphosphonate-Generated ATP-Analogs Inhibit Cell Signaling Pathways. *J Am Chem Soc,* 140**,** 7568-7578.

MARTIN, M. B., ARNOLD, W., HEATH, H. T., 3RD, URBINA, J. A. & OLDFIELD, E. 1999. Nitrogen-containing bisphosphonates as carbocation transition state analogs for isoprenoid biosynthesis. *Biochem Biophys Res Commun,* 263**,** 754-758.

MATT, S. & HOFMANN, T. G. 2016. The DNA damage-induced cell death response: a roadmap to kill cancer cells. *Cell Mol Life Sci,* 73**,** 2829-50.

MAURER-STROH, S., KORANDA, M., BENETKA, W., SCHNEIDER, G., SIROTA, F. L. & EISENHABER, F. 2007. Towards complete sets of farnesylated and geranylgeranylated proteins. *PLoS Comput Biol,* 3**,** e66.

MCCORMICK, F. 2015. The potential of targeting Ras proteins in lung cancer. *Expert Opin Ther Targets,* 19**,** 451-4.

MENG, Z., MOROISHI, T. & GUAN, K. L. 2016. Mechanisms of Hippo pathway regulation. *Genes Dev,* 30**,** 1-17.

MITROFAN, L. M., PELKONEN, J. & MONKKONEN, J. 2009. The level of ATP analog and isopentenyl pyrophosphate correlates with zoledronic acid-induced apoptosis in cancer cells in vitro. *Bone,* 45**,** 1153-60.

MIYAGI, Y., MATSUMURA, Y. & SAGAMI, H. 2007. Human geranylgeranyl diphosphate synthase is an octamer in solution. *J Biochem,* 142**,** 377-81.

MO, H. & ELSON, C. E. 2004. Studies of the isoprenoid-mediated inhibition of mevalonate synthesis applied to cancer chemotherapy and chemoprevention. *Exp Biol Med (Maywood),* 229**,** 567-85.

MOHAMMED, I., HAMPTON, S. E., ASHALL, L., HILDEBRANDT, E. R., KUTLIK, R. A., MANANDHAR, S. P., FLOYD, B. J., SMITH, H. E., DOZIER, J. K., DISTEFANO, M. D., SCHMIDT, W. K. & DORE, T. M. 2016. 8-Hydroxyquinoline-based inhibitors of the Rce1 protease disrupt Ras membrane localization in human cells. *Bioorg Med Chem,* 24**,** 160-78.

MOROHASHI, Y., KAN, T., TOMINARI, Y., FUWA, H., OKAMURA, Y., WATANABE, N., SATO, C., NATSUGARI, H., FUKUYAMA, T., IWATSUBO, T. & TOMITA, T. 2006. C-terminal fragment of presenilin is the molecular target of a dipeptidic gamma-secretase-specific inhibitor DAPT (N-[N-(3,5-difluorophenacetyl)-L-alanyl]-S-phenylglycine t-butyl ester). *J Biol Chem,* 281**,** 14670-6.

MUGONI, V., POSTEL, R., CATANZARO, V., DE LUCA, E., TURCO, E., DIGILIO, G., SILENGO, L., MURPHY, M. P., MEDANA, C., STAINIER, D. Y., BAKKERS, J. & SANTORO, M. M. 2013. Ubiad1 is an antioxidant enzyme that regulates eNOS activity by CoQ10 synthesis. *Cell,* 152**,** 504-18.

MULLEN, P. J., YU, R., LONGO, J., ARCHER, M. C. & PENN, L. Z. 2016. The interplay between cell signalling and the mevalonate pathway in cancer. *Nat Rev Cancer,* 16**,** 718-731.

NAGATA, Y., KONTANI, K., ENAMI, T., KATAOKA, K., ISHII, R., TOTOKI, Y., KATAOKA, T. R., HIRATA, M., AOKI, K., NAKANO, K., KITANAKA, A., SAKATA-YANAGIMOTO, M., EGAMI, S., SHIRAISHI, Y., CHIBA, K., TANAKA, H., SHIOZAWA, Y., YOSHIZATO, T., SUZUKI, H., KON, A., YOSHIDA, K., SATO, Y., SATO-OTSUBO, A., SANADA, M., MUNAKATA, W., NAKAMURA, H., HAMA, N., MIYANO, S., NUREKI, O., SHIBATA, T., HAGA, H., SHIMODA, K., KATADA, T., CHIBA, S., WATANABE, T. & OGAWA, S. 2016. Variegated RHOA mutations in adult T-cell leukemia/lymphoma. *Blood,* 127**,** 596-604.

NAKAGAWA, K., HIROTA, Y., SAWADA, N., YUGE, N., WATANABE, M., UCHINO, Y., OKUDA, N., SHIMOMURA, Y., SUHARA, Y. & OKANO, T. 2010. Identification of UBIAD1 as a novel human menaquinone-4 biosynthetic enzyme. *Nature,* 468**,** 117-21.

NISHIDA, S., KIKUICHI, S., HAGA, H., YOSHIOKA, S., TSUBAKI, M., FUJII, K. & IRIMAJIRI, K. 2003. Apoptosis-inducing effect of a new bisphosphonate, YM529, on various hematopoietic tumor cell lines. *Biol Pharm Bull,* 26**,** 96-100.

O'NEIL, J., GRIM, J., STRACK, P., RAO, S., TIBBITTS, D., WINTER, C., HARDWICK, J., WELCKER, M., MEIJERINK, J. P., PIETERS, R., DRAETTA, G., SEARS, R., CLURMAN, B. E. & LOOK, A. T. 2007. FBW7 mutations in leukemic cells mediate NOTCH pathway activation and resistance to gamma-secretase inhibitors. *J Exp Med,* 204**,** 1813-24.

O'NEILL, E., RUSHWORTH, L., BACCARINI, M. & KOLCH, W. 2004. Role of the kinase MST2 in suppression of apoptosis by the proto-oncogene product Raf-1. *Science,* 306**,** 2267-70.

OBLAK, E. Z., VANHEYST, M. D., LI, J., WIEMER, A. J. & WRIGHT, D. L. 2014. Cyclopropene cycloadditions with annulated furans: total synthesis of (+)- and (-)-frondosin B and (+)-frondosin A. *J Am Chem Soc,* 136**,** 4309-15.

OHTSUKA, Y., MANABE, A., KAWASAKI, H., HASEGAWA, D., ZAIKE, Y., WATANABE, S., TANIZAWA, T., NAKAHATA, T. & TSUJI, K. 2005. RAS-blocking bisphosphonate zoledronic acid inhibits the abnormal proliferation and differentiation of juvenile myelomonocytic leukemia cells in vitro. *Blood,* 106**,** 3134-41.

OKAMOTO, S., JIANG, Y., KAWAMURA, K., SHINGYOJI, M., TADA, Y., SEKINE, I., TAKIGUCHI, Y., TATSUMI, K., KOBAYASHI, H., SHIMADA, H., HIROSHIMA, K. & TAGAWA, M. 2014. Zoledronic acid induces apoptosis and S-phase arrest in mesothelioma through inhibiting Rab family proteins and topoisomerase II actions. *Cell Death Dis,* 5**,** e1517.

OLSAUSKAS-KUPRYS, R., ZLOBIN, A. & OSIPO, C. 2013. Gamma secretase inhibitors of Notch signaling. *Onco Targets Ther,* 6**,** 943-55.

PADAVANO, J., HENKHAUS, R. S., CHEN, H., SKOVAN, B. A., CUI, H. & IGNATENKO, N. A. 2015. Mutant K-RAS Promotes Invasion and Metastasis in Pancreatic Cancer Through GTPase Signaling Pathways. *Cancer Growth Metastasis,* 8**,** 95-113.

PALOMERO, T., SULIS, M. L., CORTINA, M., REAL, P. J., BARNES, K., CIOFANI, M., CAPARROS, E., BUTEAU, J., BROWN, K., PERKINS, S. L., BHAGAT, G., AGARWAL, A. M., BASSO, G., CASTILLO, M., NAGASE, S., CORDON-CARDO, C., PARSONS, R., ZUNIGA-PFLUCKER, J. C., DOMINGUEZ, M. & FERRANDO, A. A. 2007. Mutational loss of PTEN induces resistance to NOTCH1 inhibition in T-cell leukemia. *Nat Med,* 13**,** 1203-10.

PALSULEDESAI, C. C. & DISTEFANO, M. D. 2015. Protein prenylation: enzymes, therapeutics, and biotechnology applications. *ACS Chem Biol,* 10**,** 51-62.

PANDYRA, A., MULLEN, P. J., KALKAT, M., YU, R., PONG, J. T., LI, Z., TRUDEL, S., LANG, K. S., MINDEN, M. D., SCHIMMER, A. D. & PENN, L. Z. 2014. Immediate utility of two approved agents to target both the metabolic mevalonate pathway and its restorative feedback loop. *Cancer Res,* 74**,** 4772-82.

PANDYRA, A. A., MULLEN, P. J., GOARD, C. A., ERICSON, E., SHARMA, P., KALKAT, M., YU, R., PONG, J. T., BROWN, K. R., HART, T., GEBBIA, M., LANG, K. S., GIAEVER, G., NISLOW, C., MOFFAT, J. & PENN, L. Z. 2015. Genome-wide RNAi analysis reveals that simultaneous inhibition of specific mevalonate pathway genes potentiates tumor cell death. *Oncotarget,* 6**,** 26909-21.

PASSARO, D., QUANG, C. T. & GHYSDAEL, J. 2016. Microenvironmental cues for T-cell acute lymphoblastic leukemia development. *Immunol Rev,* 271**,** 156-72.

PHILIPS, M. R. & COX, A. D. 2007. Geranylgeranyltransferase I as a target for anti-cancer drugs. *J Clin Invest,* 117**,** 1223-1225.

PICCOLO, S., DUPONT, S. & CORDENONSI, M. 2014. The biology of YAP/TAZ: hippo signaling and beyond. *Physiol Rev,* 94**,** 1287-312.

PLOUFFE, S. W., LIN, K. C., MOORE, J. L., 3RD, TAN, F. E., MA, S., YE, Z., QIU, Y., REN, B. & GUAN, K. L. 2018. The Hippo pathway effector proteins YAP and TAZ have both distinct and overlapping functions in the cell. *J Biol Chem,* 293**,** 11230-11240.

POULTER, C. D., ARGYLE, J. C. & MASH, E. A. 1978. Farnesyl pyrophosphate synthetase. Mechanistic studies of the 1'-4 coupling reaction with 2-fluorogeranyl pyrophosphate. *J Biol Chem,* 253**,** 7227-33.

PREUDHOMME, C., ROUMIER, C., HILDEBRAND, M. P., DALLERY-PRUDHOMME, E., LANTOINE, D., LAI, J. L., DAUDIGNON, A., ADENIS, C., BAUTERS, F., FENAUX, P., KERCKAERT, J. P. & GALIEGUE-ZOUITINA, S. 2000. Nonrandom 4p13 rearrangements of the RhoH/TTF gene, encoding a GTP-binding protein, in non-Hodgkin's lymphoma and multiple myeloma. *Oncogene,* 19**,** 2023-32.

PUI, C. H., RELLING, M. V. & DOWNING, J. R. 2004. Acute lymphoblastic leukemia. *N Engl J Med,* 350**,** 1535-48.

QI, X. F., ZHENG, L., LEE, K. J., KIM, D. H., KIM, C. S., CAI, D. Q., WU, Z., QIN, J. W., YU, Y. H. & KIM, S. K. 2013. HMG-CoA reductase inhibitors induce apoptosis of lymphoma cells by promoting ROS generation and regulating Akt, Erk and p38 signals via suppression of mevalonate pathway. *Cell Death Dis,* 4**,** e518.

QIU, R. G., CHEN, J., MCCORMICK, F. & SYMONS, M. 1995. A role for Rho in Ras transformation. *Proc Natl Acad Sci U S A,* 92**,** 11781-5.

RADTKE, F. & RAJ, K. 2003. The role of Notch in tumorigenesis: oncogene or tumour suppressor? *Nat Rev Cancer,* 3**,** 756-67.

RADUJKOVIC, A., TOPALY, J., FRUEHAUF, S. & ZELLER, W. J. 2006. Combination treatment of imatinib-sensitive and -resistant BCR-ABL-positive CML cells with imatinib and farnesyltransferase inhibitors. *Anticancer Res,* 26**,** 2169-77.

RAMAKRISHNAN, V., KIMLINGER, T., HAUG, J., PAINULY, U., WELLIK, L., HALLING, T., RAJKUMAR, S. V. & KUMAR, S. 2012. Anti-myeloma activity of Akt inhibition is linked to the activation status of PI3K/Akt and MEK/ERK pathway. *PLoS One,* 7**,** e50005.

RAO, S. S., O'NEIL, J., LIBERATOR, C. D., HARDWICK, J. S., DAI, X., ZHANG, T., TYMINSKI, E., YUAN, J., KOHL, N. E., RICHON, V. M., VAN DER PLOEG, L. H., CARROLL, P. M., DRAETTA, G. F., LOOK, A. T., STRACK, P. R. & WINTER, C. G. 2009. Inhibition of NOTCH signaling by gamma secretase inhibitor engages the RB pathway and elicits cell cycle exit in T-cell acute lymphoblastic leukemia cells. *Cancer Res,* 69**,** 3060-8.

REID, T. S., TERRY, K. L., CASEY, P. J. & BEESE, L. S. 2004. Crystallographic analysis of CaaX prenyltransferases complexed with substrates defines rules of protein substrate selectivity. *J Mol Biol,* 343**,** 417-33.

RESZKA, A. A., HALASY-NAGY, J. & RODAN, G. A. 2001. Nitrogen-bisphosphonates block retinoblastoma phosphorylation and cell growth by inhibiting the cholesterol biosynthetic pathway in a keratinocyte model for esophageal irritation. *Mol Pharmacol,* 59**,** 193-202.

RESZKA, A. A. & RODAN, G. A. 2004. Nitrogen-containing bisphosphonate mechanism of action. *Mini Rev Med Chem,* 4**,** 711-9.

RINI, B. I. 2005. VEGF-targeted therapy in metastatic renal cell carcinoma. *Oncologist,* 10**,** 191-7.

ROELOFS, A. J., THOMPSON, K., GORDON, S. & ROGERS, M. J. 2006. Molecular mechanisms of action of bisphosphonates: current status. *Clin Cancer Res,* 12**,** 6222s-6230s.

ROGERS, M. J., JI, X. H., RUSSELL, R. G. G., BLACKBURN, G. M., WILLIAMSON, M. P., BAYLESS, A. V., EBETINO, F. H. & WATTS, D. J. 1994. Incorporation of Bisphosphonates into Adenine-Nucleotides by Amebas of the Cellular Slime-Mold Dictyostelium-Discoideum. *Biochemical Journal,* 303**,** 303-311.

ROGERS, M. J., XIONG, X., BROWN, R. J., WATTS, D. J., RUSSELL, R. G., BAYLESS, A. V. & EBETINO, F. H. 1995. Structure-activity relationships of new heterocycle-containing bisphosphonates as inhibitors of bone resorption and as inhibitors of growth of Dictyostelium discoideum amoebae. *Mol Pharmacol,* 47**,** 398-402.

ROWLEY, J. D. 1973. Letter: A new consistent chromosomal abnormality in chronic myelogenous leukaemia identified by quinacrine fluorescence and Giemsa staining. *Nature,* 243**,** 290-3.

RUSSELL, R. G. & ROGERS, M. J. 1999. Bisphosphonates: from the laboratory to the clinic and back again. *Bone,* 25**,** 97-106.
RUSSELL, R. G. G., WATTS, N. B., EBETINO, F. H. & ROGERS, M. J. 2008. Mechanisms of action of bisphosphonates: similarities and differences and their potential influence on clinical efficacy. *Osteoporosis International,* 19**,** 733-759.
SANCHEZ-MARTIN, M., AMBESI-IMPIOMBATO, A., QIN, Y., HERRANZ, D., BANSAL, M., GIRARDI, T., PAIETTA, E., TALLMAN, M. S., ROWE, J. M., DE KEERSMAECKER, K., CALIFANO, A. & FERRANDO, A. A. 2017. Synergistic antileukemic therapies in NOTCH1-induced T-ALL. *Proc Natl Acad Sci U S A,* 114**,** 2006-2011.
SANCHEZ-MARTIN, M. & FERRANDO, A. 2017. The NOTCH1-MYC highway toward T-cell acute lymphoblastic leukemia. *Blood,* 129**,** 1124-1133.
SEGAWA, H., KIMURA, S., KURODA, J., SATO, K., YOKOTA, A., KAWATA, E., KAMITSUJI, Y., ASHIHARA, E., YUASA, T., FUJIYAMA, Y., OTTMANN, O. G. & MAEKAWA, T. 2005. Zoledronate synergises with imatinib mesylate to inhibit Ph primary leukaemic cell growth. *Br J Haematol,* 130**,** 558-60.
SEVER, N., SONG, B. L., YABE, D., GOLDSTEIN, J. L., BROWN, M. S. & DEBOSE-BOYD, R. A. 2003. Insig-dependent ubiquitination and degradation of mammalian 3-hydroxy-3-methylglutaryl-CoA reductase stimulated by sterols and geranylgeraniol. *J Biol Chem,* 278**,** 52479-90.
SHARMA, V. M., CALVO, J. A., DRAHEIM, K. M., CUNNINGHAM, L. A., HERMANCE, N., BEVERLY, L., KRISHNAMOORTHY, V., BHASIN, M., CAPOBIANCO, A. J. & KELLIHER, M. A. 2006. Notch1 contributes to mouse T-cell leukemia by directly inducing the expression of c-myc. *Mol Cell Biol,* 26**,** 8022-31.
SHEN, N., SHAO, Y., LAI, S. S., QIAO, L., YANG, R. L., XUE, B., PAN, F. Y., CHEN, H. Q. & LI, C. J. 2011. GGPPS, a new EGR-1 target gene, reactivates ERK 1/2 signaling through increasing Ras prenylation. *Am J Pathol,* 179**,** 2740-50.
SHIMONO, Y., MUKOHYAMA, J., NAKAMURA, S. & MINAMI, H. 2015. MicroRNA Regulation of Human Breast Cancer Stem Cells. *J Clin Med,* 5.
SHIPMAN, C. M., CROUCHER, P. I., RUSSELL, R. G., HELFRICH, M. H. & ROGERS, M. J. 1998. The bisphosphonate incadronate (YM 175) causes apoptosis of human myeloma cels in vitro by inhibiting the mevalonate pathway. *Cancer research,* 58**,** 5294-5297.
SHULL, L. W., WIEMER, A. J., HOHL, R. J. & WIEMER, D. F. 2006. Synthesis and biological activity of isoprenoid bisphosphonates. *Bioorg Med Chem,* 14**,** 4130-6.
SJOGREN, A. K., ANDERSSON, K. M., LIU, M., CUTTS, B. A., KARLSSON, C., WAHLSTROM, A. M., DALIN, M., WEINBAUM, C., CASEY, P. J., TARKOWSKI, A., SWOLIN, B., YOUNG, S. G. & BERGO, M. O. 2007. GGTase-I deficiency reduces tumor formation and improves survival in mice with K-RAS-induced lung cancer. *J Clin Invest,* 117**,** 1294-304.
SONNEMANN, J., BUMBUL, B. & BECK, J. F. 2007. Synergistic activity of the histone deacetylase inhibitor suberoylanilide hydroxamic acid and the bisphosphonate zoledronic acid against prostate cancer cells in vitro. *Mol Cancer Ther,* 6**,** 2976-84.
SORRENTINO, G., RUGGERI, N., SPECCHIA, V., CORDENONSI, M., MANO, M., DUPONT, S., MANFRIN, A., INGALLINA, E., SOMMAGGIO, R., PIAZZA, S., ROSATO, A., PICCOLO, S. & DEL SAL, G. 2014. Metabolic control of YAP and TAZ by the mevalonate pathway. *Nat Cell Biol,* 16**,** 357-66.

STIGTER, E. A., GUO, Z., BON, R. S., WU, Y. W., CHOIDAS, A., WOLF, A., MENNINGER, S., WALDMANN, H., BLANKENFELDT, W. & GOODY, R. S. 2012. Development of selective, potent RabGGTase inhibitors. *J Med Chem,* 55**,** 8330-40.
STRESING, V., DAUBINE, F., BENZAID, I., MONKKONEN, H. & CLEZARDIN, P. 2007. Bisphosphonates in cancer therapy. *Cancer Lett,* 257**,** 16-35.
SUN, J., QIAN, Y., CHEN, Z., MARFURT, J., HAMILTON, A. D. & SEBTI, S. M. 1999. The geranylgeranyltransferase I inhibitor GGTI-298 induces hypophosphorylation of retinoblastoma and partner switching of cyclin-dependent kinase inhibitors. A potential mechanism for GGTI-298 antitumor activity. *J Biol Chem,* 274**,** 6930-4.
SZABO, C. M., MATSUMURA, Y., FUKURA, S., MARTIN, M. B., SANDERS, J. M., SENGUPTA, S., CIESLAK, J. A., LOFTUS, T. C., LEA, C. R., LEE, H. J., KOOHANG, A., COATES, R. M., SAGAMI, H. & OLDFIELD, E. 2002. Inhibition of geranylgeranyl diphosphate synthase by bisphosphonates and diphosphates: a potential route to new bone antiresorption and antiparasitic agents. *J Med Chem,* 45**,** 2185-96.
TANG, D., PARK, H. J., GEORGESCU, S. P., SEBTI, S. M., HAMILTON, A. D. & GALPER, J. B. 2006. Simvastatin potentiates tumor necrosis factor alpha-mediated apoptosis of human vascular endothelial cells via the inhibition of the geranylgeranylation of RhoA. *Life Sci,* 79**,** 1484-92.
TANG, Z., LI, C., KANG, B., GAO, G., LI, C. & ZHANG, Z. 2017. GEPIA: a web server for cancer and normal gene expression profiling and interactive analyses. *Nucleic Acids Res,* 45**,** W98-W102.
TANIDA, I., UENO, T. & KOMINAMI, E. 2008. LC3 and Autophagy. *Methods Mol Biol,* 445**,** 77-88.
TAO, W., SHI, J. F., ZHANG, Q., XUE, B., SUN, Y. J. & LI, C. J. 2013. Egr-1 enhances drug resistance of breast cancer by modulating MDR1 expression in a GGPPS-independent manner. *Biomed Pharmacother,* 67**,** 197-202.
TECLEAB, A., ZHANG, X. & SEBTI, S. M. 2014. Ral GTPase down-regulation stabilizes and reactivates p53 to inhibit malignant transformation. *J Biol Chem,* 289**,** 31296-309.
TERPOS, E., BERENSON, J., RAJE, N. & ROODMAN, G. D. 2014. Management of bone disease in multiple myeloma. *Expert Rev Hematol,* 7**,** 113-25.
TERPOS, E., ROODMAN, G. D. & DIMOPOULOS, M. A. 2013. Optimal use of bisphosphonates in patients with multiple myeloma. *Blood,* 121**,** 3325-8.
TERRY, M. R., ARYA, R., MUKHOPADHYAY, A., BERRETT, K. C., CLAIR, P. M., WITT, B., SALAMA, M. E., BHUTKAR, A. & OLIVER, T. G. 2015. Caspase-2 impacts lung tumorigenesis and chemotherapy response in vivo. *Cell Death Differ,* 22**,** 719-30.
THOMPSON, K., ROGERS, M. J., COXON, F. P. & CROCKETT, J. C. 2006. Cytosolic entry of bisphosphonate drugs requires acidification of vesicles after fluid-phase endocytosis. *Mol Pharmacol,* 69**,** 1624-32.
TSUBAKI, M., ITOH, T., SATOU, T., IMANO, M., KOMAI, M., OGAWA, N., MUKAI, J. & NISHIDA, S. 2013. Nitrogen-containing bisphosphonates induce apoptosis of hematopoietic tumor cells via inhibition of Ras signaling pathways and Bim-mediated activation of the intrinsic apoptotic pathway. *Biochem Pharmacol,* 85**,** 163-72.
TSUBAKI, M., TAKEDA, T., SAKAMOTO, K., SHIMAOKA, H., FUJITA, A., ITOH, T., IMANO, M., MASHIMO, K., FUJIWARA, D., SAKAGUCHI, K., SATOU, T. & NISHIDA, S. 2015. Bisphosphonates and statins inhibit expression and secretion of MIP-

1alpha via suppression of Ras/MEK/ERK/AML-1A and Ras/PI3K/Akt/AML-1A pathways. *Am J Cancer Res,* 5**,** 168-79.
VAN BEEK, E., LOWIK, C., VAN DER PLUIJM, G. & PAPAPOULOS, S. 1999a. The role of geranylgeranylation in bone resorption and its suppression by bisphosphonates in fetal bone explants in vitro: A clue to the mechanism of action of nitrogen-containing bisphosphonates. *J Bone Miner Res,* 14**,** 722-9.
VAN BEEK, E., PIETERMAN, E., COHEN, L., LOWIK, C. & PAPAPOULOS, S. 1999b. Farnesyl pyrophosphate synthase is the molecular target of nitrogen-containing bisphosphonates. *Biochem Biophys Res Commun,* 264**,** 108-11.
VAN DE DONK, N. W., KAMPHUIS, M. M., VAN KESSEL, B., LOKHORST, H. M. & BLOEM, A. C. 2003. Inhibition of protein geranylgeranylation induces apoptosis in myeloma plasma cells by reducing Mcl-1 protein levels. *Blood,* 102**,** 3354-62.
VERMEZOVIC, J., ADAMOWICZ, M., SANTARPIA, L., RUSTIGHI, A., FORCATO, M., LUCANO, C., MASSIMILIANO, L., COSTANZO, V., BICCIATO, S., DEL SAL, G. & D'ADDA DI FAGAGNA, F. 2015. Notch is a direct negative regulator of the DNA-damage response. *Nat Struct Mol Biol,* 22**,** 417-24.
WANG, J. Y., NADERI, S. & CHEN, T. T. 2001. Role of retinoblastoma tumor suppressor protein in DNA damage response. *Acta Oncol,* 40**,** 689-95.
WANG, X., MARTINDALE, J. L. & HOLBROOK, N. J. 2000. Requirement for ERK activation in cisplatin-induced apoptosis. *J Biol Chem,* 275**,** 39435-43.
WANG, X., XU, W., ZHAN, P., XU, T., JIN, J., MIU, Y., ZHOU, Z., ZHU, Q., WAN, B., XI, G., YE, L., LIU, Y., GAO, J., LI, H., LV, T. & SONG, Y. 2018. Overexpression of geranylgeranyl diphosphate synthase contributes to tumour metastasis and correlates with poor prognosis of lung adenocarcinoma. *J Cell Mol Med,* 22**,** 2177-2189.
WASKO, B. M., DUDAKOVIC, A. & HOHL, R. J. 2011. Bisphosphonates induce autophagy by depleting geranylgeranyl diphosphate. *J Pharmacol Exp Ther,* 337**,** 540-6.
WEISSENRIEDER, J. S., REILLY, J. E., NEIGHBORS, J. D. & HOHL, R. J. 2018. Inhibiting geranylgeranyl diphosphate synthesis reduces nuclear androgen receptor signaling and neuroendocrine differentiation in prostate cancer cell models. *Prostate*.
WENG, A. P., FERRANDO, A. A., LEE, W., MORRIS, J. P. T., SILVERMAN, L. B., SANCHEZ-IRIZARRY, C., BLACKLOW, S. C., LOOK, A. T. & ASTER, J. C. 2004. Activating mutations of NOTCH1 in human T cell acute lymphoblastic leukemia. *Science,* 306**,** 269-71.
WENG, A. P., MILLHOLLAND, J. M., YASHIRO-OHTANI, Y., ARCANGELI, M. L., LAU, A., WAI, C., DEL BIANCO, C., RODRIGUEZ, C. G., SAI, H., TOBIAS, J., LI, Y., WOLFE, M. S., SHACHAF, C., FELSHER, D., BLACKLOW, S. C., PEAR, W. S. & ASTER, J. C. 2006. c-Myc is an important direct target of Notch1 in T-cell acute lymphoblastic leukemia/lymphoma. *Genes Dev,* 20**,** 2096-109.
WENNERBERG, K., ROSSMAN, K. L. & DER, C. J. 2005. The Ras superfamily at a glance. *J Cell Sci,* 118**,** 843-6.
WHYTE, D. B., KIRSCHMEIER, P., HOCKENBERRY, T. N., NUNEZ-OLIVA, I., JAMES, L., CATINO, J. J., BISHOP, W. R. & PAI, J. K. 1997. K- and N-Ras are geranylgeranylated in cells treated with farnesyl protein transferase inhibitors. *J Biol Chem,* 272**,** 14459-64.
WIEMER, A. J., HOHL, R. J. & WIEMER, D. F. 2009. The intermediate enzymes of isoprenoid metabolism as anticancer targets. *Anticancer Agents Med Chem,* 9**,** 526-542.

WIEMER, A. J., TONG, H., SWANSON, K. M. & HOHL, R. J. 2007. Digeranyl bisphosphonate inhibits geranylgeranyl pyrophosphate synthase. *Biochem Biophys Res Commun,* 353**,** 921-5.
WIEMER, A. J., WERNIMONT, S. A., CUNG, T. D., BENNIN, D. A., BEGGS, H. E. & HUTTENLOCHER, A. 2013. The focal adhesion kinase inhibitor PF-562,271 impairs primary CD4+ T cell activation. *Biochem Pharmacol,* 86**,** 770-81.
WIEMER, A. J. & WIEMER, D. F. 2015. Prodrugs of phosphonates and phosphates: crossing the membrane barrier. *Top Curr Chem,* 360**,** 115-60.
WIEMER, A. J., WIEMER, D. F. & HOHL, R. J. 2011. Geranylgeranyl diphosphate synthase: an emerging therapeutic target. *Clin Pharmacol Ther,* 90**,** 804-12.
WIEMER, A. J., YU, J. S., LAMB, K. M., HOHL, R. J. & WIEMER, D. F. 2008a. Mono- and dialkyl isoprenoid bisphosphonates as geranylgeranyl diphosphate synthase inhibitors. *Bioorg Med Chem,* 16**,** 390-9.
WIEMER, A. J., YU, J. S., SHULL, L. W., BARNEY, R. J., WASKO, B. M., LAMB, K. M., HOHL, R. J. & WIEMER, D. F. 2008b. Pivaloyloxymethyl-modified isoprenoid bisphosphonates display enhanced inhibition of cellular geranylgeranylation. *Bioorg Med Chem,* 16**,** 3652-60.
WILKE, M., GOBEL, A., RAUNER, M., BENAD-MEHNER, P., SCHUTZE, N., FUSSEL, S., HADJI, P., HOFBAUER, L. C. & RACHNER, T. D. 2014. Zoledronic acid and atorvastatin inhibit alphavbeta3-mediated adhesion of breast cancer cells. *J Bone Oncol,* 3**,** 10-7.
WILLS, V. S., ALLEN, C., HOLSTEIN, S. A. & WIEMER, D. F. 2015. Potent Triazole Bisphosphonate Inhibitor of Geranylgeranyl Diphosphate Synthase. *ACS Med Chem Lett,* 6**,** 1195-8.
WU, J., WONG, W. W., KHOSRAVI, F., MINDEN, M. D. & PENN, L. Z. 2004. Blocking the Raf/MEK/ERK pathway sensitizes acute myelogenous leukemia cells to lovastatin-induced apoptosis. *Cancer Res,* 64**,** 6461-8.
XIA, Y., LIU, Y. L., XIE, Y., ZHU, W., GUERRA, F., SHEN, S., YEDDULA, N., FISCHER, W., LOW, W., ZHOU, X., ZHANG, Y., OLDFIELD, E. & VERMA, I. M. 2014. A combination therapy for KRAS-driven lung adenocarcinomas using lipophilic bisphosphonates and rapamycin. *Sci Transl Med,* 6**,** 263ra161.
XU, Y. F., HANNAFON, B. N. & DING, W. Q. 2017. microRNA regulation of human pancreatic cancer stem cells. *Stem Cell Investig,* 4**,** 5.
YANAE, M., TSUBAKI, M., SATOU, T., ITOH, T., IMANO, M., YAMAZOE, Y. & NISHIDA, S. 2011. Statin-induced apoptosis via the suppression of ERK1/2 and Akt activation by inhibition of the geranylgeranyl-pyrophosphate biosynthesis in glioblastoma. *J Exp Clin Cancer Res,* 30**,** 74.
YANG, W., SOARES, J., GRENINGER, P., EDELMAN, E. J., LIGHTFOOT, H., FORBES, S., BINDAL, N., BEARE, D., SMITH, J. A., THOMPSON, I. R., RAMASWAMY, S., FUTREAL, P. A., HABER, D. A., STRATTON, M. R., BENES, C., MCDERMOTT, U. & GARNETT, M. J. 2013. Genomics of Drug Sensitivity in Cancer (GDSC): a resource for therapeutic biomarker discovery in cancer cells. *Nucleic Acids Res,* 41**,** D955-61.
YOSHIDA, T., CLARK, M. F. & STERN, P. H. 2009. The small GTPase RhoA is crucial for MC3T3-E1 osteoblastic cell survival. *J Cell Biochem,* 106**,** 896-902.

YU, D. C., LIU, J., CHEN, J., SHAO, J. J., SHEN, X., XIA, H. G., LI, C. J., XUE, B. & DING, Y. T. 2014. GGPPS1 predicts the biological character of hepatocellular carcinoma in patients with cirrhosis. *BMC Cancer,* 14**,** 248.

YU, R., LONGO, J., VAN LEEUWEN, J. E., MULLEN, P. J., BA-ALAWI, W., HAIBE-KAINS, B. & PENN, L. Z. 2018. Statin-Induced Cancer Cell Death Can Be Mechanistically Uncoupled from Prenylation of RAS Family Proteins. *Cancer Res,* 78**,** 1347-1357.

YU, X., SHEN, N., ZHANG, M. L., PAN, F. Y., WANG, C., JIA, W. P., LIU, C., GAO, Q., GAO, X., XUE, B. & LI, C. J. 2011. Egr-1 decreases adipocyte insulin sensitivity by tilting PI3K/Akt and MAPK signal balance in mice. *EMBO J,* 30**,** 3754-65.

ZAFAR, S., COATES, D. E., CULLINAN, M. P., DRUMMOND, B. K., MILNE, T. & SEYMOUR, G. J. 2014. Zoledronic acid and geranylgeraniol regulate cellular behaviour and angiogenic gene expression in human gingival fibroblasts. *J Oral Pathol Med,* 43**,** 711-21.

ZAGOURAS, P., STIFANI, S., BLAUMUELLER, C. M., CARCANGIU, M. L. & ARTAVANIS-TSAKONAS, S. 1995. Alterations in Notch signaling in neoplastic lesions of the human cervix. *Proc Natl Acad Sci U S A,* 92**,** 6414-8.

ZHANG, T., GUO, L., CREIGHTON, C. J., LU, Q., GIBBONS, D. L., YI, E. S., DENG, B., MOLINA, J. R., SUN, Z., YANG, P. & YANG, Y. 2016. A genetic cell context-dependent role for ZEB1 in lung cancer. *Nat Commun,* 7**,** 12231.

ZHANG, Y., CAO, R., YIN, F., HUDOCK, M. P., GUO, R. T., KRYSIAK, K., MUKHERJEE, S., GAO, Y. G., ROBINSON, H., SONG, Y., NO, J. H., BERGAN, K., LEON, A., CASS, L., GODDARD, A., CHANG, T. K., LIN, F. Y., VAN BEEK, E., PAPAPOULOS, S., WANG, A. H., KUBO, T., OCHI, M., MUKKAMALA, D. & OLDFIELD, E. 2009. Lipophilic bisphosphonates as dual farnesyl/geranylgeranyl diphosphate synthase inhibitors: an X-ray and NMR investigation. *J Am Chem Soc,* 131**,** 5153-62.

ZHANG, Y., ZHU, W., LIU, Y. L., WANG, H., WANG, K., LI, K., NO, J. H., AYONG, L., GULATI, A., PANG, R., FREITAS-JUNIOR, L., MORITA, C. T. & OLD-FIELD, E. 2013. Chemo-Immunotherapeutic Anti-Malarials Targeting Isoprenoid Biosynthesis. *ACS Med Chem Lett,* 4**,** 423-427.

ZHAO, B., WEI, X., LI, W., UDAN, R. S., YANG, Q., KIM, J., XIE, J., IKENOUE, T., YU, J., LI, L., ZHENG, P., YE, K., CHINNAIYAN, A., HALDER, G., LAI, Z. C. & GUAN, K. L. 2007. Inactivation of YAP oncoprotein by the Hippo pathway is involved in cell contact inhibition and tissue growth control. *Genes Dev,* 21**,** 2747-61.

ZHOU, X., FERREE, S. D., WILLS, V. S., BORN, E. J., TONG, H., WIEMER, D. F. & HOLSTEIN, S. A. 2014. Geranyl and neryl triazole bisphosphonates as inhibitors of geranylgeranyl diphosphate synthase. *Bioorg Med Chem,* 22**,** 2791-8.

ZHOU, X., QIAN, J., HUA, L., SHI, Q., LIU, Z., XU, Y., SANG, B., MO, J. & YU, R. 2013. Geranylgeranyltransferase I promotes human glioma cell growth through Rac1 membrane association and activation. *J Mol Neurosci,* 49**,** 130-9.

ZHU, Y., CASEY, P. J., KUMAR, A. P. & PERVAIZ, S. 2013. Deciphering the signaling networks underlying simvastatin-induced apoptosis in human cancer cells: evidence for non-canonical activation of RhoA and Rac1 GTPases. *Cell Death Dis,* 4**,** e568.